MITOCHONDRIAL RESPIRATION PROMOTES NON-SMALL CELL LUNG CANCER CELL PROLIFERATION AND FUNCTION

by

Md Maksudul Alam

APPROVED BY SUPERVISORY COMMITTEE:

_____

Dr. Li Zhang, Chair

_____

Dr. John G. Burr

_____

Dr. Ernest M. Hannig

_____

Dr. Michael Q. Zhang

Dedicated to my late father Gazi Mohd. Omar Ali

MITOCHONDRIAL RESPIRATION PROMOTES NON-SMALL CELL LUNG CANCER CELL PROLIFERATION AND FUNCTION

by

MD MAKSUDUL ALAM, MS

DISSERTATION

Presented to the Faculty of

The University of Texas at Dallas

in Partial Fulfillment

of the Requirements

for the Degree of

DOCTOR OF PHILOSOPHY IN

MOLECULAR AND CELL BIOLOGY

THE UNIVERSITY OF TEXAS AT DALLAS

December 2016

ACKNOWLEDGMENTS

My academic achievements would not be possible without the help of my parents, family and teachers. Notably, I would like to thank my uncles, MA Halim and Din Mohammad for their support and advice throughout my academic career. I am ever grateful to my PhD supervisor Dr. Li Zhang for taking me as a PhD student and guiding me to the completion of my project. Without her help and support it would be impossible to get my PhD degree. I would also like to thank my Undergraduate teacher and mentor Dr. Haseena Khan for introducing me to the realm of research world.

My dissertation committee members; Dr. John G. Burr, Dr. Michael Q. Zhang, and Dr. Ernest M. Hannig should also be thanked for their valuable suggestions and comments in preparing my PhD thesis.

I would like to thank my lab members, Dr. Xiao Yao and Dr. Daniela Cadinu for teaching me many fundamental techniques of cell culture. I am also grateful to my lab members; Sagar Sohoni, Dr. Jagmohan Hooda, Dr. Ajit Shah, Sneha Lal, Sarada Preta and other lab members of Dr. Li Zhang's lab for their helping hands. I am thankful to my previous lab mates Dr. Inder Kalra and Dr. Ashwinikumar Kulkarni for their constant support. Finally I would like to thank my best friends Hussainul, Anwarul, Fahim and Niloy for their inspiration and support.

October, 2016

PREFACE

This dissertation was produced in accordance with guidelines that permit the inclusion as part of the dissertation the text of an original paper, or papers, submitted for publication. The dissertation must still conform to all other requirements explained in the "Guide for the preparation of Master's Thesis, Doctoral Dissertations, and Doctor of Chemistry Practica Reports at the University of Texas at Dallas". It must include a comprehensive abstract, a full introduction and literature review, and a final overall conclusion. Additional material (procedural and design data as well as descriptions of equipments) must be provided in sufficient detail to allow a clear and precise judgment to be made of the importance and originality of the research reported.

It is acceptable for this dissertation to include as chapters authentic copies of papers already published, provided they meet type size, margin, and legibility requirements. In such cases, connecting texts that provide logical bridges between different manuscripts are mandatory. Where the student is not the sole author of a manuscript, the student is required to make an explicit statement in the introductory material to that manuscript describing the student's contribution to the work and acknowledging the contributions of the other author(s). The signatures of the Supervising Committee that precede all other material in the dissertation attest to the accuracy of this statement.

MITOCHONDRIAL RESPIRATION PROMOTES NON-SMALL CELL LUNG CANCER CELL PROLIFERATION AND FUNCTION

Publication No. _____

Md Maksudul Alam, PhD
The University of Texas at Dallas, 2016

Supervising Professor: Dr. Li Zhang

Lung cancer is the leading cause of cancer related death both in the USA and worldwide. More than 80% of the lung cancer cases are non-small cell lung cancer (NSCLC). Since Otto Warburg made the first observation that the rate of aerobic glycolisis is increased in tumor cells, substantial amount of research has been done on altered cancer cell metabolism and bioenergetics. Recently, the use of more advanced metabolomics and genomics technologies has revealed the remarkable plasticity of tumor metabolism and bioenergetics. Many types of tumor cells have been shown to generate most of the cellular energy via mitochondrial respiration and oxidative phosphorylation. In this dissertation project it has been shown that the rate of respiration is intensified in an array of NSCLCs compared to the normal lung cell line. We also found that the respiration is greatly reduced when NSCLCs are grown in glutamine deprived media, whereas the respiration is unaffected when the cells are grown in glucose deprived media. In this project we have also shown that Hedgehog (Hh) signaling inhibitors Cyclopamine tartrate

(CycT) and SNAT1 disrupt mitochondrial function and aerobic respiration. Our results showed that CycT, like glutamine depletion, caused a substantial decrease in oxygen consumption in a number of NSCLC cell lines, suppressed NSCLC cell proliferation, and induced apoptosis. Further, we found that CycT increased reactive oxygen species (ROS) generation, causes mitochondrial membrane hyperpolarization, and mitochondrial fragmentation, thereby disrupting mitochondrial function in NSCLC cells.

Furthermore, using two isogenic cell lines representing matched pairs of normal and cancer cells, we have identified changes in protein levels accompanying transformation of normal lung epithelial cells to cancer cells. Surprisingly, a substantial number of proteins involved in actin cytoskeleton were preferentially downregualted in cancer cells. However, similar numbers of proteins in other organelles were either up or down regulated. The formation of stress fibers and focal adhesions were also markedly decreased in cancer cells. Protein network analysis showed that the altered proteins are highly connected.

TABLE OF CONTENTS

LIST OF FIGURES

LIST OF TABLES

CHAPTER 1

A HOLISTIC VIEW OF CANCER BIOENERGETICS: MITOCHONDRIAL FUNCTION AND RESPIRATION PLAY FUNDAMENTAL ROLES IN THE DEVELOPMENT AND PROGRESSION OF DIVERSE TUMORS

Author – Md Maksudul Alam

Literature analysis and organization – Li Zhang, Md Maksudul Alam

Literature research – Md Maksudul Alam, Sneha Lal, Keely E FitzGerald

Department of Biological Sciences

The University of Texas at Dallas

800 West Campbell Road

Richardson, Texas 75080

PREFACE

In this chapter, I will discuss the bioenergetics of tumors, particularly the role of mitochondrial respiration and function on various processes of cancer development and progression. This chapter is published in the manuscript: "A holistic view of cancer bioenergetics: mitochondrial function and respiration play fundamental roles in the development and progression of diverse tumors"

Alam et al. Clin Trans Med (2016) 5:3

DOI 10.1186/s40169-016-0082-9

ABSTRACT

Since Otto Warburg made the first observation that tumor cells exhibit altered metabolism and bioenergetics in the 1920s, many scientists have tried to further the understanding of tumor bioenergetics. Particularly, in the past decade, the application of the state-of the-art metabolomics and genomics technologies has revealed the remarkable plasticity of tumor metabolism and bioenergetics. Firstly, a wide array of tumor cells has been shown to be able to use not only glucose, but also glutamine for generating cellular energy, reducing power, and metabolic building blocks for biosynthesis. Secondly, many types of cancer cells generate most of their cellular energy via mitochondrial respiration and oxidative phosphorylation. Glutamine is the preferred substrate for oxidative phosphorylation in tumor cells. Thirdly, tumor cells exhibit remarkable versatility in using bioenergetics substrates. Notably, tumor cells can use metabolic substrates donated by stromal cells for cellular energy generation via oxidative

phosphorylation. Further, it has been shown that mitochondrial transfer is a critical mechanism for tumor cells with defective mitochondria to restore oxidative phosphorylation. The restoration is necessary for tumor cells to gain tumorigenic and metastatic potential. It is also worth noting that heme is essential for the biogenesis and proper functioning of mitochondrial respiratory chain complexes. Hence, it is not surprising that recent experimental data showed that heme flux and function are elevated in non-small cell lung cancer (NSCLC) cells and that elevated heme function promotes intensified oxygen consumption, thereby fueling tumor cell proliferation and function. Finally, emerging evidence increasingly suggests that clonal evolution and tumor genetic heterogeneity contribute to bioenergetic versatility of tumor cells, as well as tumor recurrence and drug resistance. Although mutations are found only in several metabolic enzymes in tumors, diverse mutations in signaling pathways and networks can cause changes in the expression and activity of metabolic enzymes, which likely enable tumor cells to gain their bioenergetic versatility. A better understanding of tumor bioenergetics should provide a more holistic approach to investigate cancer biology and therapeutics. This review therefore attempts to comprehensively consider and summarize the experimental data supporting our latest view of cancer bioenergetics.

KEY WORDS

Tumor bioenergetics, Glutamine, Tumor heterogeneity, Metabolic Mutations, Mitochondrial Respiration, Oxidative phosphorylation, Heme, Hemoprotein, Mitochondrial transfer.

INTRODUCTION

Terrestrial organisms vary in many ways, but one characteristic common to all living organisms is the need for cellular energy. The universal energy currency is ATP. Eukaryotes ranging from yeast to humans generate ATP via glycolysis and oxidative phosphorylation. The term glycolysis comes from the Greek "glyco-," meaning "sweet," and "-lysis," meaning "to split." The name is apt, as the glycolytic pathway involves the splitting of sugar to produce ATP. Oxidative phosphorylation (OXPHOS) is so named because it combines inorganic phosphate with ADP to form ATP in the presence of oxygen. Human cells can use various fuels, including glucose, amino acids, and fat for adenosine triphosphate (ATP) production to support cellular function and proliferation. Fuel usage for ATP generation is dependent on the conditions of the body. For example, in healthy, well-fed individuals, skeletal muscle is degraded and regenerated frequently. The amino acid pool in humans remains relatively unchanged. To keep the amino acid pool constant during starvation, the degradation of skeletal muscles increases. This occurs so that the body can continue to provide energy for essential functions. Glutamine and alanine constitute the majority of amino acids released from skeletal muscles during starvation. One consequence of unlimited cancer cell proliferation is likely to make the human body feel starved and respond in a way similar to the body's response to starvation. Hence, it is conceivable that glutamine can be a preferred fuel for many types of cancer cells. The importance of glutamine in tumor metabolism and bioenergetics is further confirmed by recent metabolomics studies showing that α-ketoglutarate from glutamine can undergo reductive carboxylation to generate citrate, which can be turned into malate for generating nicotinamide adenine dinucleotide phosphate (NADPH) via malic enzyme. This provides an alternative pathway for cancer cells to

generate citrate and NADPH for sustaining anabolic reactions. Another noteworthy development in cancer bioenergetics research is the finding that stromal cells in the tumor microenvironment can provide cancer cells with bioenergetic substrates. Below, we consider previous and emerging research results and attempt to provide a holistic and up-to-date view of tumor bioenergetics.

REVIEW

High glycolytic rates occur concomitantly with oxidative phosphorylation (OXPHOS) in cells of most tumors

Glycolysis was first studied by Louis Pasteur in an attempt to understand the process of fermentation in 1856 [1]. Glycolysis as we understand it today was finalized by Buchner in 1947 [2]. Glycolysis consumes 2 ATP and produces 4 ATP for a net yield of 2 ATP (Figure 1.1). In the absence of oxygen, glycolysis is the metabolic pathway of choice. In the presence of oxygen, however, glycolysis only begins the process of aerobic respiration. In the presence of oxygen, pyruvate is consumed by the tricarboxylic acid (TCA) cycle (Figure 1.1). Albert Szent-Gyorgyi made major contributions elucidating the TCA cycle, also known as the Krebs cycle, in the 1920s and 1930s [3-7]. In 1945, coenzyme A was discovered by Fritz Lipmann [8]. However, the most important and well-known contributor to the discovery and understanding of the TCA cycle is Hans Krebs, who discovered that cycle began with citrate [9]. The TCA cycle does not produce ATP directly, although it produces 1 GTP, which is easily converted to ATP (Figure 1.1). However, the TCA cycle is extremely important for energy production because it provides the precursor molecules, namely NADH and $FADH_2$, for OXPHOS (Figure 1.1). Breakthroughs in OXPHOS were made from 1944 to 1980, beginning with Dickens, McIlwain, Neuberger,

Norris, Obrien, and Young and ending with Boyer [10-12]. OXPHOS is the preferred energy-generating method of many life forms, including mammals, in the presence of oxygen. This is because OXPHOS creates up to 38 ATP molecules per one molecule of glucose, as compared to only 2 ATP molecules generated anaerobically by glycolysis (Figure 1.1). Both TCA cycle and OXPHOS occur in mitochondria.

How cancer cells gain sufficient ATP to support their unabated proliferation and function has fascinated many scientists for nearly a century. The German scientist Otto Warburg and co-workers performed the first quantitative study of cancer cell metabolism in the 1920s [13, 14]. They showed that tumor tissues metabolize approximately tenfold more glucose to lactate in a given time than normal tissues, even when presented with enough oxygen to metabolize glucose completely to CO_2. This phenomenon is widely known as the Warburg effect and is the origin of the perception that a high glycolytic rate is typical of cancer/tumor cells [15]. The rationale for the high glycolytic rate was that tumor mitochondria have impaired respiration, which is compensated by an unusually high contribution of aerobic glycolysis to sustain ATP generation. The hallmark of aerobic glycolysis is a high rate of lactate production from glucose in the presence of oxygen. Warburg's observation has motivated generations of cancer biologists and biochemists to refine his hypothesis and provide mechanistic explanations for it.

However, immediately after the publication of Warburg's paper "On the Origin of Cancer Cells" [15], Weinhouse contested Warburg's ideas based on results in his laboratory showing that neoplastic tissues have a normal OXPHOS (oxidative phosphorylation) capacity when supplemented with NAD^+ [16, 17]. In 1979, Reitzer and co-workers showed that in cultured HeLa cells, more than half of the ATP requirement (determined by comparing $^{14}CO_2$ production

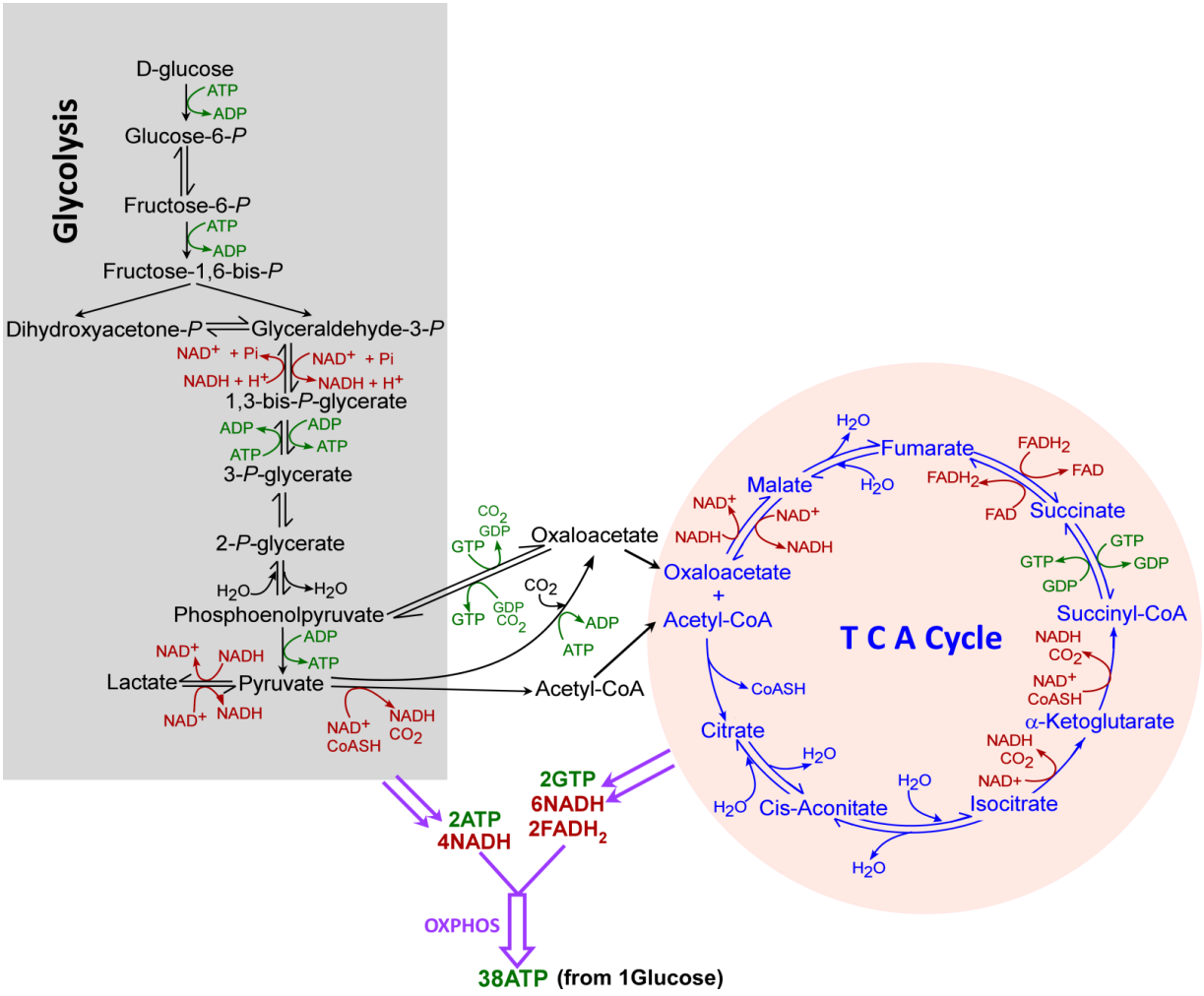

Figure 1.1. The metabolic steps of glycolysis and TCA cycle. The steps involved in glycolysis and TCA cycle are demarcated separately. ATP/GTP utilization or synthesis is shown in green, while NAD+/NADH and FAD/FADH2 are shown in red. Also indicated are the numbers of NADH, FADH2, and ATP/GTP generated when one molecule of glucose is consumed following glycolysis, TCA cycle, and oxidative phosphorylation. Abbreviations: *Glucose-6-P* glucose 6-phosphate, *Fructose-6-P* fructose 6-phosphate, *Fructose -1,6-bis-P* fructose 1,6-bisphosphate, *Dihydroxyacetone-P* dihydroxyacetone phosphate, *Glyceraldehyde-3-P* glyceraldehyde 3-phosphate, *1,3-Bis-P-glycerate* 1,3-bisphosphoglycerate, *3-P-Glycerate* 3-phosphoglycerate,*2-P-Glycerate* 2-phosphoglycerate, *OXPHOS* oxidative phosphorylation.

from ^{14}C-glutamine and ^{14}C-lactate production from ^{14}C-glucose) comes from glutamine even when a high concentration (10 mM) of glucose is present [18]. When fructose or galactose is the carbohydrate, glutamine provides greater than 98% of energy by aerobic oxidation from the TCA cycle. Experimental studies in recent years have confirmed the idea that glutamine is a major nutrient in cancer cells [19-22]. Additionally, ample experimental evidence showed that glutamine is a good substrate for oxidative metabolism in various tumor and cancer cells [23-26]. It is also worth noting that the authors' lab recently showed that glutamine enables an array of non-small cell lung cancer (NSCLC) cells to increase oxygen consumption substantially when glucose is depleted [27]. Taken together, various studies have shown that glucose and glutamine are key nutrients and fuels for cancer cells [21, 28]. Different cancer cells may exhibit varying dependence on glucose or glutamine [29, 30].

Both glucose and glutamine are important nutrients for many types of cancer cells and tumors

The importance of glutamine as a nutrient and fuel is consistent with the fact that it is the most abundant amino acid released from skeletal muscle, and it is the most abundant amino acid in plasma [31]. The importance of glucose and glutamine in cancer metabolism and bioenergetics can be easily gleaned from the architecture of metabolic pathways (Figure 1.2). Both glucose and glutamine have dual roles in ATP production and biosynthesis (anabolism). Although glucose can generate ATP via glycolysis, its most prominent function is evidently in anabolism (biosynthesis). As shown in Figure 1.2, glucose can generate the precursor ribulose-5-P and the reducing power NADPH via the pentose phosphate pathway. The glycolysis intermediate

glyceraldehyde 3-P can yield glycerol-3-P, which serves as a backbone for the synthesis of phosphatidic acid, a precursor for the synthesis of triacylglycerol and phospholipids. Another glycolysis intermediate, 3-P glycerate, is a precursor for serine, which can be used to synthesize ceramide and is a precursor for one-carbon metabolism. Ultimately, pyruvate generated from glucose via glycolysis can be turned into Acetyl CoA and serves as a substrate feeding the TCA cycle. Under conditions permitting mitochondrial respiration, NADH and FADH2 generated from the TCA cycle will lead to high yield of ATP, via the electron transport chain and OXPHOS (Figure 1.1).

Glutamine is a very versatile nutrient feeding into many pathways for ATP generation, redox homeostasis, and biosynthesis [22]. Firstly, glutamine is the main substrate supporting TCA cycle anaplerosis. Glutamine can be readily turned into α-ketoglutarate, which feeds the TCA cycle (Figure 1.2), leading to the generation of NADH and $FADH_2$, which is used to generate ATP via electron transport and OXPHOS (Figure 1.1). This can lead to the generation of various TCA cycle intermediates, which can support many biosynthetic reactions and gluconeogenesis. Secondly, under hypoxic conditions or when mitochondria are defective, α-ketoglutarate from glutamine can undergo reductive carboxylation to generate citrate, providing a mechanism to sustain anabolic reactions [32-34] (Figure 1.2). Additionally, citrate generated in this way can be turned into malate, which provides another mechanism to generate NADPH via malic enzyme 1 [35, 36] (Figure 1.2).

Cancer cells also exhibit an increased demand for fatty acids, besides glucose and glutamine [37, 38] . Fatty acids can be synthesized endogenously (Figure 1.2) or taken up from exogenous sources. In prostate tumors, which import less glucose than other tumors [39], β-

oxidation of fatty acids provides an important energy source [40, 41]. Additionally, two recent studies showed that acetate is a bioenergetic substrate for glioblastoma and brain metastases, and it is important for biosynthesis and histone modification in a wide spectrum of tumors [42, 43]. Overall, metabolic phenotypes in cancer cells are plastic, and cancer cells exhibit greater plasticity than normal cells [44].

Stromal cells and adipocytes can provide building blocks and fuels to tumor cells

Like other aspects of cancer biology, our understanding of tumor metabolism is continuously evolving. Particularly in recent years, some researchers have investigated tumor metabolism in the context of the whole tumor microenvironment. These studies suggest a two-compartment model for understanding tumor metabolism [45-49]. In this model, under the education of cancer cells and inflammatory cytokines, stromal cells and adipocytes become "food donors." Tumor stromal cells principally include cancer-associated fibroblasts (CAFs), tumor endothelial cells (TECs), and tumor-associated macrophages (TAMs). Catabolism in stromal cells and adipocytes provides fuels and building blocks (see Figure 1.2) for the anabolic growth of cancer cells via metabolic coupling [48, 49]. For example, by examining MCF7 breast cancer cells cultured alone or co-cultured with nontransformed fibroblasts, Ko et al. showed that CAFs undergo an autophagic program, leading to the generation and secretion of high glutamine levels into the tumor microenvironment [50]. The glutamine released from CAFs fuel cancer cell mitochondrial activity, driving a vicious cycle of catabolism in the tumor stroma and anabolic tumor cell expansion. Likewise, Nieman et al showed that triglyceride catabolism in adipocytes drives ovarian cancer metastasis by providing fatty acids as mitochondrial fuels [51].

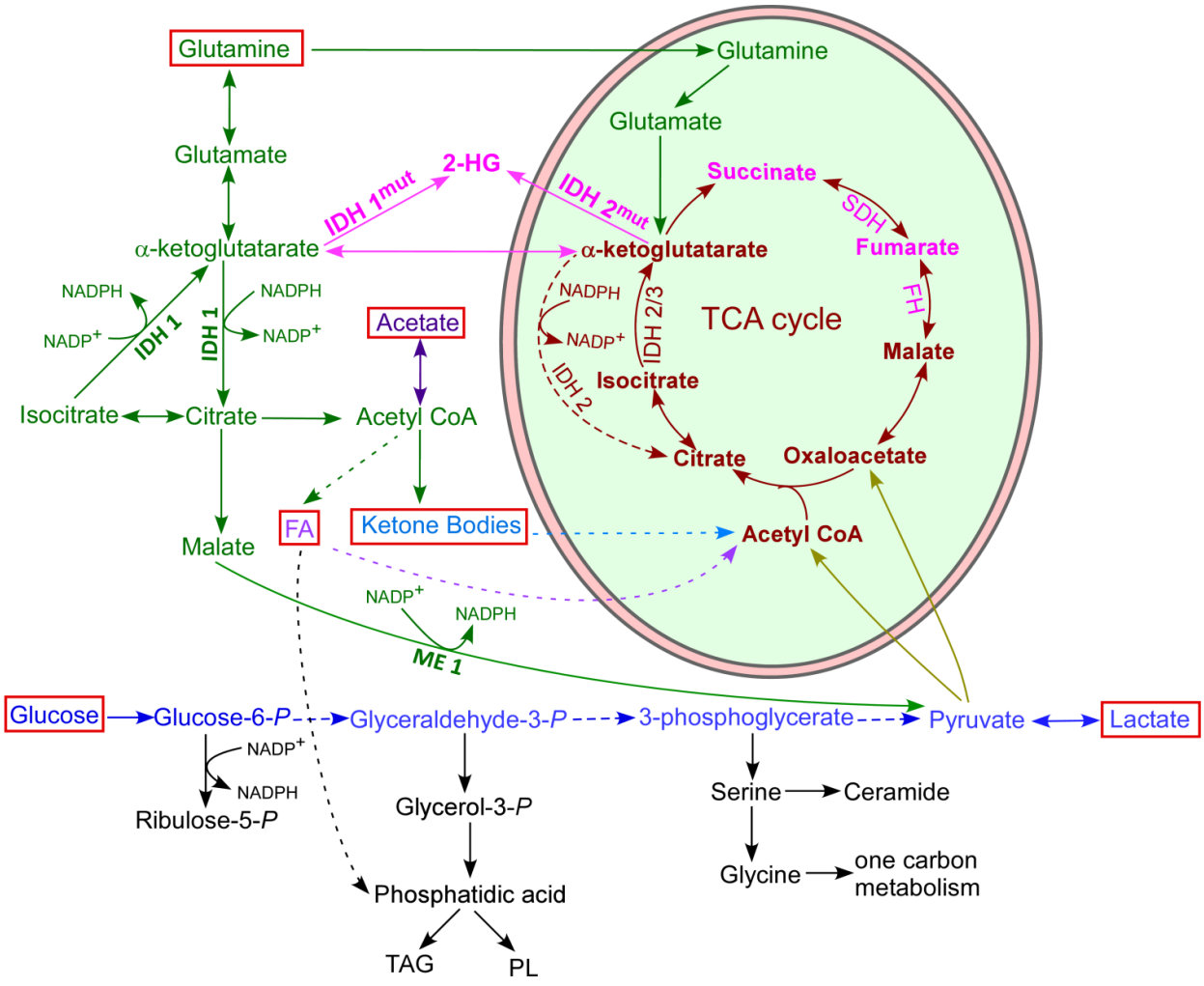

Figure 1.2. Metabolic fuels for tumor cells. Tumor cells are able to use a variety of bioenergetic substrates, including glutamine, glucose, fatty acids (FA), ketone bodies, and acetate (highlighted by *red boxes*). These substrates can be provided by stromal cells in the microenvironment. Much of the cellular energy for tumor cells is likely generated by TCA cycle coupled to oxidative phosphorylation. The pathways for the generation and metabolism of these substrates are outlined. Notably, glutamine and glucose can also provide building blocks for the synthesis of many biomolecules. Also indicated in pink are the metabolic enzymes whose mutations are found in various tumors and the accumulated oncometabolites in these tumors.

Furthermore, a study by Sotgia et al. suggested that glycolytic stromal cells produce mitochondrial fuels, L-lactate and ketone bodies, which are transferred to oxidative epithelial cancer cells, driving OXPHOS and mitochondrial metabolism [52]. This is strongly supported by their finding that metastatic breast cancer cells amplify OXPHOS and that adjacent stromal cells are glycolytic and lack detectable mitochondria. In essence, these observations and the two-compartment model are still consistent with Warburg's original observation that tumors show a metabolic shift towards aerobic glycolysis.

The metabolic enzymes found to be mutated in tumors include isocitrate dehydrogenase, succinate dehydrogenase, and fumarate hydratase

With the increased interest in tumor metabolism in recent years, mutations in metabolic enzymes have been intensely studied. To date, the metabolic mutations associated with cancer are found mainly in isocitrate dehydrogenase (IDH), succinate dehydrogenase (SDH), and fumarate hydratase (FH). IDH catalyzes the oxidative decarboxylation of isocitrate to produce α-ketoglutarate (α–KG). In humans, there are three different IDH isoforms: IDH1, IDH2 and IDH3 (Figure 1.2). IDH1 is located in the cytosol and peroxisomes, while IDH2 and IDH3 are located in mitochondria. IDH1 and IDH2 use $NADP^+$ as a cofactor, while IDH3 uses NAD^+ as a cofactor in the TCA cycle for energy metabolism [53, 54]. All three enzymes convert isocitrate to α–KG.

In 2008, the R132H IDH1 mutation was first found in human glioblastoma multiforme [55]. Subsequently, mutations of the R132 residues were found in leukemic cells of myeloid leukemia (AML) patients [56]. These findings were quickly confirmed by multiple studies involving direct sequencing of IDH1 and its homologue IDH2. Mutations in IDH1 and IDH2

were found in 75% of grade 2 to 3 gliomas and secondary glioblastoma, and in about 20% of AML [57-69]. Additionally, IDH1 and IDH2 mutations were found in several other human tumors, including cartilaginous tumors (75%), intrahepatic cholangiocarcinoma (10%), and thyroid carcinomas (16%) [70-77]. The most common cancer mutations map to single arginine residues in the catalytic pockets: IDH1 (R132) and IDH2 (R172 or R140) [55, 56, 61]. Mutant IDH1/2 forms a dimer with the wild-type protein from the normal allele and displays a neomorphic activity that allows the heterodimeric enzyme to catalyze the reduction of α-KG directly to D-2-hydroxyglutarate (D-2-HG, also known as R-2-HG) in the presence of NADPH [65, 69, 78, 79]. In human glioma with IDH1/2 mutation, the level of D-2-HG accumulates as high as 5–35 mmol L^{-1} [63, 79, 80].

SDH is a highly conserved protein complex with four subunits: SDHA, SDHB, SDHC, and SDHD. SDHA and SDHB are catalytic subunits, and SDHC and SDHD are ubiquinone-binding and membrane-anchorage subunits. SDH functions in the TCA cycle, and as complex II of the electron transport chain (ETC), catalyzes the oxidation of succinate to fumarate in a reaction that generates FADH2, and donates electrons to the ETC. Mutations in genes encoding SDH subunits and the SDH assembly factor 2 are found in hereditary paraganglioma and pheochromocytoma, as well as in gastrointestinal stromal tumors, renal tumors, thyroid tumors, testicular seminomas, and neuroblastomas [81]. Over 650 reported cases of *SDH* mutations have been reported, and these mutations significantly reduce SDH activity. In three cases of paragangliomatosis with *SDH* mutation, succinate accumulated to a high level of 364–517 μmol g^{-1} protein [82]. Also, Xiao et al. showed that depleting *SDH* in mice or ectopic expression of tumor-derived SDH mutants resulted in the accumulation of succinate [83].

FH exists as a homotetrameric enzyme that catalyzes the stereospecific and reversible hydration of fumarate to malate. Mutations in the *FH* gene were first identified in inherited uterine fibroids, skin leiomyoma, and papillary renal cell cancer by a combination of mapping methods [84]. *FH* mutations were also found in cerebral cavernomas, Leydig cell tumors, and ovarian mucinous cystadenoma with low frequency [85-87]. Over 300 cases of FH mutations have been reported. Like SDH mutations, FH mutations significantly reduce FH activity, resulting in the accumulation of fumarate to a level as high as 417–688 μmol/g protein in hereditary leiomyomatosis and renal cell cancer [82]. The accumulation of fumarate was also observed in cells depleted for *FH* or expressing a tumor-derived FH mutant [83].

The accumulation of D-2-HG, succinate, and fumarate all lead to impaired activity of a class of enzymes called α-KG-dependent dioxygenases. These oxygenases include prolyl hydroxylase (PHD), which causes HIF1α degradation [88]. Hence, the accumulation of D-2-HG, succinate, and fumarate causes HIF1α accumulation. Other α-KG-dependent dioxygenases include the JMJD family KDMs and the TET family of 5mC hydroxylases, which impact epigenetic events [89]. Ultimately, by impacting cellular processes such as hypoxia response and epigenetic modifications, D-2-HG, succinate, and fumarate promote tumorigenesis. Such metabolites whose abnormal accumulation causes both metabolic and nonmetabolic dysregulation and promotes tumorigenesis are often called oncometabolites. However, there is only limited evidence linking these oncometabolites to metastatic progression. For example, treatment with dimethylfumarate, a cell-permeable form of fumarate, strongly reduces invasion and metastasis formation in melanoma [90-92] , although overexpression of FH in a FH-deficient renal cell carcinoma line inhibits cellular migration and invasion [93].

Mitochondrial OXPHOS is essential for ATP generation in most tumor types

As discussed above, mutations in IDH, SDH, and FH may interfere with mitochondrial function and respiration in certain rare tumor types. However, a plethora of studies have shown that mitochondrial function and respiration are critical for many common types of tumors. Over the years, various studies have identified several modes of mitochondrial function in tumorigenesis. For example, mitochondria and cancer are linked through the generation of reactive oxygen species (ROS). Notably, mitochondria generate much of the endogenous cellular ROS through mitochondrial OXPHOS. Under normal physiological conditions, ROS production is highly regulated, at least in part, by complex I [94-98]. When the electron transport chain (ETC) is inhibited by an OXPHOS gene mutation, the ETC electron carriers accumulate excessive electrons, which can be passed directly to O_2 to generate superoxide anion ($O_2^{\cdot -}$). The $O_2^{\cdot -}$ generated by complex I is released into the mitochondrial matrix and is converted to H_2O_2 by the mitochondrial manganese superoxide dismutase (MnSOD). The $O_2^{\cdot -}$ generated from complex III is released into the mitochondrial intermembrane space and is converted to H_2O_2 by copper/zinc superoxide dismutase (Cu/ZnSOD). Mitochondrial H_2O_2 can then diffuse into other cellular compartments. Mitochondrial ROS are important signaling molecules and potent mitogens [99-101]. Increased production of ROS has long been observed to be a hallmark of many tumors and cancer cell lines [102, 103]. The mechanisms by which ROS promote tumorigenesis have been reviewed extensively elsewhere [95, 104, 105]. Additionally, it is well known that ROS can inhibit tumor progression by inducing apoptosis, and many anti-cancer agents act by generating ROS and inducing cancer cell death [106, 107].

Another link of mitochondria to tumorigenesis is OXPHOS. Although it has long been believed that the glycolytic phenotype in cancer is due to defective mitochondrial OXPHOS, as proposed by Otto Warburg [15], this view has been challenged since it was proposed [17]. Many lines of experimental evidence have shown that the function of mitochondrial OXPHOS in most tumors is intact. For example, Guppy and co-workers showed that in the MCF-7 breast cancer cell line, ATP production is 80% oxidative and 20% glycolytic [108]. Rodriguez-Enriquez et al. showed that in AS-30D hepatoma tumor cells, cellular ATP is mainly provided by OXPHOS [109]. Furthermore, Rodriguez-Enriquez et al. showed that in both human HeLa and rodent AS-30D fast-growing tumor cells, mitochondria respiration is the predominant source of ATP in both cell types (66–75%), in spite of an active glycolysis [110]. In glucose-free medium with glutamine, proliferation of both lines is diminished by 30%, but OXPHOS and the cytosolic ATP level are increased by 50%. In glutamine-free medium with glucose, proliferation, OXPHOS, and ATP concentration are diminished drastically. In 2004, Zu and Guppy reviewed a plethora of experimental studies regarding glycolytic and oxidative contribution to ATP production in a wide array of tumor cells [111]. Their analyses of previous data showed that the vast majority of tumor cells generate ATP via oxidative phosphorylation.

Notably, a recent study has linked OXPHOS to oncogene ablation-resistant pancreatic cancer cells [112]. Viale et al. showed that a subpopulation of dormant tumor cells surviving oncogene ablation, responsible for tumor relapse, relies on OXPHOS for survival. Furthermore, recent experimental studies have identified transcription factors that promote mitochondrial biogenesis and OXPHOS in cancer cells. For example, LeBleu and co-workers identified the transcription coactivator peroxisome proliferator-activated receptor gamma, coactivator 1alpha

(PPARGC1A or PGC-1α) as the transcription factor promoting mitochondrial biogenesis and OXPHOS in cancer cells [113]. They showed that migratory/invasive cancer cells favor mitochondrial respiration and increased ATP production. There is a strong correlation between PGC-1α expression in invasive cancer cells and the formation of distant metastases. In another study, Mauro et al. showed that NF-κB plays a role in metabolic adaptation in cancer by upregulating OXPHOS [114].

Mitochondrial transfer provides a mechanism for restoring OXPHOS in tumor cells defective in mitochondrial respiration and for promoting tumor progression

Importantly, a recent study involving mtDNA transfer between normal and tumor cells provided further evidence supporting the importance of OXPHOS in cancer progression [115]. Tan et al. showed that tumor cells without mitochondrial DNA (mtDNA) exhibit delayed tumor growth and that tumor formation is associated with the acquisition of mtDNA from host cells [115]. By following mtDNA acquisition in the 4T1 breast carcinoma model, Tan and colleagues found that stable cell lines derived from primary subcutaneous tumors that grew from 4T1ρ^0 cells showed partial recovery of mitochondrial respiration and an intermediate lag to tumor growth. Cell lines from circulating tumor cells and from lung metastases showed further and staged recovery of mitochondrial respiration, and tumor growth more similar to that of parental 4T1 cells. They demonstrated that restored mitochondrial respiration is critical for the tumorigenic potential of cancer cells without mtDNA [115]. Interestingly, the role of mitochondrial transfer has been observed in canine transmissible venereal tumor (CTVT), which is a highly adapted cancer and is transmitted as an allograft during coition [116]. Rebbeck et al. analyzed mtDNA in 37

transmissible venereal tumors in dogs and comparable mtDNA regions from 15 host animals and 43 published canine mtDNA sequences [117]. Their analyses suggested that these tumors have periodically acquired mitochondria from their hosts, perhaps over a period of 11,000 years when this tumor type originated [116, 117]. It was estimated that the transfer of mitochondria into malignant cells with heavily mutated mtDNA occurs once in about 100 years [117]. Clearly, ample experimental evidence exists to demonstrate the importance of mitochondrial respiration in the progression of many cancers.

Heme is an essential factor for the proper functioning of OXPHOS complexes and directly regulates many molecular and cellular processes

Mitochondrial respiration is carried out by the OXPHOS complexes I-V (Figure 1.3) [118]. Complex I, the NADH-coenzyme Q reductase or NADH dehydrogenase, is constituted of 45 polypeptides, of which seven (ND1, -2, -3, -4, -4L, -5, and -6) are encoded by the mtDNA, and the rest are encoded by nuclear DNA [119, 120]. Complex II, succinate-coenzyme Q reductase or succinate dehydrogenase, contains four nDNA-encoded protein subunits. Complex III, cytochrome bc1 complex or ubiquinol-cytochrome c oxidoreductase, contains 11 subunits, of which one (cytochrome *b*) is encoded by the mtDNA. Complex IV, cytochrome c reductase, is composed of 13 subunits, of which three (COI, -II, and -III) are from the mtDNA. Complex V, ATP synthase, contains approximately 16 subunits, of which two (ATP6 and -8) are from the mtDNA. Complexes I, III, IV, and V retain mtDNA-encoded protein subunits and transport protons (Figure 1.3). Importantly, three complexes, II, III, and IV, require heme for proper

functioning. Particularly, multiple subunits in complexes III and IV require heme as a prosthetic group, and different forms of heme are present (Figure 1.3) [121].

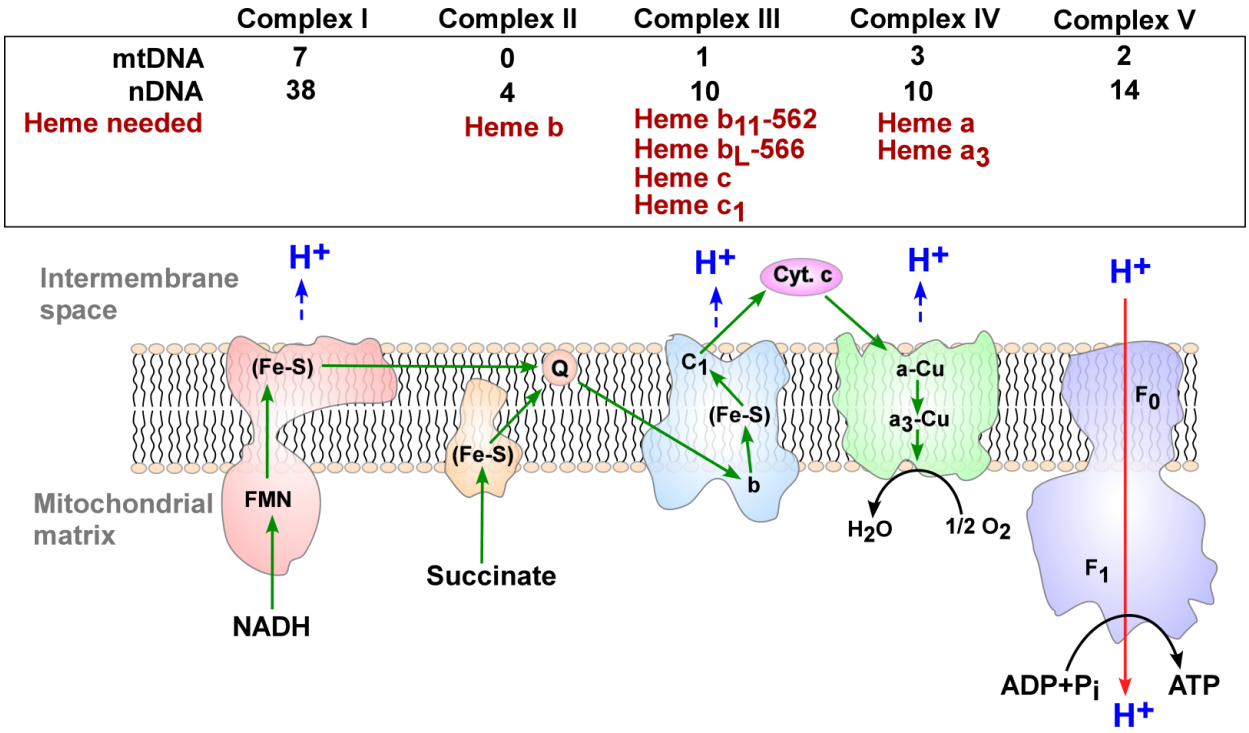

Figure 1.3. The function and composition of mitochondrial OXPHOS complexes I-V. Shown here are the directions of electron and proton transport by the OXPHOS complexes. Also indicated are the origins of DNA encoding the subunits and the hemes needed for complexes II-IV. *nDNA* nuclear DNA, *mtDNA* mitochondrial DNA.

The function of heme as a prosthetic group in proteins and enzymes involved in the transport, storage, and utilization of oxygen is well-known [122]. Furthermore, heme directly regulates the expression of proteins and enzymes involved in using oxygen [123]. In humans, heme plays essential roles in many physiological processes, including erythropoiesis, neurogenesis, cell

growth and differentiation [123-125]. Heme constitutes 95% of functional iron in the human body, as well as two-thirds of the average person's iron intake in developed countries. In the human body, erythroid and hepatic cells use the most heme. Most, if not all, human cells need a basal level of heme for survival. Mammalian cells can synthesize heme endogenously in the mitochondria, or they can import heme from the circulation via heme transporters (Figure 1.4) [126]and references therein]. In mammalian cells, intracellular heme is used to synthesize various hemoproteins, such as cytochromes, or it can be degraded by heme oxygenase (Figure 1.4) [127].

It is also worth noting that heme can serve as a regulatory and signaling molecule and directly regulate transcription, translation, and cell growth and differentiation [125]. For example, in erythroid precursor cells, heme regulates the transcription of globin chains and heme oxygenase genes by modulating the activity of transcriptional regulators, such as NF-E2 and Bach1 [128-131]. Additionally, heme regulates the translation of globin chains by directly controlling the activity of the heme-regulated eIF-2α kinase (HRI) [132, 133] . These mechanisms ensure the coordination of globin chain synthesis with heme synthesis. In neuronal cells, heme can modulate the activity of the NMDA receptor and the Ras-ERK1/2 signaling pathway [134-137]. Furthermore, heme directly regulates the activity of the nuclear receptors REV-ERBα and REV-ERBβ [138, 139], microRNA processing protein DiGeorge critical region-8 (DGCR8) [140], and ion channels (SloBK potassium channel and epithelial sodium channel ENaCs) [141-143], in an array of mammalian cells (Figure 1.4).

Elevated heme flux and function are critical for the proliferation and function of non-small cell lung cancer cells

Interestingly, it has long been observed that inhibiting heme synthesis in various cancer cell lines suppresses cell proliferation and induces apoptosis [144-146]. However, it is not clear how heme deficiency impacts normal cells. This was clarified recently by a study carried out in the authors' laboratory [147]. In this study, we took advantage of a matched pair of cell lines representing the normal, nonmalignant bronchial epithelial and non-small cell lung cancer (NSCLC) cells developed from the same patient [148, 149]. Using this pair of cell lines and several other NSCLC lines, we examined the differences in bioenergetic activities in normal and cancer cells. We found that the rates of both glucose and oxygen consumption in NSCLC cells are elevated, with the elevation of oxygen consumption greater than glucose consumption [147]. Next, we showed that the rate of heme synthesis is increased significantly in the NSCLC cells, compared to the normal lung cells. Additionally, we showed that the expression level of the rate-limiting heme synthetic enzyme, ALAS1, is highly elevated in NSCLC cells and tumors. Further, the levels of two heme transporters HCP1 and HRG1 [150, 151] are dramatically increased in NSCLC cells and tumors, compared to the normal cells [147]. The increased availability of heme is expected to intensify the production of oxygen-utilizing hemoproteins. Indeed, we found that the levels of cytoglobin, cytochrome c, cytochrome P450 CYP1B1, and Cox-2 are significantly increased in NSCLC cells and tumors [147]. Our results revealed that both heme biosynthesis and uptake are intensified to enhance heme availability for the production of oxygen-utilizing hemoproteins in cancer cells and xenograft tumors [147]. Increased levels of heme and oxygen-utilizing hemoproteins presumably contribute to intensified oxygen consumption in cancer cells.

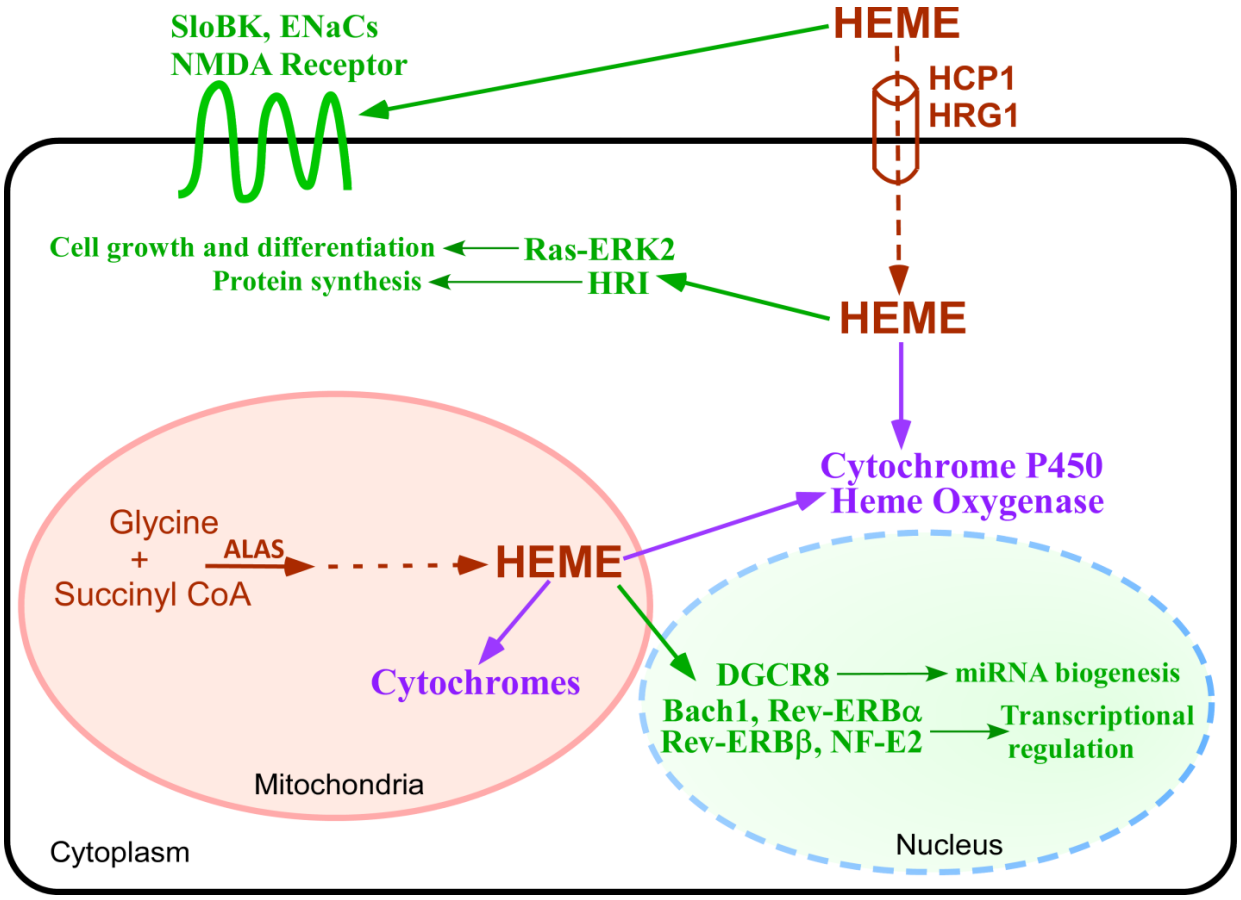

Figure 1.4. The signaling and structural functions of heme in human cells. Human cells can synthesize heme de novo in mitochondria (the first and rate-limiting enzyme is ALAS, 5-aminolevulinate synthase) or import heme via heme transporters, such as HRG1 and HCP1. Inside cells, heme serves as a prosthetic group in numerous enzymes and proteins that transport, store, or use oxygen, such as mitochondrial cytochromes and cytochrome P450. Additionally, heme directly regulates the activity of diverse cellular signaling and regulatory molecules, such as Bach1, Rev-ERBα, and Rev-ERBβ (transcriptional regulators), as well as DGCR8 (an essential miRNA processing factor) in the nucleus. Heme also regulates HRI (the heme-regulated inhibitor kinase controlling protein synthesis) and the Ras-ERK signaling pathway in the cytoplasm. Furthermore, heme regulates the activity of the NMDA receptor, the SloBK potassium channel, and the ENaCs sodium channel on the cell membrane.

Conversely, depleting heme in cancer cells is expected to cause a lack of hemoproteins, leading to reduced oxygen consumption and cellular energy generation. Indeed, we found that oxygen consumption in the NSCLC cells is selectively reduced when cells are cultured in heme-depleted medium [147].

In contrast, heme depletion in the medium does not affect oxygen consumption in normal cells. Further, we showed that lowering heme levels strongly suppresses NSCLC cell proliferation, colony formation, and migration [147]. Together, our results showed that heme availability is significantly increased in cancer cells and tumors, which leads to elevated production of hemoproteins, resulting in intensified oxygen consumption and cellular energy production for fueling cancer cell progression [147].

The selective importance of heme in tumor cell proliferation and function is also consistent with the previous observation that NSCLC cells require serum (containing heme) for maintenance and proliferation, whereas the normal lung cells survive and proliferate better with growth factors in the absence of serum [148, 149]. Further, the preferential requirement of NSCLC cells for heme is in complete agreement with the critical roles of heme in mitochondrial respiratory chain complexes. As shown in Figure 1.3, OXPHOS complexes II, III, and IV all require heme for proper functioning. By logical reasoning, tumor cells that depend mainly on OXPHOS for ATP generation should require elevated levels of heme and hemoproteins for proliferation and function.

Clonal evolution and genetic heterogeneity likely contribute to the remarkable versatility of tumor cells in the use of bioenergetic substrates

In recent years, whole-genome and whole-exome sequencing studies have provided an ever-expanding survey of somatic aberrations in cancers [152-156]. Such large-scale sequencing studies have revealed a high degree of genetic heterogeneity among patients with the same type of cancer, namely inter-tumor heterogeneity, and that within a single tumor or sample, namely intra-tumor heterogeneity [157-165]. For example, Gerlinger et al. found that over half the mutations in primary tumor and its various metastases of the same advanced renal cell carcinoma are different [166]. Likewise, several groups have demonstrated the vast heterogeneous mutational landscape of pancreatic cancer by analyzing data from whole-genome and whole-exome sequencing [167-169] . Additionally, Ellsworth et al. found genomic heterogeneity within primary breast carcinomas and among regional LN metastases [170]. They concluded that metastasis is a complex process influenced by primary tumor heterogeneity and variability in the timing of dissemination. Furthermore, Leiserson et al. performed a pan-cancer analysis of mutated networks in 3,281 samples from 12 cancer types from the Cancer Genome Atlas (TCGA) [171]. They identified 16 significantly mutated subnetworks that comprise well-known cancer signaling pathways as well as subnetworks with less characterized roles in cancer, including cohesin, condensin, and others. In a comprehensive review, Vogelstein et al. summarized the genes altered in a high percentage of tumors and a much larger number of genes altered infrequently [163]. They reported ~140 driver genes whose intragenic mutations can promote or drive tumorigenesis. These driver genes can be classified into 12 signaling pathways that regulate three core cellular processes: cell fate, cell survival, and genome maintenance.

Data from these large-scale cancer genome sequencing studies also support clonal evolution as the mechanism responsible for generating intra-tumor heterogeneity (ITH). Clonal evolution was initially proposed by Nowell [172]. It refers to the process in which cancer cells accumulate genetic and epigenetic changes over time, giving rise to new subclones. It suggests that cancer evolves by a process of clonal expansion, diversification, and selection within the tissue ecosystems. Clonal evolution can be linear evolution or branched evolution [159, 160]. Evidence of clonal evolution is found in many tumors. For example, evaluation of genomic heterogeneity within primary breast carcinomas and among axillary LN metastases indicated that multiple clonal cell lineages exist in every primary tumor and between many metastatic deposits from the same patient [170]. Two recent studies revealed substantial intra-tumoral heterogeneity within lung adenocarcinomas [173, 174]. Cancer evolution and tumor heterogeneity likely contribute to tumor recurrence and the emergence of drug-resistant disease [175-177]. Under therapeutic pressure, those tumor clones that are most adaptive or resistant to treatment will be selected. These clones will then dominate and populate the tumor rendering it highly resistant to the given therapy. Further, some of these resistance pathways lead to multidrug resistance, generating an even more difficult clinical problem to overcome. Likewise, high mutational heterogeneity and subclonal mutation fraction can lead to increased likelihood of tumor recurrence.

Very likely, changes in tumor cell bioenergetic characteristics accompany tumor progression, recurrence, and drug resistance. Tumor cells are remarkably versatile in their ability to adapt to and take advantage of the environment to support their proliferation and function. Firstly, tumor cells use a variety of fuels, including glucose, glutamine, fatty acids, ketone bodies, and acetate [37-43]. Secondly, tumor cells from the same type of tumors can exhibit great

variations in metabolic and bioenergetic phenotypes. Notably, different NSCLC cell lines exhibit a wide range of dependence on glutamine [30]. These cell lines also show a varying degree of increased oxygen consumption rates, as well as heme synthesis and uptake rates. Evidently, tumor cells adapt to the environment and adopt specific bioenergetic features in order to take advantage of whatever fuels are available. For example, tumor cells in an environment rich in adipocytes would likely adapt to preferentially use fatty acids, while tumor cells in an environment rich in myocytes may adapt to preferentially use glutamine. Clonal evolution enables different tumor cells to adopt metabolic and bioenergetic phenotypes fit to their environment. Such variations in tumor bioenergetic characteristics are likely underpinned by genetic heterogeneity. That is, the aforementioned diverse mutations in signaling pathways and networks would ultimately impact the expression and activity of metabolic enzymes, thereby enabling tumor cells to adopt specific bioenergetic features fit for their unique environment.

CONCLUSIONS

Recent advances in cancer research have clarified many issues relating to tumor bioenergetics. Some important points include the following: (1) High glycolytic rates in tumors and mitochondrial respiration often operate simultaneously in tumors. Increased glycolysis most likely contributes building blocks for biosynthesis. (2) Glutamine is the preferred oxidative fuel for tumor cells. (3) Tumor cells can use a range of fuels including glucose, glutamine, fatty acids, and acetate. (4) Mutations in metabolic enzymes are found mainly in three enzymes involved in the TCA cycle. (5) Mitochondrial respiration can be restored by mitochondrial transfer in tumor cells defective in OXPHOS, and it is critical for the initiation and metastasis of diverse tumors.

(6) Elevated heme flux and function lead to intensified oxygen consumption in NSCLC cells, fueling cancer cell proliferation, migration, and colony formation. (7) Lowered heme availability selectively diminishes the proliferation and function of NSCLC cells. (8) Clonal evolution contributes to a high degree of genetic heterogeneity in tumors, which likely underpin metabolic and bioenergetic versatility of tumor cells, as well as tumor recurrence and drug resistance. Evidently, clonal evolution likely enables NSCLC cells to enhance heme synthesis and uptake, in order to increase their cellular energy generation. Heme coordinates the production and function of OXPHOS complexes. Hence, increasing heme availability provides an effective way to upregulate OXPHOS complexes and mitochondrial respiration for energy generation. It is likely that this mechanism involving elevated heme flux and function operates in other types of tumors besides NSCLC tumors to promote tumor development and progression.

Recent research has also provided ample evidence showing that many types of tumors indeed consume larger amounts of glucose, compared to normal tissues, as Warburg originally observed [15]. However, his hypothesis that tumor mitochondria have impaired respiration is largely incorrect for most types of tumors, as discussed extensively in this review. The observed large increases in glucose consumption in tumor tissues can be attributed to increased demand for building blocks in tumor cells and to increased glucose consumption in stromal cells, which in turn provide oxidative fuels, such as lactate, to tumor cells. Nonetheless, Warburg's original observation has motivated generations of scientists to better understand tumor bioenergetics, and this will undoubtedly lead to a more holistic approach in cancer research and therapeutics.

ABBREVIATIONS

ALAS1: 5'-Aminolevulinate synthase 1

ETC: Electron transport chain

HCP1: Heme carrier protein 1

HIF1α: Hypoxia-inducible factor 1α

HRG1: Heme-responsive gene 1

HRI: Heme-regulated eIF-2α kinase

IDH: Isocitrate dehydrogenase

NMDA: N-Methyl-D-aspartate

NSCLC: Non-small cell lung cancer

OXPHOS: Oxidative phosphorylation

ROS: Reactive oxygen species

SDH: Succinate dehydrogenase

REFERENCES

[1] Pasteur L. Mémoire sur la Fermentation Alcoolique. Paris: Imprimerie de Mallet-Bachelier; 1860.

[2] Buchner E. Uber ein phosphat ubertragendes Garungsferment. Biochimica et Biophysica Acta. 1947:292-314.

[3] Szent-Gyorgyi A. Zellatmung IV. Mitteilung: Uber den Oxydationsmechanismus der Kartoffeln. Aus dem physiologicshen Laboratorium der Reichsuniveritat zu Groningen. 1925.

[4] Szent-Gyorgyi A. Zellatmung V. Mitteilung: Uber den Oxydationsmechanismus einiger Pflanzen. 1927.

[5] Szent-Gyorgyi A. Uber den Mechanismus der Hauptatmung des Taubenbrustmuskels. 1934.

[6] Szent-Gyorgyi A. Uber die Bedeutung der Fumarsaure fur die Tierische Gewebsatmung: Einleitung, Ubersicht,Methoden. 1935.

[7] Szent-Gyorgyi A. Uber die Bedeutung der Fumarsaure fur die Tierische Gewebsatmung. III. Mitteilung: Einleitung,Ubersicht, Methoden. 1936.

[8] Lipmann F. On chemistry and function of coenzyme A. Bacteriol Rev. 1953;17:1-16.

[9] Krebs HA. The citric acid cycle and the Szent-Gyorgyi cycle in pigeon breast muscle. Biochem J. 1940;34:775-9.

[10] Dickens F. Annual Reports on the Progress of Chemistry. RSC Journal Archives. 1944;41.

[11] Boyer PD, Ariki M. 18O-probes of phosphoenzyme formation and cooperativity with sarcoplasmic reticulum ATPase. Fed Proc. 1980;39:2410-4.

[12] Boyer PD, Cross RL, Momsen W. A new concept for energy coupling in oxidative phosphorylation based on a molecular explanation of the oxygen exchange reactions. Proc Natl Acad Sci U S A. 1973;70:2837-9.

[13] Koppenol WH, Bounds PL, Dang CV. Otto Warburg's contributions to current concepts of cancer metabolism. Nat Rev Cancer. 2011;11:325-37.

[14] Warburg O, Wind F, Negelein E. The Metabolism of Tumors in the Body. J Gen Physiol. 1927;8:519-30.

[15] Warburg O. On the origin of cancer cells. Science. 1956;123:309-14.

[16] Wenner CE, Weinhouse S. Metabolism of neoplastic tissue. III. Diphosphopyridine nucleotide requirements for oxidations by mitochondria of neoplastic and non-neoplastic tissues. Cancer research. 1953;13:21-6.

[17] Weinhouse S. On respiratory impairment in cancer cells. Science. 1956;124:267-9.

[18] Reitzer LJ, Wice BM, Kennell D. Evidence that glutamine, not sugar, is the major energy source for cultured HeLa cells. J Biol Chem. 1979;254:2669-76.

[19] Anastasiou D, Cantley LC. Breathless cancer cells get fat on glutamine. Cell Res. 2012;22:443-6.

[20] DeBerardinis RJ, Cheng T. Q's next: the diverse functions of glutamine in metabolism, cell biology and cancer. Oncogene. 2010;29:313-24.

[21] Ward PS, Thompson CB. Metabolic reprogramming: a cancer hallmark even warburg did not anticipate. Cancer Cell. 2012;21:297-308.

[22] Hensley CT, Wasti AT, DeBerardinis RJ. Glutamine and cancer: cell biology, physiology, and clinical opportunities. J Clin Invest. 2013;123:3678-84.

[23] Kovacevic Z, Morris HP. The role of glutamine in the oxidative metabolism of malignant cells. Cancer research. 1972;32:326-33.

[24] Lanks KW, Hitti IF, Chin NW. Substrate utilization for lactate and energy production by heat-shocked L929 cells. J Cell Physiol. 1986;127:451-6.

[25] Goossens V, Grooten J, Fiers W. The oxidative metabolism of glutamine. A modulator of reactive oxygen intermediate-mediated cytotoxicity of tumor necrosis factor in L929 fibrosarcoma cells. J Biol Chem. 1996;271:192-6.

[26] Fan J, Kamphorst JJ, Mathew R, Chung MK, White E, Shlomi T, et al. Glutamine-driven oxidative phosphorylation is a major ATP source in transformed mammalian cells in both normoxia and hypoxia. Mol Syst Biol. 2013;9:712.

[27] Hooda J, Alam MM, Zhang L. Evaluating the Association of Heme and Heme Metabolites with Lung Cancer Bioenergetics and Progression. Metabolomics : open access. 2015;5:1000150.

[28] Vander Heiden MG, Cantley LC, Thompson CB. Understanding the Warburg effect: the metabolic requirements of cell proliferation. Science. 2009;324:1029-33.

[29] Griguer CE, Oliva CR, Gillespie GY. Glucose metabolism heterogeneity in human and mouse malignant glioma cell lines. J Neurooncol. 2005;74:123-33.

[30] van den Heuvel AP, Jing J, Wooster RF, Bachman KE. Analysis of glutamine dependency in non-small cell lung cancer: GLS1 splice variant GAC is essential for cancer cell growth. Cancer Biol Ther. 2012;13:1185-94.

[31] Bergstrom J, Furst P, Noree LO, Vinnars E. Intracellular free amino acid concentration in human muscle tissue. J Appl Physiol. 1974;36:693-7.

[32] Wise DR, Ward PS, Shay JE, Cross JR, Gruber JJ, Sachdeva UM, et al. Hypoxia promotes isocitrate dehydrogenase-dependent carboxylation of alpha-ketoglutarate to citrate to support cell growth and viability. Proc Natl Acad Sci U S A. 2011;108:19611-6.

[33] Metallo CM, Gameiro PA, Bell EL, Mattaini KR, Yang J, Hiller K, et al. Reductive glutamine metabolism by IDH1 mediates lipogenesis under hypoxia. Nature. 2012;481:380-4.

[34] Mullen AR, Wheaton WW, Jin ES, Chen PH, Sullivan LB, Cheng T, et al. Reductive carboxylation supports growth in tumour cells with defective mitochondria. Nature. 2012;481:385-8.

[35] Son J, Lyssiotis CA, Ying H, Wang X, Hua S, Ligorio M, et al. Glutamine supports pancreatic cancer growth through a KRAS-regulated metabolic pathway. Nature. 2013;496:101-5.

[36] Schulze A, Harris AL. How cancer metabolism is tuned for proliferation and vulnerable to disruption. Nature. 2012;491:364-73.

[37] Zaidi N, Lupien L, Kuemmerle NB, Kinlaw WB, Swinnen JV, Smans K. Lipogenesis and lipolysis: the pathways exploited by the cancer cells to acquire fatty acids. Prog Lipid Res. 2013;52:585-9.

[38] Menendez JA, Lupu R. Fatty acid synthase and the lipogenic phenotype in cancer pathogenesis. Nat Rev Cancer. 2007;7:763-77.

[39] Price DT, Coleman RE, Liao RP, Robertson CN, Polascik TJ, DeGrado TR. Comparison of [18 F]fluorocholine and [18 F]fluorodeoxyglucose for positron emission tomography of androgen dependent and androgen independent prostate cancer. J Urol. 2002;168:273-80.

[40] Liu Y, Zuckier LS, Ghesani NV. Dominant uptake of fatty acid over glucose by prostate cells: a potential new diagnostic and therapeutic approach. Anticancer Res. 2010;30:369-74.

[41] Zha S, Ferdinandusse S, Hicks JL, Denis S, Dunn TA, Wanders RJ, et al. Peroxisomal branched chain fatty acid beta-oxidation pathway is upregulated in prostate cancer. Prostate. 2005;63:316-23.

[42] Comerford SA, Huang Z, Du X, Wang Y, Cai L, Witkiewicz AK, et al. Acetate dependence of tumors. Cell. 2014;159:1591-602.

[43] Mashimo T, Pichumani K, Vemireddy V, Hatanpaa KJ, Singh DK, Sirasanagandla S, et al. Acetate is a bioenergetic substrate for human glioblastoma and brain metastases. Cell. 2014;159:1603-14.

[44] Berridge MV, Herst PM, Tan AS. Metabolic flexibility and cell hierarchy in metastatic cancer. Mitochondrion. 2010;10:584-8.

[45] Bonuccelli G, Tsirigos A, Whitaker-Menezes D, Pavlides S, Pestell RG, Chiavarina B, et al. Ketones and lactate "fuel" tumor growth and metastasis: Evidence that epithelial cancer cells use oxidative mitochondrial metabolism. Cell Cycle. 2010;9:3506-14.

[46] Pavlides S, Whitaker-Menezes D, Castello-Cros R, Flomenberg N, Witkiewicz AK, Frank PG, et al. The reverse Warburg effect: aerobic glycolysis in cancer associated fibroblasts and the tumor stroma. Cell Cycle. 2009;8:3984-4001.

[47] Icard P, Kafara P, Steyaert JM, Schwartz L, Lincet H. The metabolic cooperation between cells in solid cancer tumors. Biochim Biophys Acta. 2014;1846:216-25.

[48] Lisanti MP, Martinez-Outschoorn UE, Sotgia F. Oncogenes induce the cancer-associated fibroblast phenotype: metabolic symbiosis and "fibroblast addiction" are new therapeutic targets for drug discovery. Cell Cycle. 2013;12:2723-32.

[49] Martinez-Outschoorn UE, Lisanti MP, Sotgia F. Catabolic cancer-associated fibroblasts transfer energy and biomass to anabolic cancer cells, fueling tumor growth. Semin Cancer Biol. 2014;25:47-60.

[50] Ko YH, Lin Z, Flomenberg N, Pestell RG, Howell A, Sotgia F, et al. Glutamine fuels a vicious cycle of autophagy in the tumor stroma and oxidative mitochondrial metabolism in epithelial cancer cells: implications for preventing chemotherapy resistance. Cancer Biol Ther. 2011;12:1085-97.

[51] Nieman KM, Kenny HA, Penicka CV, Ladanyi A, Buell-Gutbrod R, Zillhardt MR, et al. Adipocytes promote ovarian cancer metastasis and provide energy for rapid tumor growth. Nat Med. 2011;17:1498-503.

[52] Sotgia F, Whitaker-Menezes D, Martinez-Outschoorn UE, Flomenberg N, Birbe RC, Witkiewicz AK, et al. Mitochondrial metabolism in cancer metastasis: visualizing tumor cell mitochondria and the "reverse Warburg effect" in positive lymph node tissue. Cell Cycle. 2012;11:1445-54.

[53] Frezza C, Pollard PJ, Gottlieb E. Inborn and acquired metabolic defects in cancer. J Mol Med (Berl). 2011;89:213-20.

[54] Yang H, Ye D, Guan KL, Xiong Y. IDH1 and IDH2 mutations in tumorigenesis: mechanistic insights and clinical perspectives. Clin Cancer Res. 2012;18:5562-71.

[55] Parsons DW, Jones S, Zhang X, Lin JC, Leary RJ, Angenendt P, et al. An integrated genomic analysis of human glioblastoma multiforme. Science. 2008;321:1807-12.

[56] Mardis ER, Ding L, Dooling DJ, Larson DE, McLellan MD, Chen K, et al. Recurring mutations found by sequencing an acute myeloid leukemia genome. N Engl J Med. 2009;361:1058-66.

[57] Balss J, Meyer J, Mueller W, Korshunov A, Hartmann C, von Deimling A. Analysis of the IDH1 codon 132 mutation in brain tumors. Acta Neuropathol. 2008;116:597-602.

[58] Bleeker FE, Lamba S, Leenstra S, Troost D, Hulsebos T, Vandertop WP, et al. IDH1 mutations at residue p.R132 (IDH1(R132)) occur frequently in high-grade gliomas but not in other solid tumors. Hum Mutat. 2009;30:7-11.

[59] Hartmann C, Meyer J, Balss J, Capper D, Mueller W, Christians A, et al. Type and frequency of IDH1 and IDH2 mutations are related to astrocytic and oligodendroglial differentiation and age: a study of 1,010 diffuse gliomas. Acta Neuropathol. 2009;118:469-74.

[60] Watanabe T, Nobusawa S, Kleihues P, Ohgaki H. IDH1 mutations are early events in the development of astrocytomas and oligodendrogliomas. Am J Pathol. 2009;174:1149-53.

[61] Yan H, Parsons DW, Jin G, McLendon R, Rasheed BA, Yuan W, et al. IDH1 and IDH2 mutations in gliomas. N Engl J Med. 2009;360:765-73.

[62] Chou WC, Hou HA, Chen CY, Tang JL, Yao M, Tsay W, et al. Distinct clinical and biologic characteristics in adult acute myeloid leukemia bearing the isocitrate dehydrogenase 1 mutation. Blood. 2010;115:2749-54.

[63] Dang L, Jin S, Su SM. IDH mutations in glioma and acute myeloid leukemia. Trends Mol Med. 2010;16:387-97.

[64] Gravendeel LA, Kloosterhof NK, Bralten LB, van Marion R, Dubbink HJ, Dinjens W, et al. Segregation of non-p.R132H mutations in IDH1 in distinct molecular subtypes of glioma. Hum Mutat. 2010;31:E1186-99.

[65] Gross S, Cairns RA, Minden MD, Driggers EM, Bittinger MA, Jang HG, et al. Cancer-associated metabolite 2-hydroxyglutarate accumulates in acute myelogenous leukemia with isocitrate dehydrogenase 1 and 2 mutations. J Exp Med. 2010;207:339-44.

[66] Ho PA, Alonzo TA, Kopecky KJ, Miller KL, Kuhn J, Zeng R, et al. Molecular alterations of the IDH1 gene in AML: a Children's Oncology Group and Southwest Oncology Group study. Leukemia. 2010;24:909-13.

[67] Tefferi A, Lasho TL, Abdel-Wahab O, Guglielmelli P, Patel J, Caramazza D, et al. IDH1 and IDH2 mutation studies in 1473 patients with chronic-, fibrotic- or blast-phase essential thrombocythemia, polycythemia vera or myelofibrosis. Leukemia. 2010;24:1302-9.

[68] Wagner K, Damm F, Gohring G, Gorlich K, Heuser M, Schafer I, et al. Impact of IDH1 R132 mutations and an IDH1 single nucleotide polymorphism in cytogenetically normal acute myeloid leukemia: SNP rs11554137 is an adverse prognostic factor. J Clin Oncol. 2010;28:2356-64.

[69] Ward PS, Patel J, Wise DR, Abdel-Wahab O, Bennett BD, Coller HA, et al. The common feature of leukemia-associated IDH1 and IDH2 mutations is a neomorphic enzyme activity converting alpha-ketoglutarate to 2-hydroxyglutarate. Cancer Cell. 2010;17:225-34.

[70] Amary MF, Bacsi K, Maggiani F, Damato S, Halai D, Berisha F, et al. IDH1 and IDH2 mutations are frequent events in central chondrosarcoma and central and periosteal chondromas but not in other mesenchymal tumours. J Pathol. 2011;224:334-43.

[71] Pansuriya TC, van Eijk R, d'Adamo P, van Ruler MA, Kuijjer ML, Oosting J, et al. Somatic mosaic IDH1 and IDH2 mutations are associated with enchondroma and spindle cell hemangioma in Ollier disease and Maffucci syndrome. Nat Genet. 2011;43:1256-61.

[72] Wang P, Dong Q, Zhang C, Kuan PF, Liu Y, Jeck WR, et al. Mutations in isocitrate dehydrogenase 1 and 2 occur frequently in intrahepatic cholangiocarcinomas and share hypermethylation targets with glioblastomas. Oncogene. 2013;32:3091-100.

[73] Hemerly JP, Bastos AU, Cerutti JM. Identification of several novel non-p.R132 IDH1 variants in thyroid carcinomas. Eur J Endocrinol. 2010;163:747-55.

[74] Murugan AK, Bojdani E, Xing M. Identification and functional characterization of isocitrate dehydrogenase 1 (IDH1) mutations in thyroid cancer. Biochem Biophys Res Commun. 2010;393:555-9.

[75] Kang MR, Kim MS, Oh JE, Kim YR, Song SY, Seo SI, et al. Mutational analysis of IDH1 codon 132 in glioblastomas and other common cancers. Int J Cancer. 2009;125:353-5.

[76] Gaal J, Burnichon N, Korpershoek E, Roncelin I, Bertherat J, Plouin PF, et al. Isocitrate dehydrogenase mutations are rare in pheochromocytomas and paragangliomas. J Clin Endocrinol Metab. 2010;95:1274-8.

[77] Borger DR, Tanabe KK, Fan KC, Lopez HU, Fantin VR, Straley KS, et al. Frequent mutation of isocitrate dehydrogenase (IDH)1 and IDH2 in cholangiocarcinoma identified through broad-based tumor genotyping. Oncologist. 2012;17:72-9.

[78] Dang L, White DW, Gross S, Bennett BD, Bittinger MA, Driggers EM, et al. Cancer-associated IDH1 mutations produce 2-hydroxyglutarate. Nature. 2009;462:739-44.

[79] Kalinina J, Carroll A, Wang L, Yu Q, Mancheno DE, Wu S, et al. Detection of "oncometabolite" 2-hydroxyglutarate by magnetic resonance analysis as a biomarker of IDH1/2 mutations in glioma. J Mol Med (Berl). 2012;90:1161-71.

[80] Elkhaled A, Jalbert LE, Phillips JJ, Yoshihara HA, Parvataneni R, Srinivasan R, et al. Magnetic resonance of 2-hydroxyglutarate in IDH1-mutated low-grade gliomas. Sci Transl Med. 2012;4:116ra5.

[81] Bardella C, Pollard PJ, Tomlinson I. SDH mutations in cancer. Biochim Biophys Acta. 2011;1807:1432-43.

[82] Pollard PJ, Briere JJ, Alam NA, Barwell J, Barclay E, Wortham NC, et al. Accumulation of Krebs cycle intermediates and over-expression of HIF1alpha in tumours which result from germline FH and SDH mutations. Hum Mol Genet. 2005;14:2231-9.

[83] Xiao M, Yang H, Xu W, Ma S, Lin H, Zhu H, et al. Inhibition of alpha-KG-dependent histone and DNA demethylases by fumarate and succinate that are accumulated in mutations of FH and SDH tumor suppressors. Genes Dev. 2012;26:1326-38.

[84] Tomlinson IP, Alam NA, Rowan AJ, Barclay E, Jaeger EE, Kelsell D, et al. Germline mutations in FH predispose to dominantly inherited uterine fibroids, skin leiomyomata and papillary renal cell cancer. Nat Genet. 2002;30:406-10.

[85] Campione E, Terrinoni A, Orlandi A, Codispoti A, Melino G, Bianchi L, et al. Cerebral cavernomas in a family with multiple cutaneous and uterine leiomyomas associated with a new mutation in the fumarate hydratase gene. The Journal of investigative dermatology. 2007;127:2271-3.

[86] Carvajal-Carmona LG, Alam NA, Pollard PJ, Jones AM, Barclay E, Wortham N, et al. Adult leydig cell tumors of the testis caused by germline fumarate hydratase mutations. J Clin Endocrinol Metab. 2006;91:3071-5.

[87] Ylisaukko-oja SK, Cybulski C, Lehtonen R, Kiuru M, Matyjasik J, Szymanska A, et al. Germline fumarate hydratase mutations in patients with ovarian mucinous cystadenoma. Eur J Hum Genet. 2006;14:880-3.

[88] Zhao S, Lin Y, Xu W, Jiang W, Zha Z, Wang P, et al. Glioma-derived mutations in IDH1 dominantly inhibit IDH1 catalytic activity and induce HIF-1alpha. Science. 2009;324:261-5.

[89] Yang H, Xiong Y, Guan K. Metabolic alteration in tumorigenesis. Sci China Life Sci. 2013;56:1067-75.

[90] Loewe R, Valero T, Kremling S, Pratscher B, Kunstfeld R, Pehamberger H, et al. Dimethylfumarate impairs melanoma growth and metastasis. Cancer research. 2006;66:11888-96.

[91] Valero T, Steele S, Neumuller K, Bracher A, Niederleithner H, Pehamberger H, et al. Combination of dacarbazine and dimethylfumarate efficiently reduces melanoma lymph node metastasis. The Journal of investigative dermatology. 2010;130:1087-94.

[92] Yamazoe Y, Tsubaki M, Matsuoka H, Satou T, Itoh T, Kusunoki T, et al. Dimethylfumarate inhibits tumor cell invasion and metastasis by suppressing the expression and activities of matrix metalloproteinases in melanoma cells. Cell biology international. 2009;33:1087-94.

[93] Sudarshan S, Shanmugasundaram K, Naylor SL, Lin S, Livi CB, O'Neill CF, et al. Reduced expression of fumarate hydratase in clear cell renal cancer mediates HIF-2alpha accumulation and promotes migration and invasion. PLoS One. 2011;6:e21037.

[94] Kushnareva Y, Murphy AN, Andreyev A. Complex I-mediated reactive oxygen species generation: modulation by cytochrome c and NAD(P)+ oxidation-reduction state. Biochem J. 2002;368:545-53.

[95] Sullivan LB, Chandel NS. Mitochondrial reactive oxygen species and cancer. Cancer Metab. 2014;2:17.

[96] McCord JM. The evolution of free radicals and oxidative stress. Am J Med. 2000;108:652-9.

[97] Hansen JM, Go YM, Jones DP. Nuclear and mitochondrial compartmentation of oxidative stress and redox signaling. Annu Rev Pharmacol Toxicol. 2006;46:215-34.

[98] Genova ML, Pich MM, Biondi A, Bernacchia A, Falasca A, Bovina C, et al. Mitochondrial production of oxygen radical species and the role of Coenzyme Q as an antioxidant. Exp Biol Med (Maywood). 2003;228:506-13.

[99] Lander HM. An essential role for free radicals and derived species in signal transduction. Faseb J. 1997;11:118-24.

[100] Gupta SC, Hevia D, Patchva S, Park B, Koh W, Aggarwal BB. Upsides and downsides of reactive oxygen species for cancer: the roles of reactive oxygen species in tumorigenesis, prevention, and therapy. Antioxid Redox Signal. 2012;16:1295-322.

[101] Burdon RH. Superoxide and hydrogen peroxide in relation to mammalian cell proliferation. Free Radic Biol Med. 1995;18:775-94.

[102] Szatrowski TP, Nathan CF. Production of large amounts of hydrogen peroxide by human tumor cells. Cancer research. 1991;51:794-8.

[103] Ishikawa K, Takenaga K, Akimoto M, Koshikawa N, Yamaguchi A, Imanishi H, et al. ROS-generating mitochondrial DNA mutations can regulate tumor cell metastasis. Science. 2008;320:661-4.

[104] Sabharwal SS, Schumacker PT. Mitochondrial ROS in cancer: initiators, amplifiers or an Achilles' heel? Nat Rev Cancer. 2014;14:709-21.

[105] Singh KK. Mitochondria damage checkpoint, aging, and cancer. Ann N Y Acad Sci. 2006;1067:182-90.

[106] Ozben T. Oxidative stress and apoptosis: impact on cancer therapy. Journal of pharmaceutical sciences. 2007;96:2181-96.

[107] Fang J, Seki T, Maeda H. Therapeutic strategies by modulating oxygen stress in cancer and inflammation. Advanced drug delivery reviews. 2009;61:290-302.

[108] Guppy M, Leedman P, Zu X, Russell V. Contribution by different fuels and metabolic pathways to the total ATP turnover of proliferating MCF-7 breast cancer cells. Biochem J. 2002;364:309-15.

[109] Rodriguez-Enriquez S, Torres-Marquez ME, Moreno-Sanchez R. Substrate oxidation and ATP supply in AS-30D hepatoma cells. Arch Biochem Biophys. 2000;375:21-30.

[110] Rodriguez-Enriquez S, Vital-Gonzalez PA, Flores-Rodriguez FL, Marin-Hernandez A, Ruiz-Azuara L, Moreno-Sanchez R. Control of cellular proliferation by modulation of oxidative phosphorylation in human and rodent fast-growing tumor cells. Toxicol Appl Pharmacol. 2006;215:208-17.

[111] Zu XL, Guppy M. Cancer metabolism: facts, fantasy, and fiction. Biochem Biophys Res Commun. 2004;313:459-65.

[112] Viale A, Pettazzoni P, Lyssiotis CA, Ying H, Sanchez N, Marchesini M, et al. Oncogene ablation-resistant pancreatic cancer cells depend on mitochondrial function. Nature. 2014;514:628-32.

[113] LeBleu VS, O'Connell JT, Gonzalez Herrera KN, Wikman H, Pantel K, Haigis MC, et al. PGC-1alpha mediates mitochondrial biogenesis and oxidative phosphorylation in cancer cells to promote metastasis. Nat Cell Biol. 2014;16:992-1003, 1-15.

[114] Mauro C, Leow SC, Anso E, Rocha S, Thotakura AK, Tornatore L, et al. NF-kappaB controls energy homeostasis and metabolic adaptation by upregulating mitochondrial respiration. Nat Cell Biol. 2011;13:1272-9.

[115] Tan AS, Baty JW, Dong LF, Bezawork-Geleta A, Endaya B, Goodwin J, et al. Mitochondrial genome acquisition restores respiratory function and tumorigenic potential of cancer cells without mitochondrial DNA. Cell Metab. 2015;21:81-94.

[116] Strakova A, Murchison EP. The cancer which survived: insights from the genome of an 11000 year-old cancer. Curr Opin Genet Dev. 2015;30:49-55.

[117] Rebbeck CA, Leroi AM, Burt A. Mitochondrial capture by a transmissible cancer. Science. 2011;331:303.

[118] Wallace DC, Fan W, Procaccio V. Mitochondrial energetics and therapeutics. Annu Rev Pathol. 2010;5:297-348.

[119] Efremov RG, Baradaran R, Sazanov LA. The architecture of respiratory complex I. Nature. 2010;465:441-5.

[120] Efremov RG, Sazanov LA. Structure of the membrane domain of respiratory complex I. Nature. 2011;476:414-20.

[121] Kim HJ, Khalimonchuk O, Smith PM, Winge DR. Structure, function, and assembly of heme centers in mitochondrial respiratory complexes. Biochim Biophys Acta. 2012;1823:1604-16.

[122] Bock KW, De Matteis F, Aldridge WN. Heme and Hemoproteins. New York: Springer-Verlag; 1978.

[123] Padmanaban G, Venkateswar V, Rangarajan PN. Haem as a multifunctional regulator. Trends Biochem Sci. 1989;14:492-6.

[124] Chen JJ, London IM. Regulation of protein synthesis by heme-regulated eIF-2 alpha kinase. Trends Biochem Sci. 1995;20:105-8.

[125] Zhang L. HEME BIOLOGY: The Secret Life of Heme in Regulating Diverse Biological Processes: World Scientific; 2011.

[126] Hooda J, Shah A, Zhang L. Heme, an essential nutrient from dietary proteins, critically impacts diverse physiological and pathological processes. Nutrients. 2014;6:1080-102.

[127] Anderson KE, Sassa S, Bishop DF, Desnick RJ. Disorders of heme biosynthesis: X-linked sideroblastic anemia and the porphyrias. In: Scriver CR, Beaudt AL, Sly WS, Valle D, Barton C, Kinzler KW, et al., editors. The metabolic and molecular bases of inherited disease. New York: The McGraw-Hill Companies, Inc.; 2001. p. 2991-3062.

[128] Sassa S. Novel effects of heme and heme-related compounds in biological systems. Current Med Chem. 1996;3:273-90.

[129] Suzuki H, Tashiro S, Hira S, Sun J, Yamazaki C, Zenke Y, et al. Heme regulates gene expression by triggering Crm1-dependent nuclear export of Bach1. Embo J. 2004;23:2544-53.

[130] Zenke-Kawasaki Y, Dohi Y, Katoh Y, Ikura T, Ikura M, Asahara T, et al. Heme induces ubiquitination and degradation of the transcription factor Bach1. Mol Cell Biol. 2007;27:6962-71.

[131] Hira S, Tomita T, Matsui T, Igarashi K, Ikeda-Saito M. Bach1, a heme-dependent transcription factor, reveals presence of multiple heme binding sites with distinct coordination structure. IUBMB Life. 2007;59:542-51.

[132] Uma S, Matts RL, Guo Y, White S, Chen JJ. The N-terminal region of the heme-regulated eIF2alpha kinase is an autonomous heme binding domain. Eur J Biochem. 2000;267:498-506.

[133] Rafie-Kolpin M, Chefalo PJ, Hussain Z, Hahn J, Uma S, Matts RL, et al. Two heme-binding domains of heme-regulated eukaryotic initiation factor-2alpha kinase. N terminus and kinase insertion. J Biol Chem. 2000;275:5171-8.

[134] Sengupta A, Hon T, Zhang L. Heme deficiency suppresses the expression of key neuronal genes and causes neuronal cell death. Brain Res Mol Brain Res. 2005;137:23-30.

[135] Zhu Y, Hon T, Ye W, Zhang L. Heme deficiency interferes with the Ras-mitogen-activated protein kinase signaling pathway and expression of a subset of neuronal genes. Cell Growth Differ. 2002;13:431-9.

[136] Chernova T, Nicotera P, Smith AG. Heme deficiency is associated with senescence and causes suppression of N-methyl-D-aspartate receptor subunits expression in primary cortical neurons. Mol Pharmacol. 2006;69:697-705.

[137] Chernova T, Steinert JR, Guerin CJ, Nicotera P, Forsythe ID, Smith AG. Neurite degeneration induced by heme deficiency mediated via inhibition of NMDA receptor-dependent extracellular signal-regulated kinase 1/2 activation. J Neurosci. 2007;27:8475-85.

[138] Raghuram S, Stayrook KR, Huang P, Rogers PM, Nosie AK, McClure DB, et al. Identification of heme as the ligand for the orphan nuclear receptors REV-ERBalpha and REV-ERBbeta. Nat Struct Mol Biol. 2007;14:1207-13.

[139] Yin L, Wu N, Curtin JC, Qatanani M, Szwergold NR, Reid RA, et al. Rev-erbalpha, a heme sensor that coordinates metabolic and circadian pathways. Science. 2007;318:1786-9.

[140] Faller M, Matsunaga M, Yin S, Loo JA, Guo F. Heme is involved in microRNA processing. Nat Struct Mol Biol. 2007;14:23-9.

[141] Tang XD, Xu R, Reynolds MF, Garcia ML, Heinemann SH, Hoshi T. Haem can bind to and inhibit mammalian calcium-dependent Slo1 BK channels. Nature. 2003;425:531-5.

[142] Wang S, Publicover S, Gu Y. An oxygen-sensitive mechanism in regulation of epithelial sodium channel. Proc Natl Acad Sci U S A. 2009;106:2957-62.

[143] Sahoo N, Goradia N, Ohlenschlager O, Schonherr R, Friedrich M, Plass W, et al. Heme impairs the ball-and-chain inactivation of potassium channels. Proc Natl Acad Sci U S A. 2013;110:E4036-44.

[144] Weinbach EC, Ebert PS. Effects of succinylacetone on growth and respiration of L1210 leukemia cells. Cancer Lett. 1985;26:253-9.

[145] Ye WZ, Zhang L. Heme Deficiency Causes Apoptosis But Does Not Increase ROS Generation in HeLa Cells. Biochem Biophys Res Commun. 2004;319:1065-71.

[146] Ye WZ, Zhang L. Heme controls the expression of cell cycle regulators and cell proliferation in HeLa Cells. Biochem Biophys Res Commun. 2004;315:546-54.

[147] Hooda J, Cadinu D, Alam MM, Shah A, Cao TM, Sullivan LA, et al. Enhanced heme function and mitochondrial respiration promote the progression of lung cancer cells. PLoS One. 2013;8:e63402.

[148] Ramirez RD, Sheridan S, Girard L, Sato M, Kim Y, Pollack J, et al. Immortalization of human bronchial epithelial cells in the absence of viral oncoproteins. Cancer research. 2004;64:9027-34.

[149] Whitehurst AW, Bodemann BO, Cardenas J, Ferguson D, Girard L, Peyton M, et al. Synthetic lethal screen identification of chemosensitizer loci in cancer cells. Nature. 2007;446:815-9.

[150] Latunde-Dada GO, Takeuchi K, Simpson RJ, McKie AT. Haem carrier protein 1 (HCP1): Expression and functional studies in cultured cells. FEBS Lett. 2006;580:6865-70.

[151] Rajagopal A, Rao AU, Amigo J, Tian M, Upadhyay SK, Hall C, et al. Haem homeostasis is regulated by the conserved and concerted functions of HRG-1 proteins. Nature. 2008;453:1127-31.

[152] Network CGA. Comprehensive molecular characterization of human colon and rectal cancer. Nature. 2012;487:330-7.

[153] Network CGA. Comprehensive molecular portraits of human breast tumours. Nature. 2012;490:61-70.

[154] Network CGA. Comprehensive molecular characterization of urothelial bladder carcinoma. Nature. 2014;507:315-22.

[155] Network CGA. Comprehensive molecular profiling of lung adenocarcinoma. Nature. 2014;511:543-50.

[156] Network CGA. Genomic and epigenomic landscapes of adult de novo acute myeloid leukemia. N Engl J Med. 2013;368:2059-74.

[157] Chang DK, Grimmond SM, Biankin AV. Pancreatic cancer genomics. Curr Opin Genet Dev. 2014;24:74-81.

[158] Gruber M, Wu CJ. Evolving understanding of the CLL genome. Semin Hematol. 2014;51:177-87.

[159] Devarakonda S, Morgensztern D, Govindan R. Genomic alterations in lung adenocarcinoma. Lancet Oncol. 2015;16:e342-51.

[160] Guieze R, Wu CJ. Genomic and epigenomic heterogeneity in chronic lymphocytic leukemia. Blood. 2015;126:445-53.

[161] McGranahan N, Swanton C. Biological and therapeutic impact of intratumor heterogeneity in cancer evolution. Cancer Cell. 2015;27:15-26.

[162] De Sousa EMF, Vermeulen L, Fessler E, Medema JP. Cancer heterogeneity--a multifaceted view. EMBO Rep. 2013;14:686-95.

[163] Vogelstein B, Papadopoulos N, Velculescu VE, Zhou S, Diaz LA, Jr., Kinzler KW. Cancer genome landscapes. Science. 2013;339:1546-58.

[164] Wyatt AW, Mo F, Wang Y, Collins CC. The diverse heterogeneity of molecular alterations in prostate cancer identified through next-generation sequencing. Asian J Androl. 2013;15:301-8.

[165] Shibata D. Cancer. Heterogeneity and tumor history. Science. 2012;336:304-5.

[166] Gerlinger M, Rowan AJ, Horswell S, Larkin J, Endesfelder D, Gronroos E, et al. Intratumor heterogeneity and branched evolution revealed by multiregion sequencing. N Engl J Med. 2012;366:883-92.

[167] Biankin AV, Waddell N, Kassahn KS, Gingras MC, Muthuswamy LB, Johns AL, et al. Pancreatic cancer genomes reveal aberrations in axon guidance pathway genes. Nature. 2012;491:399-405.

[168] Alexandrov LB, Nik-Zainal S, Wedge DC, Aparicio SA, Behjati S, Biankin AV, et al. Signatures of mutational processes in human cancer. Nature. 2013;500:415-21.

[169] Yachida S, Jones S, Bozic I, Antal T, Leary R, Fu B, et al. Distant metastasis occurs late during the genetic evolution of pancreatic cancer. Nature. 2010;467:1114-7.

[170] Ellsworth RE, Toro AL, Blackburn HL, Decewicz A, Deyarmin B, Mamula KA, et al. Molecular Heterogeneity in Primary Breast Carcinomas and Axillary Lymph Node Metastases Assessed by Genomic Fingerprinting Analysis. Cancer Growth Metastasis. 2015;8:15-24.

[171] Leiserson MD, Vandin F, Wu HT, Dobson JR, Eldridge JV, Thomas JL, et al. Pan-cancer network analysis identifies combinations of rare somatic mutations across pathways and protein complexes. Nat Genet. 2015;47:106-14.

[172] Nowell PC. The clonal evolution of tumor cell populations. Science. 1976;194:23-8.

[173] de Bruin EC, McGranahan N, Mitter R, Salm M, Wedge DC, Yates L, et al. Spatial and temporal diversity in genomic instability processes defines lung cancer evolution. Science. 2014;346:251-6.

[174] Zhang J, Fujimoto J, Wedge DC, Song X, Seth S, Chow CW, et al. Intratumor heterogeneity in localized lung adenocarcinomas delineated by multiregion sequencing. Science. 2014;346:256-9.

[175] Gerlinger M, Swanton C. How Darwinian models inform therapeutic failure initiated by clonal heterogeneity in cancer medicine. Br J Cancer. 2010;103:1139-43.

[176] Greaves M, Maley CC. Clonal evolution in cancer. Nature. 2012;481:306-13.

[177] Yates LR, Campbell PJ. Evolution of the cancer genome. Nat Rev Genet. 2012;13:795-806.

CHAPTER 2

CYCLOPAMINE TARTRATE, AN INHIBITOR OF HEDGEHOG SIGNALING, STRONGLY INTERFERES WITH MITOCHONDRIAL FUNCTION AND SUPPRESSES AEROBIC RESPIRATION IN LUNG CANCER CELLS

Author – Md Maksudul Alam

Conception and design – Li Zhang, Md Maksudul Alam

Experiments – Md Maksudul Alam, Sagar Sohoni, Sarada Preeta Kalainayakan

Analysis – Li Zhang, Md Maksudul Alam

Administrative, technical, or material support – Li Zhang, Massoud Garrossian

Department of Biological Sciences

The University of Texas at Dallas

800 West Campbell Road

Richardson, Texas 75080

PREFACE

In this chapter, we will discuss the effect of CycT on NSCLC's respiration and mitochondrial functions. In previous chapter we have discussed that, mitochondrial respiration is critical for NSCLC's tumorigenicity. Majority of the data shown in this chapter is published in the manuscript: "Cyclopamine tartrate, an inhibitor of Hedgehog signaling, strongly interferes with mitochondrial function and suppresses aerobic respiration in lung cancer cells." Alam et al. BMC Cancer (2016) 16:150

DOI 10.1186/s12885-016-2200-x

ACKNOWLEDGMENTS

We thank Dr. Massoud Garrossian for providing Cyclopamine Tartrate. We also thank Dr. John Minna's Lab for providing HCC4017 and HBEC30KT cell lines.

ABSTRACT

Hedgehog (Hh) signaling is critical for normal embryonic development and for the maintenance, renewal and regeneration of adult tissues. Aberrant Hh signaling is associated with the development of many cancers including lung cancer, pancreatic cancer, ovarian cancer, and basal cell carcinoma. Therefore, the Hh signaling pathway has been one of the most intensely investigated targets for cancer therapy, and a number of compounds inhibiting Hh signaling are being tested clinically for the treatment of many cancers. Cyclopamine was the first compound found to inhibit Hh signaling and has been invaluable for understanding Hh signaling in development and cancer. Here, using an improved analogue of cyclopamine, cyclopamine

tartrate (CycT), we performed an in-depth analysis of the effect of inhibiting Hh signaling on an array of non-small-cell lung cancer (NSCLC) cell lines. We discovered that CycT, as well as another Hh inhibitor SANT1, has a novel activity in disrupting mitochondrial function and aerobic respiration. We found that CycT, like glutamine depletion, caused a substantial decrease in oxygen consumption in a number of NSCLC cell lines. Concomitantly, CycT initiated apoptosis and suppressed proliferation of NSCLC cells. Further analyses showed that CycT increased ROS generation, which is likely a result of mitochondrial membrane hyperpolarization and the cause for apoptosis. Notably, Mitotracker staining showed that CycT caused mitochondrial fragmentation, which coincided with the localization of Drp1 at various mitochondrial fission sites. Together, these results demonstrate that CycT, and evidently other Hh signaling inhibitors, can interfere with mitochondrial function and induce apoptosis in NSCLC cells.

KEY WORDS

Non-small-cell lung cancer (NSCLC), Hedgehog signaling, Cyclopamine tartrate, SANT1, Oxygen consumption, Mitochondrial fragmentation, ROS, Apoptosis, Glutamine depletion.

INTRODUCTION

Hedgehog (Hh) signaling is a key regulator of development and stem cell fate in animals [1]. Dysregulation of the Hh pathway is responsible for various developmental malformations, such as holoprosencephaly [2]. Aberrant activation of the Hh signaling is implicated in a variety of cancers, such as prostate cancer, gastrointestinal cancer, lung cancer, pancreatic cancer, ovarian

cancer, and basal cell carcinoma [3-8]. Therefore, Hh signaling pathway has become a therapeutic target for treating many types of cancers. Particularly, a great deal of efforts have been focused on targeting smoothened (SMO), a G protein-coupled receptor mediating Hedgehog (Hh) signaling [9]. Many SMO inhibitors have been generated and tested, and all have shown efficacy as anti-tumor agents [10]. For example, vismodegib is the first FDA-approved SMO inhibitor for the treatment of advanced and metastatic basal cell carcinoma. Currently, vismodegib and many other SMO inhibitors are being investigated in clinical trials in a range of advanced cancers [9, 10]. Consequently, understanding the molecular actions of such inhibitors can be of great value to improving therapeutic strategies for many types of cancers.

The first identified inhibitor of Hh signaling was cyclopamine, a molecule isolated from corn lilies [11, 12]. Cyclopamine binds to and inhibits SMO. Cyclopamine has been very valuable for understanding the function of Hh signaling and has been widely used as an Hh inhibitor in cell and murine models of various tumors [3-5, 13-15]. However, the usefulness of cyclopamine (Cyc) as a therapeutic drug is hindered by its poor aqueous solubility [16]. To improve the solubility and efficacy of Cyc, Dr. Garrossian, a contributor of this manuscript, generated cyclopamine tartrate (CycT) [17]. Indeed, CycT is water soluble, and its activity in inhibiting Hh signaling is higher than Cyc. Furthermore, CycT is effective in causing tumor shrinkage in two mouse models of basal cell carcinomas [17]. Therefore, we decided to examine the efficacy of CycT in inhibiting the proliferation and function of an array of non-small-cell lung cancer (NSCLC) cell lines.

Previously, using a matched pair of cell lines representing normal nonmalignant and NSCLC cells developed from the same patient, we found that oxygen consumption is intensified

in NSCLC cells and tumors [18]. Specifically, the rates of both glucose and oxygen consumption in NSCLC HCC4017 cells are elevated, with the elevation of oxygen consumption greater than that of glucose consumption. Inhibition of mitochondrial respiration interferes strongly with NSCLC cell function, proliferation and migration [18]. In this paper, we sought ways to suppress aerobic respiration, which may lead to novel therapeutic strategies to treat lung cancer and other cancers as well. Firstly, we found that oxygen consumption is intensified in an array of NSCLC cell lines. Secondly, we demonstrated that CycT and another SMO inhibitor SANT1, like glutamine depletion, suppress the rates of oxygen consumption and the rates of cancer cell proliferation. Further analyses of various cellular functions showed that CycT, as well as SANT1, increase ROS generation and mitochondrial membrane potential in NSCLC cells. Ultimately, these SMO inhibitors cause mitochondrial fragmentation, leading to apoptosis. Our studies uncovered a novel mode of anticancer action of an Hh inhibitor, which may have broad implications in the development and application of many Hh inhibitors currently being tested.

RESULTS

Cyclopamine tartrate (CycT), like glutamine depletion, strongly suppresses oxygen consumption in NSCLC cells

Previously, we showed that the rate of oxygen consumption in NSCLC HCC4017 cells is intensified compared to the nonmalignant HBEC cells representing normal lung epithelial cells from the same patient [18], as shown in Figure 2.1A. Additionally, we measured oxygen consumption rates in five other NSCLC cell lines and found that they were substantially increased in all NSCLC cell lines (Figure 2.1A). Furthermore, we examined the effect of glucose

depletion, glutamine depletion, and CycT on the rates of oxygen consumption in these NSCLC cell lines. We found that glucose depletion generally enhances oxygen consumption rates, while glutamine depletion diminishes the rates (Figure 2.1B-2.1G). Glucose and glutamine are two critical fuels for cancer cells [19, 20]. When glucose is limiting, the cells use glutamine, and vice versa. Thus, these results showed that in the absence of glucose, glutamine supports intensified oxygen consumption in cancer cells. In the absence of glutamine, even in the presence of glucose, oxygen consumption was substantially reduced (Figure 2.1B-2.1G). Notably, CycT diminished the rates of oxygen consumption in cancer cells largely to the same extent as glutamine depletion. Likewise, another SMO inhibitor SANT1 [21, 22] diminished oxygen consumption in NSCLC cells, as expected. These results indicate that CycT can cause the same effect as glutamine depletion on cancer cell metabolism and aerobic respiration.

CycT suppress proliferation and causes apoptosis in NSCLC cells

The data shown above revealed a strong effect of CycT on aerobic respiration. Thus, we further examined the effect of CycT on NSCLC cell proliferation. We found that CycT diminishes the proliferation and survival of NSCLC cells, although the sensitivity of different cell lines to CycT varies (Figure 2.2). We also tested whether CycT causes apoptosis in NSCLC cells by using Annexin V and propidium iodide (PI) staining. We found that CycT indeed causes apoptosis in NSCLC cells, albeit with varying efficacy in different NSCLC cell lines

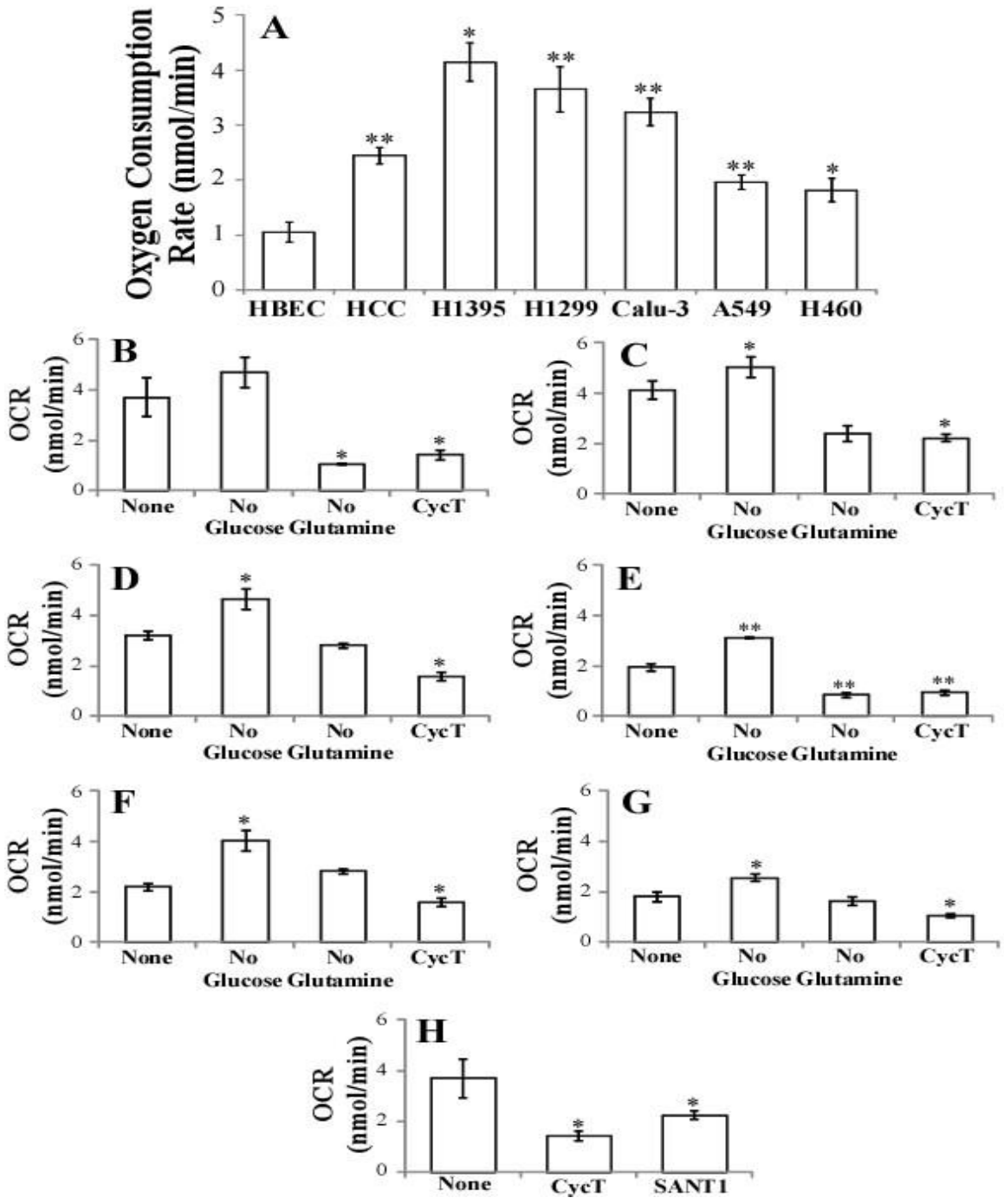

Figure 2.1. The rate of oxygen consumption (A) The rates of oxygen consumption are intensified in various NSCLC cell lines. (B-G) CycT, like glutamine depletion, strongly diminished oxygen consumption rates in NSCLC H1299 (B), H1395 (C), Calu-3 (D), A549 (E),

HCC4017 (F), and H460 (G) cells. NSCLC cell lines were cultured in their normal medium or in medium lacking glucose or glutamine, or treated with CycT, as indicated. (H) SMO inhibitor SANT1, like CycT, can diminish oxygen consumption in NSCLC cells. H1299 cells were treated with CycT or SANT1. The rates of oxygen consumption were measured. The data shown were averages of at least three independent measurements. For statistical analysis, the values were compared to that in nontumorigenic HBEC lung cells (A) or those in normal culture medium (in B-G), by using Welch 2-sample t-test. *, p value < 0.05; **, p value < 0.005.

For example, after 24 hours of treatment with CycT, H1299 cells were mostly apoptotic, as detected by Annexin V staining (Figure 2.3A). PI staining further showed that a fraction of these apoptotic H1299 cells were in the late apoptotic stage. A549 cells, as shown by the proliferation rates in Figure 2.2, were more resistant to CycT (Figure 2.3B). After 24 hours of treatment, only a fraction of the cells showed signs of apoptosis, as detected by Annexin V staining. No A549 cells were in late apoptotic stage (Figure 2.3B). Nonetheless, our results showed that CycT can cause apoptosis in NSCLC cells. Notably, another SMO inhibitor SANT1, like CycT, also exerted similar effects on NSCLC cells (Figure 2.3A & Figure 2.3B).

CycT does not exert a considerable effect on heme metabolism

Heme is a central factor in aerobic respiration and oxidative phosphorylation [23]. Previously, we have shown that limiting intracellular heme levels strongly diminish mitochondrial respiration and NSCLC cell proliferation and migration [18]. Therefore, we examined whether CycT impacts heme synthesis and metabolism. We found that CycT does not significantly affect the rate of heme synthesis in NSCLC cells (data not shown). Likewise, we found that CycT does not significantly affect the protein levels of the rate-limiting heme synthetic enzyme ALAS1 and

the degradation enzyme HO1 (Figure 2.4A & 2.4B). For a control, we showed that CycT reduces the level of the Hh signaling target Gli1 (Figure 2.4C), as expected. Furthermore, we found that CycT treatment reduced the levels of phosphorylated p44/42 MAPK. The activation of p44/42 MAPK signaling pathway has been shown to be critical for Hh signaling previously [24]. These results show that CycT does not affect aerobic respiration by impacting heme metabolism.

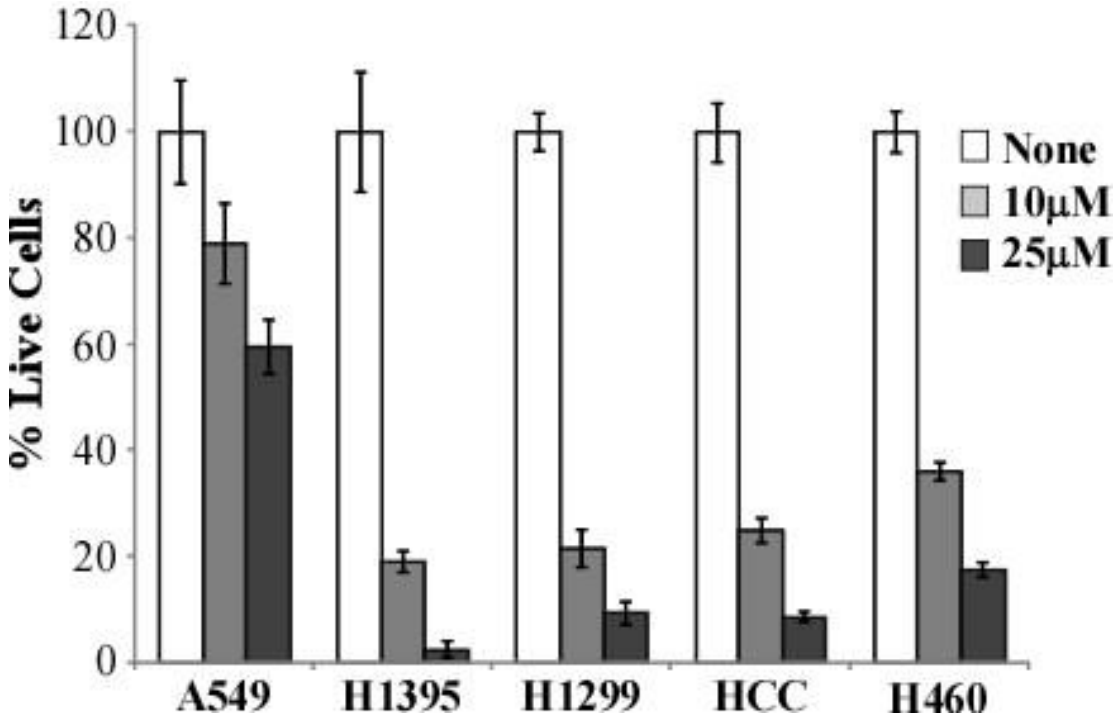

Figure 2.2. The effect of CycT treatment on NSCLC cancer cell proliferation. %live cells was calculated by dividing the number of treated cells with the number of untreated cells (seeded with the same number of cells). It shows the relative proliferative rates of treated cells (10 or 25 μM) vs. untreated cells (None). For statistical analysis, the values for treated cells were compared to the values for untreated cells, by using Welch 2-sample t-test. *, p value < 0.05; **, p value < 0.005.

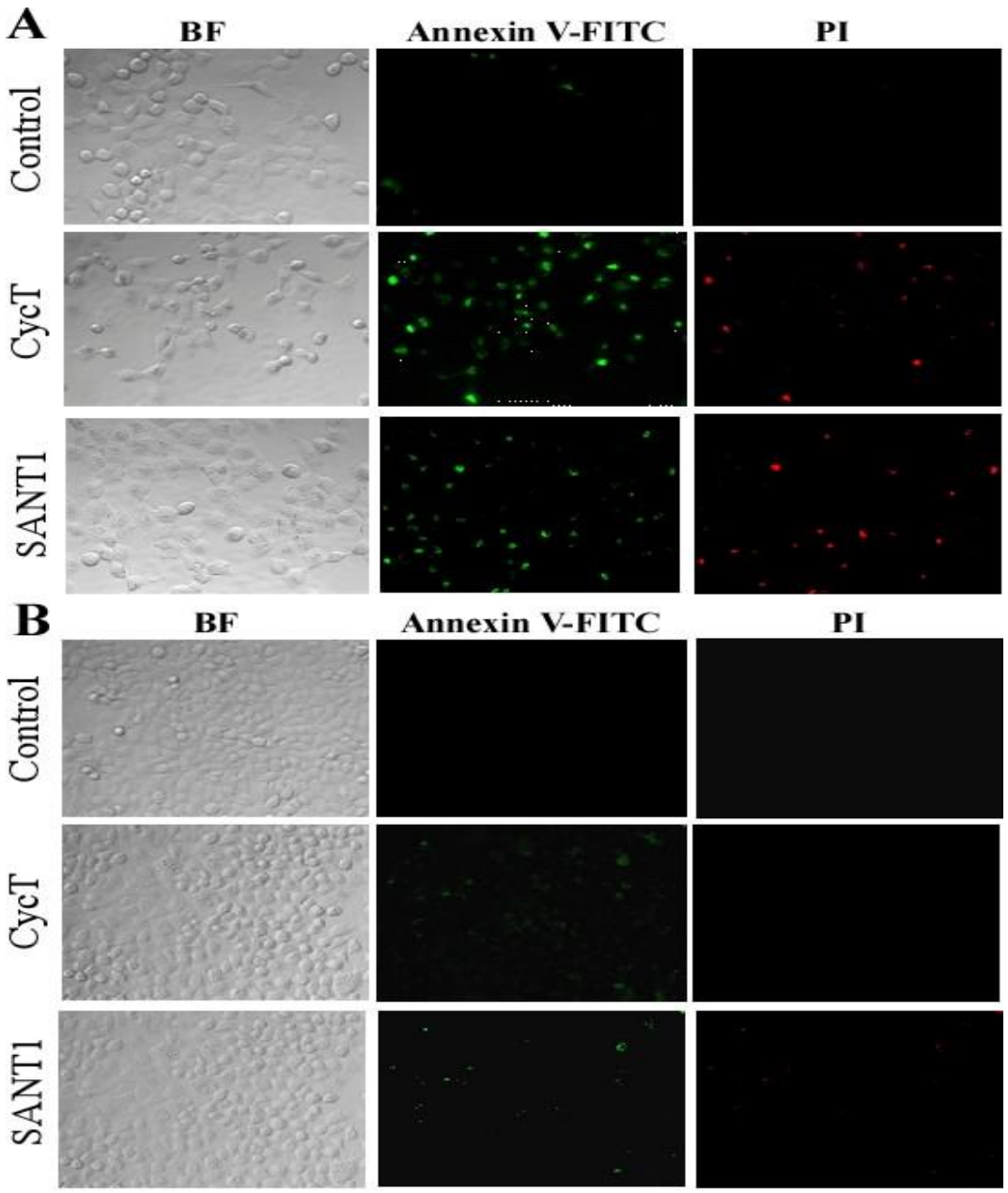

Figure 2.3. CycT and SANT1 induce apoptosis in NSCLC cells. H1299 (A) and A549 (B) cells were treated with CycT or SANT1 for 24 hours. Then cells were subjected to apoptosis assay by using Annexin V-FITC and Propidium Iodide (PI) staining. The images of cells were captured with bright field microscopy (BF) or with fluorescentmicroscopy with a FITC or rhodamine (for PI) filter.

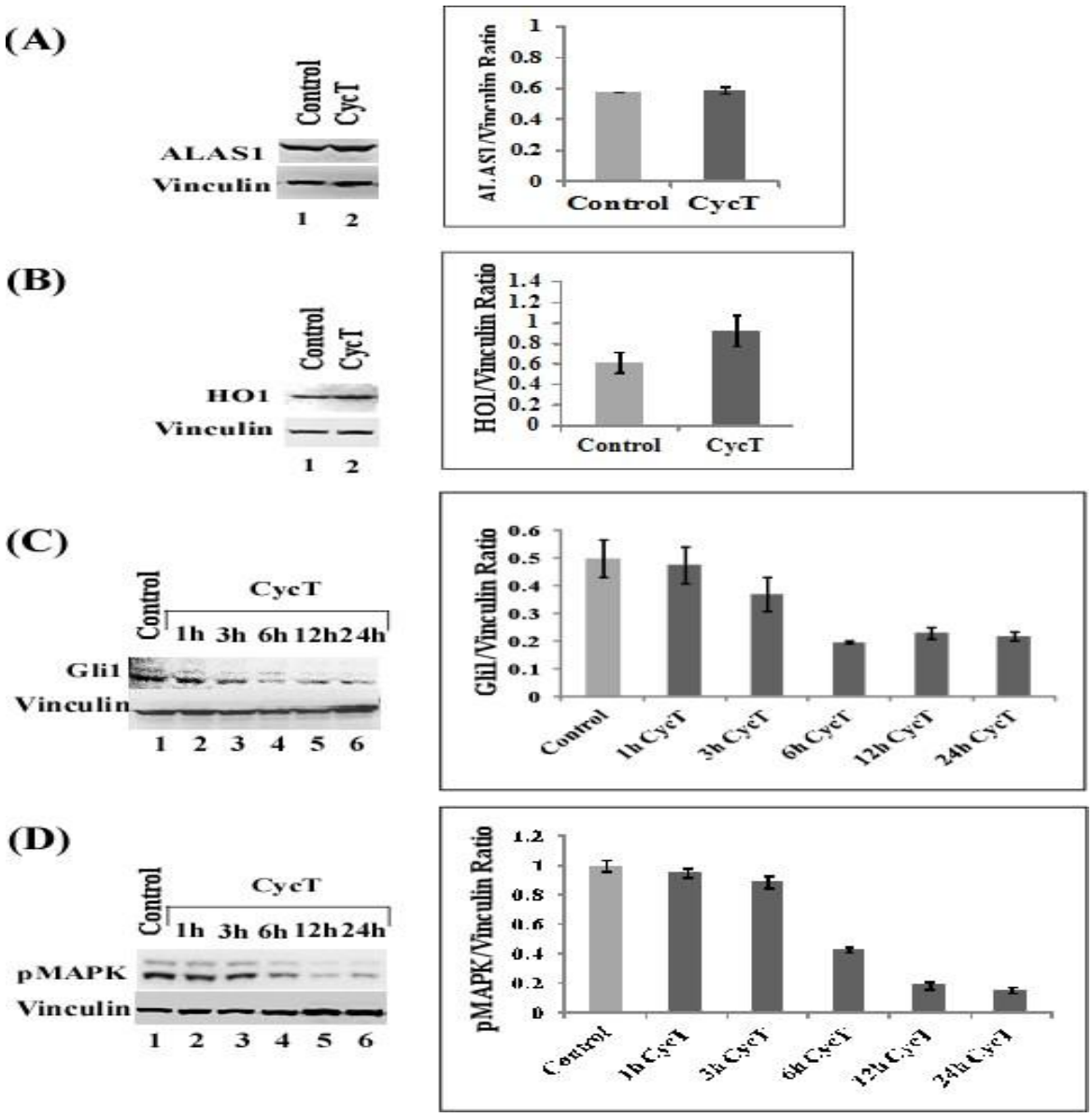

Figure 2.4. The effect of CycT treatment on the levels of ALAS1 (A), HO1 (B), Gli1 (C), and phospho-p44/p42 MAPK (D). The NSCLC A549 cells were cultured and treated with CycT for 24 hours. Protein extracts were prepared and the levels of the proteins were detected by Western blotting. The protein level of vinculin was used for normalization. For statistical analysis, the levels in treated cells were compared to the levels in untreated cells, by using Welch 2-sample t-test. *, p value < 0.05.

CycT increases ROS generation and interferes with mitochondrial function in NSCLC cells

To further investigate the mode by which CycT causes NSCLC cell death, we measured ROS generation in CycT-treated and untreated NSCLC cells. We found that CycT causes a substantial increase in ROS generation in NSCLC cells, including H1299 (Figure 2.5A), A549 (Figure 2.5B), and H460 (Figure 2.5C) cells.

In addition, we found that another SMO inhibitor SANT1 increased ROS generation in NSCLC cells (Figure 2.5D). Because of the dominant role of mitochondria in oxygen metabolism, mitochondria are mainly responsible for the generation of cellular ROS.

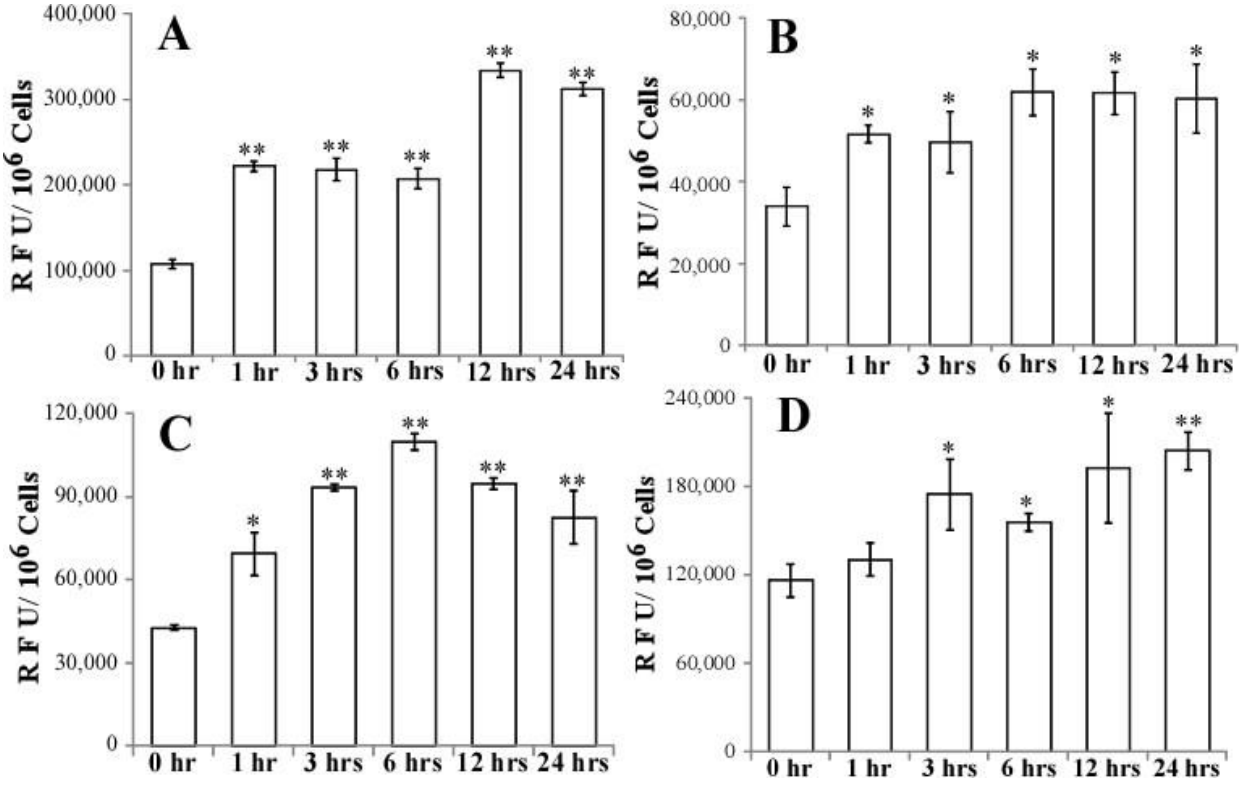

Figure 2.5. CycT and SANT1 treatment increases ROS production in NSCLC cells. H1299 (A), A549 (B), H460 (C) and SANT1 treatment on H1299 (D). NSCLC cells were treated with CycT or SANT1 for the indicated time periods. Then cells were incubated with 2,7-

dichlorodihydrofluorescein diacetate (DCFH-DA) for 30 minutes. Fluorescence intensity was measured and normalized according to cell density. For statistical analysis, the levels in CycT-treated cells were compared to the levels in untreated cells, by using Welch 2-sample t-test. *, p value < 0.05; **, p value < 0.005.

Therefore, we also examined the effect of CycT on mitochondrial function. First, we measured and compared mitochondrial membrane potential in CycT-treated and CycT-untreated cells.

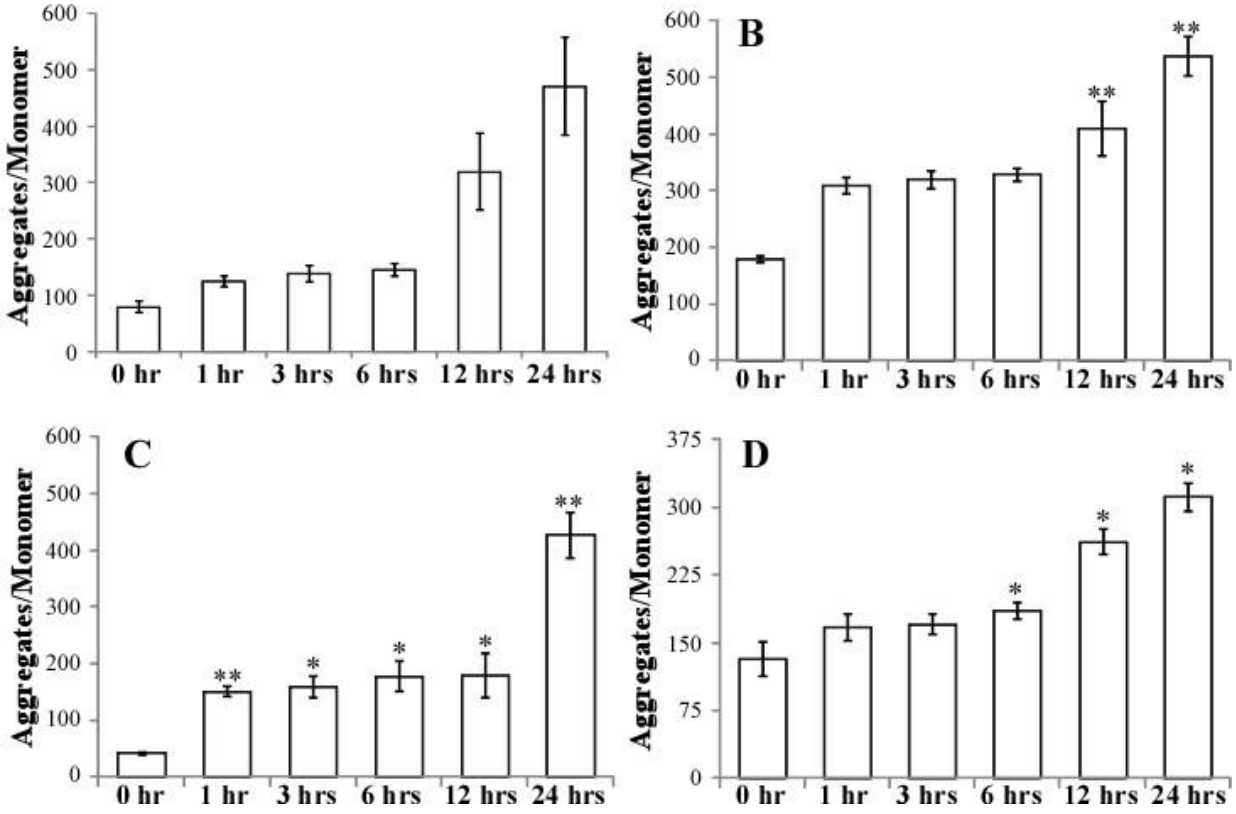

Figure 2.6. The effect of CycT and SANT1 treatment on mitochondrial membrane potential in NSCLC cells. H1299 (A), A549 (B), H460 (C) and SANT1 treatment on H1299 cells (D). NSCLC cells were treated with CycT or SANT1 for the indicated time periods. Then mitochondrial membrane potential in these cells was measured by using JC-1 staining. Mitochondrial membrane potential was expressed as the ratio of aggregates/monomer, which

was calculated by dividing red fluorescence intensity with green fluorescence intensity. For statistical analysis, the levels in CycT-treated cells were compared to the levels in untreated cells, by using Welch 2-sample t-test. *, p value < 0.05; **, p value < 0.005.

We found that CycT increases mitochondrial membrane potential substantially in NSCLC cells (Figure 2.6A, 2.6B, & 2.6C). This effect of CycT appeared to be stronger in H1299 (Figure 2.6A) and H460 (Figure 2.6C) cells than in A549 cells (Figure 2.6B). Likewise, another SMO inhibitor SANT1 increased mitochondrial membrane potential in NSCLC cells (Figure 2.6D).

CycT causes mitochondrial fragmentation in NSCLC cells

Mitochondrial morphology is closely linked to mitochondrial function [25]. Changes in mitochondrial morphology regulate many mitochondrial functions, such as the respiratory activity of the electron transport chain and apoptosis [26]. We therefore examined the effect of CycT on mitochondrial morphology in NSCLC cells by using MitoTracker Red. Figure 2.7 shows that CycT treatment caused mitochondrial fragmentation in NSCLC cells, H1299 (Figure 2.7A), A549 (Figure 2.7B), and H460 (Figure 2.7C) cells. SANT1 exerted similar effects on the NSCLC cells (not shown).

Because Drp1 is the main protein promoting mitochondrial fission and fragmentation [27], we also examined the effect of CycT on Drp1 distribution. Figure 2.8 shows the localization of Drp1 in CycT-treated NSCLC cells, H1299 (Figure 2.8A) and A549 (Figure 2.8B), Drp1 was indeed selectively localized to various mitochondrial fission sites.

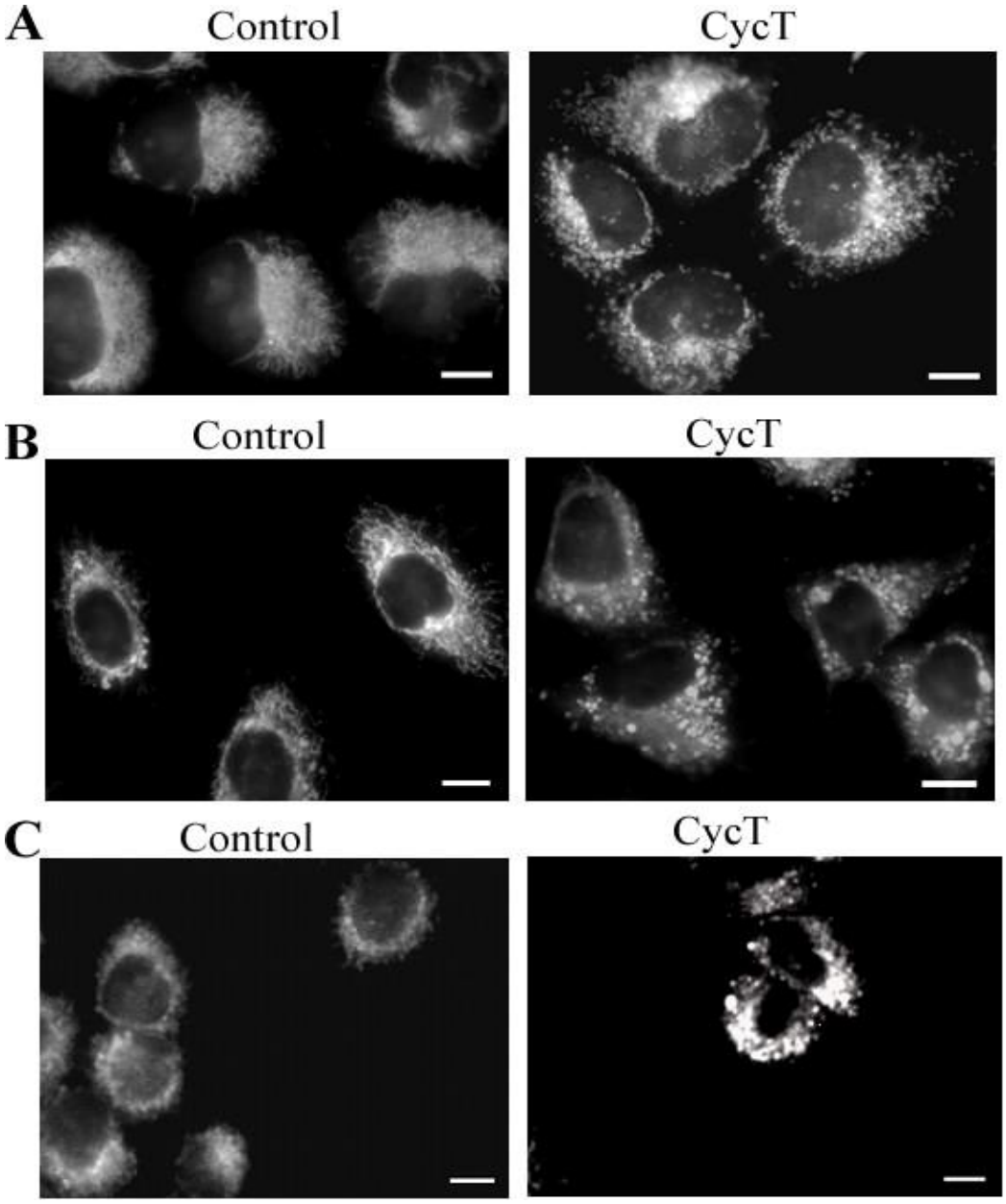

Figure 2.7. CycT treatment causes mitochondrial fragmentation in NSCLC cells. H1299 (A), A549 (B), and H460 (C) **.** NSCLC cells were treated with CycT for 24 hours, and then stained with MitoTracker Red. Fluorescent images were acquired and shown here. The scale bar indicates 10 μm

The localization pattern of Drp1 completely coincided with the MitoTracker Red staining pattern. These results demonstrated that CycT can induce Drp1 to promote mitochondrial fission and fragmentation. Moreover, the level of Drp1 is also increased in CycT treated cells (data not shown)

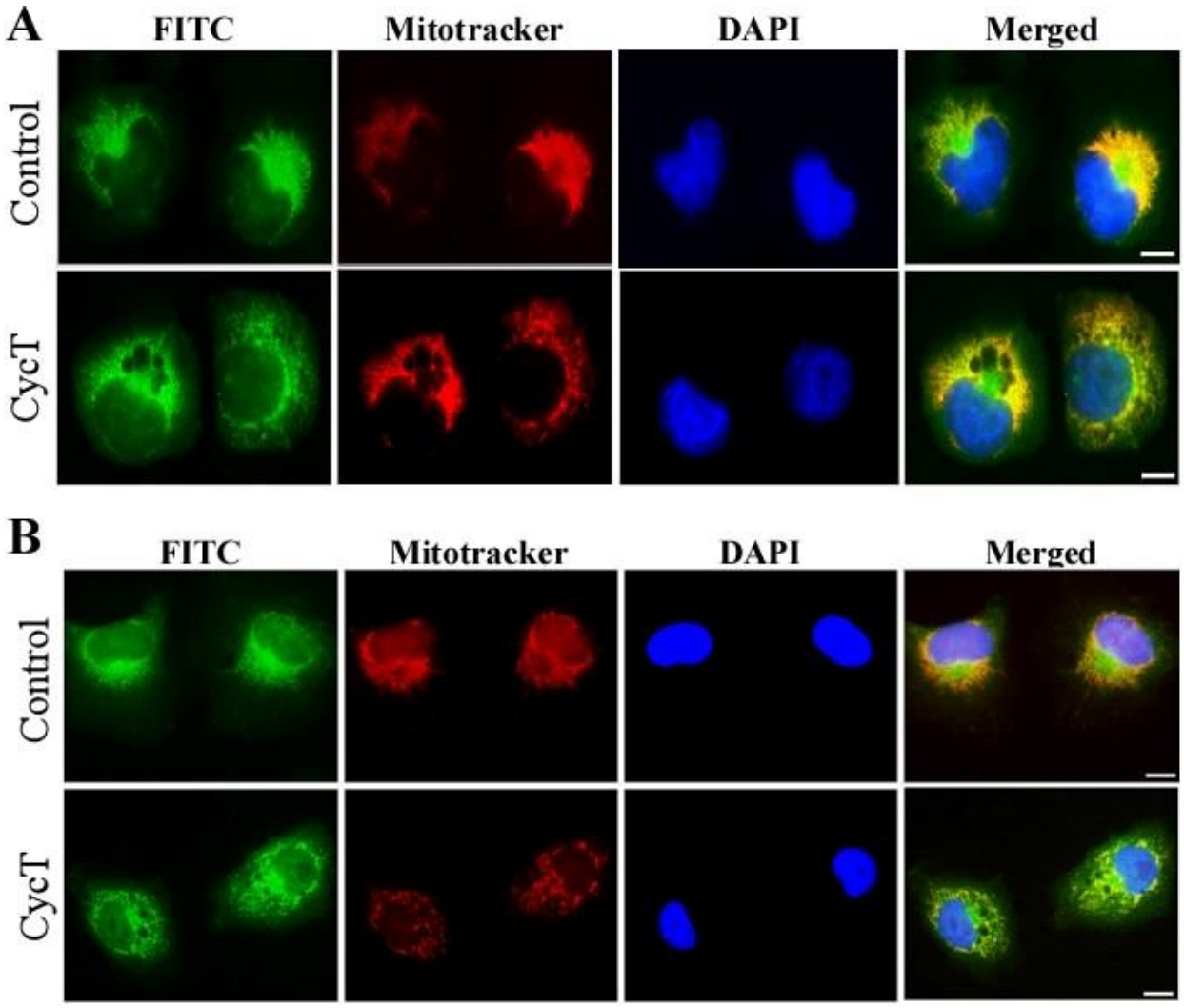

Figure 2.8. Drp1 localizes to the mitochondrial fission sites in CycT-treated NSCLC cells. H1299 (A) and A549 (B). NSCLC cells were treated with CycT for 24 hours. Cells were incubated with anti-Drp1 antibodies, and then with FITC-conjugated goat anti-rabbit secondary

antibody, MitoTracker, as well as DAPI. FITC, MitoTracker and DAPI fluorescent images were captured and are shown here. The scale bar indicates 10 μm

DISCUSSION

Targeting Hh signaling is an important strategy that is being developed to treat a variety of metastatic and advanced cancers [9, 28]. Vismodegib, a SMO antagonist, was the first Hh inhibitor to receive approval from the USA FDA in January 2012 for the treatment of locally advanced or metastatic basal cell carcinoma (BCC) [29]. Currently, NIH lists 91 ongoing or completed clinical trials testing Hh inhibitors against a variety of cancers (https://clinicaltrials.gov/ct2/results?term=HEDGEHOG). Therefore, a comprehensive understanding of the modes of Hh inhibitor action can benefit the treatment of a wide range of cancers. Here, by using the well-studied Hh inhibitor cyclopamine tartrate, we identified a new activity of this drug against aerobic respiration and mitochondrial function in NSCLC cancer cells.

First, we found that oxygen consumption is intensified in an array of NSCLC cell lines and that glutamine has a prominent role in promoting oxygen consumption, because glucose depletion in the presence of glutamine enhanced oxygen consumption while glutamine depletion in the presence of glucose diminished oxygen consumption substantially (Figure 2.1). This is entirely consistent with previous studies showing glutamine as the dominant respiratory substrate in tumor cells [30, 31]. Remarkably, we found that CycT exerted largely the same effect on oxygen consumption as glutamine depletion (Figure 2.1B-2.1G). Glutamine provides a crucial source of cellular energy and building blocks for cancer cells, and targeting glutamine uptake and metabolisms has become an important approach in treating drug-resistant cancers [32, 33].

Our finding linking both CycT treatment and glutamine depletion with diminished aerobic respiration provides a new way to control cancer cell bioenergetics. Although different NSCLC cell lines exhibited varying rates of oxygen consumption (Figure 2.1B-2.1G), CycT, like glutamine depletion, strongly diminished oxygen consumption in all cell lines, suggesting that CycT can be an effective inhibitor of cellular energy production in all these lines. The same effect of glutamine depletion and CycT treatment suggests that Hh inhibitors may be used in substitution of drugs targeting glutamine metabolism in cancer therapy.

Second, we showed that CycT strongly suppressed NSCLC cell proliferation (Figure 2.2) and induced apoptosis (Figure 2.3). Notably, apoptosis of NSCLC cells was preceded by increased ROS generation (Figure 2.5) and increased mitochondrial membrane potential (Figure 2.6). At first sight, increased mitochondrial membrane potential accompanying apoptosis may seem paradoxical. However, hyperpolarization of mitochondrial membrane potential induced by various stress factors have been observed in a wide array of cells ranging from neuronal to blood cells [34]. For example, both glucose and oxygen deprivation induces mitochondrial membrane potential hyperpolarization [35]. Hyperpolarization of mitochondrial membrane potential will lead to excessive ROS production [34, 36]. The connection between the $\Delta\Psi m$ and ROS is exponential when $\Delta\Psi m$ exceeds 140 mV [37]. Ultimately, increased ROS generation will lead to apoptosis [38, 39], as indicated in Figures 2.5 and 2.6.

Third, we found that CycT strongly induced mitochondrial fission and fragmentation (Figure 2.7). As expected, CycT-induced mitochondrial fragmentation accompanied the increased level and recruitment of Drp1 to the mitochondrial outer membrane and fission sites (Figure 2.8), consistent with previous models of mitochondrial fission [27]. Mitochondrial

fragmentation is often associated with apoptosis, although it can occur in a variety of conditions independently of apoptosis [25, 40]. Here our results suggest that CycT-induced apoptosis in NSCLC cells is associated with mitochondrial fragmentation. Interestingly, while CycT caused strong mitochondrial fragmentation in both A549 and H1299 cells, apoptosis was much less prominent in A549 cells (Figure 2.3), suggesting differential sensitivity of NSCLC cells to mitochondrial fragmentation and CycT.

In sum, our results provide novel insights into the potential mechanisms of action of Hh signaling pathway inhibitors. Previous studies have shown that Gli transcriptional factors are the key mediators of Hh signaling [1, 2]. Furthermore, genome-wide analyses using gene expression profiling and chromatin immunoprecipitation have identified many Gli target genes [41-43]. A careful examination of these target genes showed that there are 30 genes encoding for mitochondrial functions, such as MRPL23, GLUL, SLC25A13, PRDX6, and ATP6V1E1 [41]. These targets also include NDUFS8, a subunit of mitochondrial NADH:ubiquinone oxidoreductase, or Complex I; Cyb5b, a cytochrome b5 outer mitochondrial membrane isoform; 1810063B05Rik, cytochrome c oxidase assembly factor 6; and catalase. Although the identification of such a relatively small number of mitochondrial targets does not allow the inference of a global effect of Hh signaling or Hh inhibitors on mitochondria, it does lend support to our new finding that the Hh inhibitor CycT impacts mitochondrial morphology and function, thereby modulating mitochondrial respiration and apoptosis. Further studies comparing SMO inhibitors, such as CycT, and Gli inhibitors may provide additional insights into which proteins in the Hh signaling pathway play a dominant role in mitochondrial morphology and function.

CONCLUSIONS

The major findings of our study are: a) CycT, like glutamine depletion, causes a substantial decrease in oxygen consumption in a number of NSCLC cell lines; b) CycT suppresses proliferation and induces apoptosis in NSCLC cells; c) CycT and evidently other Hh inhibitors promote mitochondrial fission and fragmentation, mitochondrial membrane hyperpolarization, and ROS generation; and d) Hh signaling inhibitors can act on mitochondria and cause broad and dramatic changes in mitochondrial morphology, respiration and function. These new findings can shed light on the mechanisms underlying various cancers associated with aberrant Hh signaling and can provide novel insights into how to optimize anti-Hh signaling strategy for treating cancer.

METHODS

Lung cell lines, antibodies and reagents

HBEC30KT and HCC4017 cell lines representing normal and NSCLC cells [44, 45] were provided by Dr. John Minna's lab (UTSW) as a gift. They were developed from the same patient and were maintained in ACL4 supplemented with 2% FBS under 5% CO_2 at 37^{o}C [45]. All other NSCLC cell lines, H1395, H1299, Calu-3, A549 and H460 were purchased from ATCC, and were maintained according to ATCC procedures. All tissue culture media, including those lacking glucose or glutamine, were purchased from Invitrogen Life Technologies. HBEC30KT, HCC4017, H1299 and A549, were authenticated by using the services provided by Genetica DNA Laboratories, and they were found to be 100% match. Other NSCLC cell lines were used for measurements immediately following the purchase. Cyclopamine tartrate (CycT) was

provided by Logan Natural Products (Plano, Texas). SANT1 was purchased from Santa Cruz Biotechnology. For measuring the effect of CycT or SANT1 on lung cell proliferation, cells were seeded in 48-well plate at a density of 10^4 cells/well. After culturing for 24 hours, cells were treated with the indicated concentrations for 24 hours or the indicated time points. At the indicated times, the number of live cells was counted by using trypan blue staining and a hemocytometer. Polyclonal anti-ALAS1, anti-HO1, anti-Gli1 and anti-Drp1 were purchased from Santa Cruz Biotechnology. Monoclonal anti-vinculin antibody was purchased from Sigma-Aldrich. Polyclonal anti-phospho-p44/42 MAPK antibody was purchased from Cell Signaling Technology.

Measurement of oxygen consumption rates

NSCLC cells (~70% confluence) were maintained in medium with 25 μM CycT or 50 μM SANT1, or in medium lacking glucose or glutamine for 24 hours. Then oxygen consumption was measured, as described previously [46]. Briefly, cells with about 80% confluence were trypsinized and resuspended in fresh, air-saturated medium. For each measurement, 10^6 cells (in 350 μl) were introduced in the chamber of an Oxygraph system (Hansatech Instruments), with a Clark-type electrode placed at the bottom of the respiratory chamber. During measurements, the chamber was thermostated at 37°C by a circulating water bath. An electromagnetic stirrer bar was used to mix the contents of the chamber. Each measurement was replicated at least three times. Standard deviations were calculated, and p values were calculated by using Welch 2-sample t-test (R program).

Measurement of ROS generation and mitochondrial membrane potential

The intracellular ROS levels were measured by using 2,7-dichlorodihydrofluorescein diacetate (DCFH-DA) (Cayman Chemical), which is oxidized into highly fluorescent 2,7-dichlorofluorescein in the presence of intracellular ROS. Cells were seeded in 96-well plates with black walls and clear bottoms at a density of 10,000 cells per well. Cells were treated with 25 μM CycT or 50 μM SANT1 for the indicated times. Cells were then incubated for 30 min with 10 μM DCFH-DA dissolved in fresh media. Cells were then rinsed twice with PBS, and each well was filled with 100 μl PBS. Fluorescence was detected by using a fluorescent plate reader (Bio Tek, Synergy Mx microplate reader) with the excitation and emission wavelengths at 490 and 535 nm, respectively.

Changes in the mitochondrial membrane potential ($\Delta\Psi m$) were measured quantitatively by staining with the cationic dye JC-1(Molecular probes), which accumulates in the mitochondria, showing green fluorescence at lower membrane potential and forming J-aggregates with red fluorescence at higher membrane potential. Cells were seeded in 96 well black wall and clear bottom plates at a density of 10,000 cells per well. Cells were treated with 25 μM CycT or 50 μM SANT1 for the indicated times. Cells were then incubated with 200 μl of fresh medium containing 2μg/μl of JC-1 dye for 30 min in the dark. The cells were washed twice with PBS, and the plates were immediately read with a fluorescent plate reader (Bio Tek, Synergy Mx microplate reader) with excitation and emission wavelengths set at 540 and 595 nm, respectively, for red fluorescence; and 485 and 535 nm, respectively, for green fluorescence.

Preparation of protein extracts and Western blotting

NSCLC cells were treated, collected, and lysed by using the RIPA buffer (Cell Signaling Technology) containing the protease inhibitor cocktail. Protein concentrations were determined by using the BCA assay kit (Thermo Scientific). 50 μg of proteins from each treatment condition were electrophoresed on 9% SDS–Polyacrylamide gels, and then transferred onto the Immuno-Blot PVDF Membrane (Bio-Rad). The membranes were probed with polyclonal antibodies, followed by detection with a chemiluminescence Western blotting kit (Roche Diagnostics). The signals were detected by using a Carestream image station 4000MM Pro and quantitation was performed by using the Carestream molecular imaging software version 5.0.5.30 (Carestream Health, Inc.). Antibodies used were purchased from Santa Cruz Biotechnology and Sigma-Aldrich.

Mitochondria imaging and indirect immunofluorescence staining

Mitochondria were visualized by using Mito Tracker Red CMXRos (Molecular probes), which passively diffuses across the plasma membrane and accumulates in active mitochondria. Cells were grown on chamber slides and treated with CycT for 24 hours. Cells were then stained with 200 nM of CMXRos in complete growth medium for 30 min at 37 ^{o}C, washed with prewarmed PBS three times, and fixed with 4% formaldehyde in PBS for 10 min. After washing twice with PBS the slides were covered, and fluorescent images were captured with a multi-channel Zeiss Axio Observer Z1 fluorescent microscope with a Zeiss 40X Oil immersion lens and with a high speed AxioCam MRm Rev3 monochrome camera.

Indirect immunofluorescence staining with Drp1 antibodies (purchased from Santa Cruz Biotechnology) was performed by following the procedures provided by the antibody manufacturer. FITC and DAPI fluorescent images were captured by using a multi-channel Zeiss Axio Observer Z1 fluorescent microscope. Apoptosis was detected by using the ApoAlert Annexin V-FITC Apoptosis Kit (Clontech). Cells were seeded in a 96-well black wall clear bottom plate at the density of 10,000 cells per well. After one day, cells were treated with 25μM CycT or SANT1 in fresh medium. Twenty four hours post treatment, apoptosis assay was performed according to manufacturer's protocol. Fluorescent images were captured using a multi-channel Zeiss Axio Observer Z1 fluorescent microscope with a Zeiss 20X lens and with a high speed AxioCam MRm Rev3 monochrome camera.

ABBREVIATIONS

ALAS1: 5'-Aminolevulinate synthase 1

BCC: Basal cell carcinoma

CycT: Cyclopamine tartrate

DAPI: 4′, 6-Diamidino-2-phenylindole

DCFH-DA: 2,7-dichlorodihydrofluorescein diacetate

GLUL: Glutamate-ammonia ligase

HO1: Heme oxygenase 1

MRPL23: Mitochondrial ribosomal protein L23

NDUFS8: NADH Dehydrogenase (Ubiquinone) Fe-S protein 8

NSCLC: Non-small-cell lung cancer

PRDX6: Peroxiredoxin 6

ROS: Reactive oxygen species

REFERENCES

[1] Briscoe J, Therond PP. The mechanisms of Hedgehog signalling and its roles in development and disease. Nat Rev Mol Cell Biol. 2013;14:416-29.

[2] Hui CC, Angers S. Gli proteins in development and disease. Annu Rev Cell Dev Biol. 2011;27:513-37.

[3] Karhadkar SS, Bova GS, Abdallah N, Dhara S, Gardner D, Maitra A, et al. Hedgehog signalling in prostate regeneration, neoplasia and metastasis. Nature. 2004;431:707-12.

[4] Berman DM, Karhadkar SS, Maitra A, Montes De Oca R, Gerstenblith MR, Briggs K, et al. Widespread requirement for Hedgehog ligand stimulation in growth of digestive tract tumours. Nature. 2003;425:846-51.

[5] Watkins DN, Berman DM, Burkholder SG, Wang B, Beachy PA, Baylin SB. Hedgehog signalling within airway epithelial progenitors and in small-cell lung cancer. Nature. 2003;422:313-7.

[6] Jones S, Zhang X, Parsons DW, Lin JC, Leary RJ, Angenendt P, et al. Core signaling pathways in human pancreatic cancers revealed by global genomic analyses. Science. 2008;321:1801-6.

[7] Bhattacharya R, Kwon J, Ali B, Wang E, Patra S, Shridhar V, et al. Role of hedgehog signaling in ovarian cancer. Clin Cancer Res. 2008;14:7659-66.

[8] Stecca B, Mas C, Clement V, Zbinden M, Correa R, Piguet V, et al. Melanomas require HEDGEHOG-GLI signaling regulated by interactions between GLI1 and the RAS-MEK/AKT pathways. Proc Natl Acad Sci U S A. 2007;104:5895-900.

[9] Amakye D, Jagani Z, Dorsch M. Unraveling the therapeutic potential of the Hedgehog pathway in cancer. Nat Med. 2013;19:1410-22.

[10] Di Magno L, Coni S, Di Marcotullio L, Canettieri G. Digging a hole under Hedgehog: downstream inhibition as an emerging anticancer strategy. Biochim Biophys Acta. 2015;1856:62-72.

[11] Chen JK, Taipale J, Cooper MK, Beachy PA. Inhibition of Hedgehog signaling by direct binding of cyclopamine to Smoothened. Genes Dev. 2002;16:2743-8.

[12] Taipale J, Chen JK, Cooper MK, Wang B, Mann RK, Milenkovic L, et al. Effects of oncogenic mutations in Smoothened and Patched can be reversed by cyclopamine. Nature. 2000;406:1005-9.

[13] Thayer SP, di Magliano MP, Heiser PW, Nielsen CM, Roberts DJ, Lauwers GY, et al. Hedgehog is an early and late mediator of pancreatic cancer tumorigenesis. Nature. 2003;425:851-6.

[14] Berman DM, Karhadkar SS, Hallahan AR, Pritchard JI, Eberhart CG, Watkins DN, et al. Medulloblastoma growth inhibition by hedgehog pathway blockade. Science. 2002;297:1559-61.

[15] Sanchez P, Ruiz i Altaba A. In vivo inhibition of endogenous brain tumors through systemic interference of Hedgehog signaling in mice. Mech Dev. 2005;122:223-30.

[16] Winkler JD, Isaacs A, Holderbaum L, Tatard V, Dahmane N. Design and synthesis of inhibitors of Hedgehog signaling based on the alkaloid cyclopamine. Org Lett. 2009;11:2824-7.

[17] Fan Q, Gu D, He M, Liu H, Sheng T, Xie G, et al. Tumor shrinkage by cyclopamine tartrate through inhibiting hedgehog signaling. Chin J Cancer. 2011;30:472-81.

[18] Hooda J, Cadinu D, Alam MM, Shah A, Cao TM, Sullivan LA, et al. Enhanced heme function and mitochondrial respiration promote the progression of lung cancer cells. PloS one. 2013;8:e63402.

[19] Anastasiou D, Cantley LC. Breathless cancer cells get fat on glutamine. Cell Res. 2012;22:443-6.

[20] Birsoy K, Sabatini DM, Possemato R. Untuning the tumor metabolic machine: Targeting cancer metabolism: a bedside lesson. Nat Med. 2012;18:1022-3.

[21] Leem YE, Ha HL, Bae JH, Baek KH, Kang JS. CDO, an Hh-coreceptor, mediates lung cancer cell proliferation and tumorigenicity through Hedgehog signaling. PloS one. 2014;9:e111701.

[22] Stanton BZ, Peng LF. Small-molecule modulators of the Sonic Hedgehog signaling pathway. Molecular bioSystems. 2010;6:44-54.

[23] Zhang L. HEME BIOLOGY: The Secret Life of Heme in Regulating Diverse Biological Processes. Singapore: World Scientific Publishing Company 2011.

[24] Liu H, Jian Q, Xue K, Ma C, Xie F, Wang R, et al. The MEK/ERK signalling cascade is required for sonic hedgehog signalling pathway-mediated enhancement of proliferation and inhibition of apoptosis in normal keratinocytes. Experimental dermatology. 2014;23:896-901.

[25] McCarron JG, Wilson C, Sandison ME, Olson ML, Girkin JM, Saunter C, et al. From structure to function: mitochondrial morphology, motion and shaping in vascular smooth muscle. J Vasc Res. 2013;50:357-71.

[26] Picard M, Shirihai OS, Gentil BJ, Burelle Y. Mitochondrial morphology transitions and functions: implications for retrograde signaling? Am J Physiol Regul Integr Comp Physiol. 2013;304:R393-406.

[27] van der Bliek AM, Shen Q, Kawajiri S. Mechanisms of mitochondrial fission and fusion. Cold Spring Harb Perspect Biol. 2013;5.

[28] Ng JM, Curran T. The Hedgehog's tale: developing strategies for targeting cancer. Nat Rev Cancer. 2011;11:493-501.

[29] Dlugosz A, Agrawal S, Kirkpatrick P. Vismodegib. Nat Rev Drug Discov. 2012;11:437-8.

[30] Kovacevic Z. The pathway of glutamine and glutamate oxidation in isolated mitochondria from mammalian cells. Biochem J. 1971;125:757-63.

[31] Moreadith RW, Lehninger AL. The pathways of glutamate and glutamine oxidation by tumor cell mitochondria. Role of mitochondrial NAD(P)+-dependent malic enzyme. J Biol Chem. 1984;259:6215-21.

[32] Hensley CT, Wasti AT, DeBerardinis RJ. Glutamine and cancer: cell biology, physiology, and clinical opportunities. J Clin Invest. 2013;123:3678-84.

[33] Moses MA, Neckers L. The GLU that holds cancer together: targeting GLUtamine transporters in breast cancer. Cancer Cell. 2015;27:317-9.

[34] Kadenbach B, Ramzan R, Wen L, Vogt S. New extension of the Mitchell Theory for oxidative phosphorylation in mitochondria of living organisms. Biochim Biophys Acta. 2010;1800:205-12.

[35] Korenic A, Boltze J, Deten A, Peters M, Andjus P, Radenovic L. Astrocytic mitochondrial membrane hyperpolarization following extended oxygen and glucose deprivation. PloS one. 2014;9:e90697.

[36] Kadenbach B, Ramzan R, Moosdorf R, Vogt S. The role of mitochondrial membrane potential in ischemic heart failure. Mitochondrion. 2010;11:700-6.

[37] Liu SS. Cooperation of a "reactive oxygen cycle" with the Q cycle and the proton cycle in the respiratory chain--superoxide generating and cycling mechanisms in mitochondria. J Bioenerg Biomembr. 1999;31:367-76.

[38] Le Bras M, Clement MV, Pervaiz S, Brenner C. Reactive oxygen species and the mitochondrial signaling pathway of cell death. Histol Histopathol. 2005;20:205-19.

[39] Martinez-Reyes I, Cuezva JM. The H(+)-ATP synthase: a gate to ROS-mediated cell death or cell survival. Biochim Biophys Acta. 2014;1837:1099-112.

[40] Otera H, Mihara K. Mitochondrial dynamics: functional link with apoptosis. Int J Cell Biol. 2012;2012:821676.

[41] Lee EY, Ji H, Ouyang Z, Zhou B, Ma W, Vokes SA, et al. Hedgehog pathway-regulated gene networks in cerebellum development and tumorigenesis. Proc Natl Acad Sci U S A. 2010;107:9736-41.

[42] Vokes SA, Ji H, McCuine S, Tenzen T, Giles S, Zhong S, et al. Genomic characterization of Gli-activator targets in sonic hedgehog-mediated neural patterning. Development. 2007;134:1977-89.

[43] Vokes SA, Ji H, Wong WH, McMahon AP. A genome-scale analysis of the cis-regulatory circuitry underlying sonic hedgehog-mediated patterning of the mammalian limb. Genes Dev. 2008;22:2651-63.

[44] Ramirez RD, Sheridan S, Girard L, Sato M, Kim Y, Pollack J, et al. Immortalization of human bronchial epithelial cells in the absence of viral oncoproteins. Cancer Res. 2004;64:9027-34.

[45] Whitehurst AW, Bodemann BO, Cardenas J, Ferguson D, Girard L, Peyton M, et al. Synthetic lethal screen identification of chemosensitizer loci in cancer cells. Nature. 2007;446:815-9.

[46] Papandreou I, Cairns RA, Fontana L, Lim AL, Denko NC. HIF-1 mediates adaptation to hypoxia by actively downregulating mitochondrial oxygen consumption. Cell Metab. 2006;3:187-97.

CHAPTER 3

COMPARATIVE PROTEOMIC ANALYSIS REVEALS CHARACTERISTIC MOLECULAR CHANGES ACCOMPANYING THE TRANSFORMATION OF NONMALIGNANT TO CANCER LUNG CELLS

Author – Md Maksudul Alam and Daniela Cadinu

Conception and design – Li Zhang, Md Maksudul Alam and Daniela Cadinu

Experiments – Daniela Cadinu, Md Maksudul Alam, Jagmohan Hooda and Parimaladevi Balamurugan

Analysis – Li Zhang, Robert M Henke, Jagmohan Hooda and Md Maksudul Alam

Department of Biological Sciences

The University of Texas at Dallas

800 West Campbell Road

Richardson, Texas 75080

PREFACE

In this chapter, we will discuss global changes in protein levels accompanying lung tumorigenicity using two isogenic cell lines representing normal and cancer cell line. The data shown in this chapter is published in the manuscript: "Comparative proteomic analysis reveals characteristic molecular changes accompanying the transformation of nonmalignant to cancer lung cells"

Cadinu et al. EuPA Open Proteomics (2014):3

doi:10.1016/j.euprot.2014.01.001

ACKNOWLEDGMENTS

The HCC4017 and HBEC30KT cell lines were kindly provided by Dr. John Minna's lab. Future requests of the lines should be directed to Dr. Minna. We are grateful to Bruce and Anne Stanley (PennState Hershey College of Medicine) for their effective assistance in iTRAQ mass spectrometry and data analysis. This work was supported by the Cecil H. and Ida Green funds (LZ).

ABSTRACT

To identify changes in proteins accompanying transformation of normal lung epithelial cells to cancer cells, we performed a comparative proteomic study using two cell lines representing matching normal and cancer cells. Strikingly, a good number of detected actin cytoskeletal proteins were preferentially downregulated in cancer cells, while similar numbers of proteins in other organelles were up or downregulated. We also found that the formation of stress fibers and

focal adhesions were substantially decreased in cancer cells. Protein network analysis showed that the altered proteins are highly connected. These results provide novel insights into the molecular mechanism promoting lung cancer progression.

KEYWORDS

iTRAQ, Proteomic, Lung cancer, Actin cytoskeleton, Protein network

INTRODUCTION

Lung cancer is the leading cause of cancer-related mortality in the US and worldwide, and about 85% of the cases are non-small-cell lung cancer (NSCLC) [1, 2]. Using established cancer cell lines has been very powerful in identifying molecular mechanisms underlying tumorigenesis. Notably, recent work has established a very useful pair of lung cell lines [3, 4] that can be used to identify changes accompanying the transformation of molecular changes underlying the transformation of normal cells to malignant cells. They are the HBEC30KT and HCC4017 cell lines [3, 4]. The HCC4017 cell line represents non-small-cell lung cancer (NSCLC) cells isolated from a cancer patient, while the HBEC30KT cell line represents the normal, nonmalignant bronchial epithelial cells developed from the same patient. Thus, this pair of cell lines provides a good model for identifying changes associated with cancer, not merely variations among different persons.

The advent of proteomic technologies has made it possible to systematically identify and characterize the alterations in proteins in cells undergoing various physiological and pathophysiological changes. Particularly, the *isobaric tags for relative and absolute quantitation*

(iTRAQ) profiling technology enables the quantitative and direct comparison of the levels of a large number of proteins in two or more samples [5, 6]. The iTRAQ technology employs isobaric tags with the same total mass but different reporter group mass to label peptides, which are then detected by MS/MS mass spectrometry. iTRAQ can simultaneously identify and quantify the levels of over 1000 proteins in 2-8 samples [7]. iTRAQ provides a powerful method for identifying differentially expressed proteins [5]. Thus, we decided to apply the iTRAQ technology to identify the protein changes accompanying lung epithelial cells when they become malignant.

Using iTRAQ, we were able to consistently identify and detect the levels of over 1500 proteins in lung cells. Among them, the levels of over 100 proteins exhibited statistically significant differences in cancer cells, when compared to normal cells. Particularly, the levels of 36 proteins actively involved in the function of actin cytoskeleton and cell motility were selectively downregulated in cancer cells. Further GO analysis identified significant changes in the levels of a group of nuclear regulatory proteins in cancer cells. Network analysis suggested that certain regulatory proteins may play an important role in mediating the changes in proteins in other cellular compartments, such as those involved in actin cytoskeleton. These results show that proteomic analysis can identify important molecular changes underlying cancer cell progression.

RESULTS

iTRAQ detected over 1500 proteins in normal and lung cancer cells

We extracted proteins from both the normal, non-malignant bronchial epithelial cell line HBEC30KT and the NSCLC line HCC4017 [3, 4]. We performed iTRAQ analysis of the proteins and obtained the ratios of proteins in cancer vs normal cells in 8 biological replicates (see Materials and Methods). In total, we detected 1584 proteins with high statistical confidence (Table 3.1). The Local False Discovery Rate (FDR) for the lowest ranking accepted protein ID was less than 5% with the p-value between <0.01 and <0.001. The ratios from the eight biological replicates were calculated and analyzed.

Table 3.1. Summary of the proteins identified in HCC

	Total	Nuc	Cyto-s	Cyto-p	Mito	ER	Act
Detected	1584	532	392	1182	241	192	118
Up	183 (53)	72 (17)	34 (14)	121 (38)	18 (5)	24 (8)	1(1)
Down	275 (86)	52 (17)	51 (14)	204 (69)	34 (7)	19 (6)	81(36)

The numbers shown here are the up or down regulated proteins selected by fold changes. The numbers in the parenthesis represent those with p Value <0.05. Nuc, Nucleus; Cyto-s, Cytosol; Cyto-p, Cytoplasm; Mito, Mitochondria; ER, Endoplasmic reticulum; Act, Actin Cytoskeleton.

The majority of the detected proteins were cytoplasmic, including 241 mitochondrial proteins and 118 cytoskeletal proteins (Table 3.1). 532 nuclear proteins were also detected. Evidently, iTRAQ provided the detection and comparison of the protein levels of a large number of proteins, which cannot be achieved by using other proteomic techniques, such as two-dimensional gel electrophoresis and mass spectrometry [8].

iTRAQ data analysis shows that the levels of a number of detected proteins were consistently changed in lung cancer cells

We combined eight sets of data from iTRAQ analysis and identified proteins whose levels were consistently up or downregulated in cancer cells using fold changes (see Materials and Methods). From a complete lists of 1584 up or downregulated proteins and their ratios in cancer vs normal cells, we calculated p values for the detected proteins. We further narrowed down upregulated and downregulated proteins by selecting only those with p values <0.05. Table 3.1 shows the data from both fold changes and those with p value cut off. 183 proteins (53 with p values <0.05) were consistently upregulated by at least 1.3-fold, while 275 proteins (86 with p values <0.05) were consistently downregulated by at least 1.3-fold in cancer cells (with ratio of cancer vs normal less than 0.76).

Furthermore, we confirm the detected changes by using the conventional Western blotting [9]. We performed Gene Ontology (GO) analysis to analyze the up- and downregulated proteins. Although applying p values substantially decreased the number of proteins changed in NSCLC cells, the trends of changes and the main conclusions remained remarkably unchanged (see Table 3.1 and data described below). For example, 124 (72+52; 17+17 with p value cutoff) out of 532 detected nuclear proteins were changed, while 52 (18+34; 5+7 with p value cutoff) out of 241 detected mitochondrial proteins were changed. The sensitivity of iTRAQ, not experimental artifacts, is likely responsible for the lower number of proteins with statistically significant p values. Thus, many detected changes may be valid, even though the p values

Table 3.2. A List of Actin Cytoskeletal Proteins Downregulated in NSCLC Cells

Protein ID	Gene Symbol	Description	Fold	p-value
NP_001605	ACTG1	actin, cytoplasmic 2	0.3	2.39E-03
NP_001005386	ACTR2	actin-related protein 2	0.6	1.67E-02
NP_005712	ACTR3	actin-related protein 3	0.3	3.18E-06
NP_653080	AKAP12	A-kinase anchor protein 12	0.4	7.45E-11
NP_001002858	ANXA2	annexin A2 isoform 1	0.1	3.60E-68
NP_005709	ARPC4	actin-related protein 2/3 complex subunit 4	0.5	4.10E-02
NP_004333	CALD1	caldesmon isoform 2	0.1	7.12E-10
NP_001894	CTNNA1	catenin alpha-1	0.4	1.67E-02
NP_060293	DUSP23	dual specificity protein phosphatase 23	0.1	3.09E-03
NP_001104026	FLNA	filamin-A isoform 2	0.2	4.46E-29
NP_001157791	FLNB	filamin-B isoform 4	0.6	5.50E-03
NP_001157789	FLNB	filamin-B isoform 1	0.5	4.33E-02
NP_001531	HSPB1	heat shock protein beta-1	0.1	4.17E-09
NP_003861	IQGAP1	ras GTPase-activating-like protein	0.5	1.54E-03
NP_000413	KRT17	keratin, type I cytoskeletal 17	0.1	2.67E-05
NP_005547	KRT7	keratin, type II cytoskeletal 7	0.3	3.22E-08
NP_002435	MSN	moesin	0.6	1.36E-04
NP_001243024	MYH10	myosin-10 isoform 3	0.1	1.12E-02
NP_002464	MYH9	myosin-9	0.2	2.04E-55
NP_066299	MYL6	myosin light polypeptide 6	0.4	1.06E-07
NP_006088	MYL9	myosin regulatory light polypeptide 9	0.1	1.57E-02
NP_001074419	MYO1C	myosin-Ic	0.2	1.84E-05
NP_006087	NDRG1	protein NDRG1	0.1	4.40E-04
NP_976227	PDLIM7	PDZ and LIM domain protein 7	0.2	1.90E-04
NP_005013	PFN1	profilin-1	0.6	2.04E-03
NP_004395	Sept2	Septin 2	0.6	2.98E-03
NP_003177	TAGLN	transgelin	0.2	4.10E-03
NP_003555	TAGLN2	transgelin-2	0.1	3.60E-16
NP_006280	TLN1	talin-1	0.4	1.88E-11
NP_066932	TMSB4X	thymosin beta-4	0.3	1.10E-02
NP_001018006	TPM1	tropomyosin alpha-1 chain	0.6	2.79E-03
NP_705935	TPM3	tropomyosin alpha-3 chain	0.7	2.22E-02
NP_001138632	TPM4	tropomyosin alpha-4 chain	0.3	1.52E-06
NP_006073	TUBA1B	tubulin alpha-1B chain	0.3	9.18E-09
NP_009055	UTRN	utrophin	0.1	3.09E-02
NP_003452	ZYX	zyxin	0.5	5.26E-03

are too high. The most striking change is that many (82 or 37 out of 118) of the detected proteins with functions in the formation and regulation of actin cytoskeleton were changed. Furthermore, among those actin cytoskeletal proteins changed in cancer cells, all but one of these proteins were downregulated in cancer cells (see column "Act" Table 3.1).

Network analysis reveals characteristic changes underlying the transformation of lung cancer cells

The most prominent change in lung cancer cells identified by iTRAQ and GO analysis is the downregulation of an overwhelming majority of detected proteins involved in the function and regulation of the actin cytoskeleton (see Tables 3.1 and 3.2). These proteins (Table 3.2) play important roles in the formation of actin stress fibers and in cell adhesion and motility [10-13]. These proteins form a complex network (2) connecting the functions of actin cytoskeleton, adhesion and extracellular matrix (For complete information and for comparison, changed proteins selected only by fold changes and those by both fold changes and p values are highlighted differently in the networks). The downregulation of these proteins likely leads to the changes in actin cytoskeleton, cell-cell adhesion and cell motility accompanying cancer cell transformation.

Another important class of proteins that were changed in cancer cells are the nuclear proteins. We found that 72 (17 with p value cutoff) nuclear proteins were upregulated (Table 3.3), while 52 (17 with p value cutoff) were downregulated in cancer cells (Table 3.4). These nuclear proteins can interact with each other, and they form a very interconnected network [9].

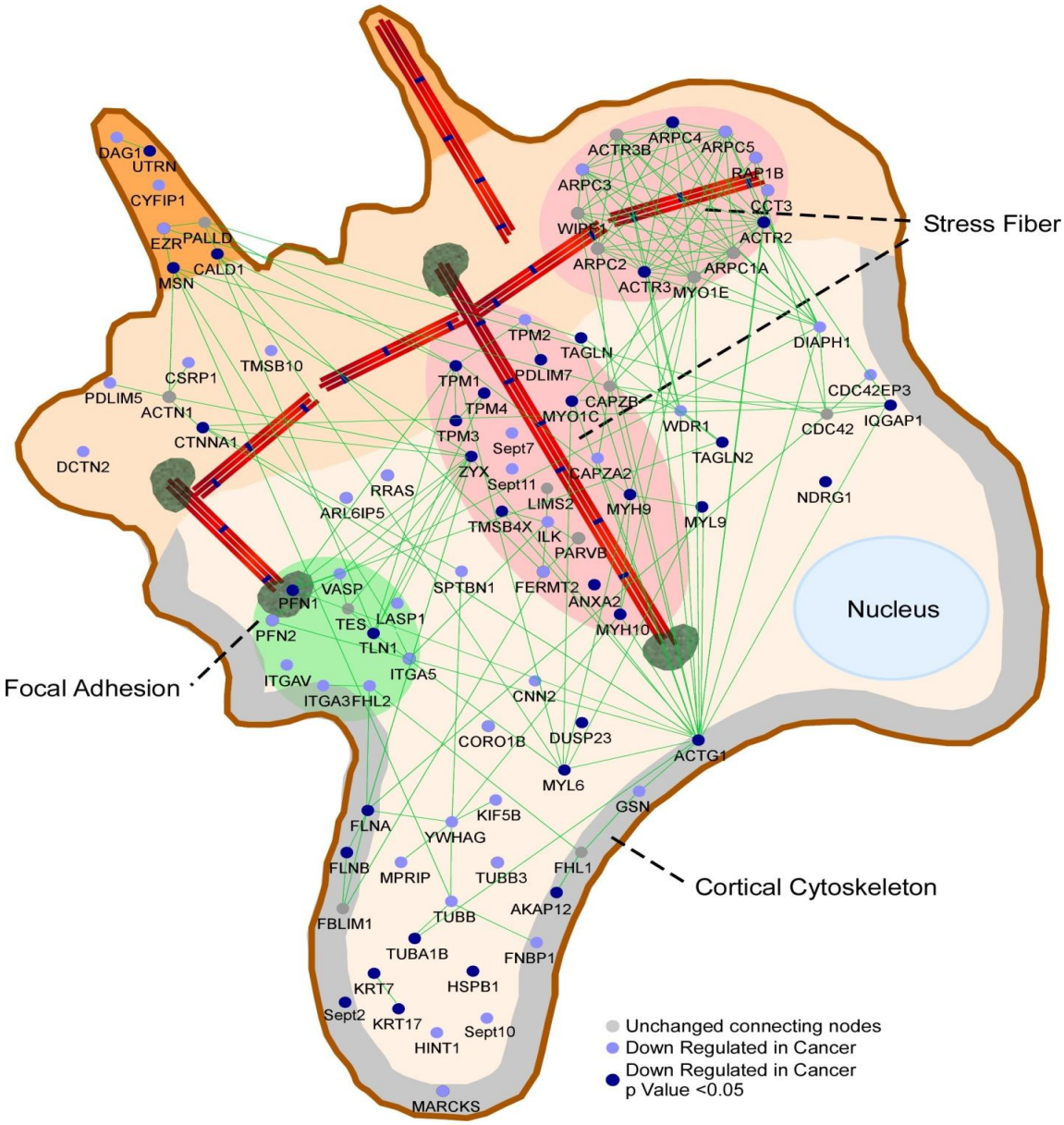

Figure 3.1. Graphical representation of protein-protein interaction networks for downregulated actin cytoskeletal proteins. The network was constructed using the tools and edge data available on the Genemania website. Node attribute assignment (GO terms and Expression) was performed in Cytoscape along with network arrangement. Final visuals were performed in CANVAS. Blue and light blue nodes represent proteins that are down regulated in cancer. Dark blue ones are selected based on both fold changes and p values, while light blue ones are selected based only on fold changes. Gray nodes represent unchanged proteins present

in the network. Where possible nodes are positioned into sub-cellular features based on GeneOntology terms. Lines represent an association of the protein to an interaction, a particular complex or functional GO term. The proteins shown in light red ovals are those involved in the formation of dorsal and ventral stress fibers. Proteins shown in the light green circle are those involved in focal adhesions. (For interpretation of the references to color in this legend, the reader is referred to the web version of the article.)

The result suggests that the coordinated changes in this network of nuclear proteins may lead to further downstream changes underlying cancer cell transformation. Indeed, many of these nuclear proteins have regulatory functions, and can affect proteins in other cellular compartments. For example, Figure 3.2 shows that many of the changed nuclear proteins are directly connected to those changed proteins in actin cytoskeleton. Very likely, the changes in these nuclear proteins contribute, at least in part, to the changes in these actin cytoskeletal proteins. For example, the changes in NCL (nucleolin) and PPP1CB may contribute to changes in the expression of actin cytoskeletal proteins, such as MYH9 and MYL9 (see Figure 3.2).

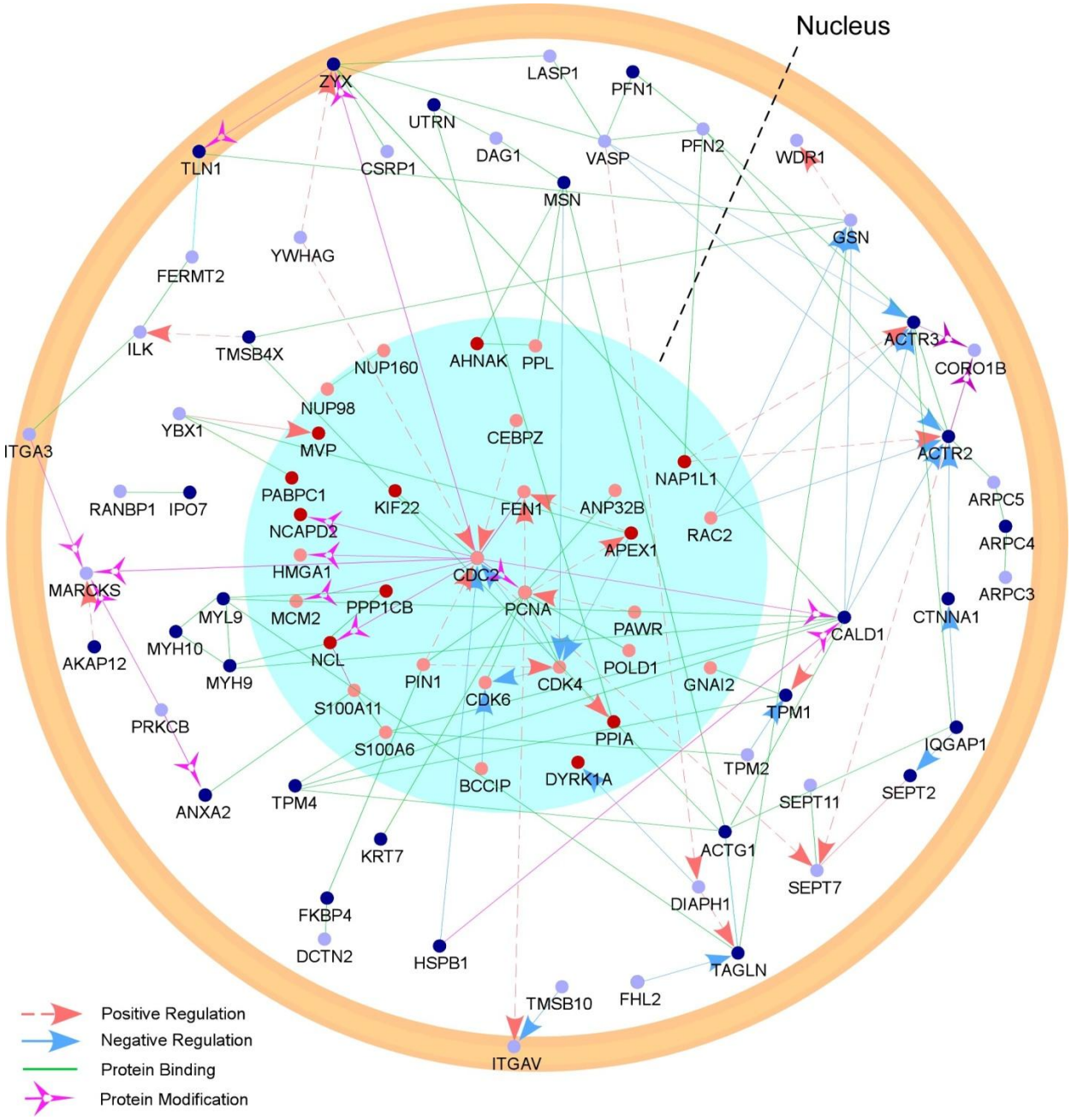

Figure 3.2. Graphical representation of interaction networks for altered nuclear proteins and downregulated actin cytoskeletal proteins. The network was constructed using tools and edge data provided by the Pathway Studios program version 7. Cytoscape was used for network arrangement and CANVAS for final visuals. Red and blue arrows represent positive and negative regulatory edge interaction, respectively. Red and light red nodes represent altered nuclear

proteins, selected based on both fold changes and p values and on fold changes, respectively. Blue and light blue nodes represent downregulated actin cytoskeletal proteins, selected based on both fold changes and p values and on fold changes, respectively. (For interpretation of the references to color in this legend, the reader is referred to the web version of the article.)

Table 3.3. A List of Nuclear Proteins Upregulated in NSCLC Cells

Protein ID	Gene Symbol	Description	Fold	p-value
NP_001632	APEX1	D-(apurinic or apyrimidinic site) lyase	2.6	7.38E-05
NP_005785	DHRS2	dehydrogese/reductase SDR family member 2	3.2	2.23E-05
NP_002005	FKBP4	peptidyl-prolyl cis-trans isomerase FKBP4	2.2	1.90E-03
NP_005508	HMGN2	non-histone chromosomal protein HMG-17	3.5	4.27E-02
NP_006382	IPO7	importin-7	3	2.40E-06
NP_573566	LRPPRC	leucine-rich PPR motif-containing protein	3.9	4.71E-14
NP_004528	NAP1L1	nucleosome assembly protein 1-like 1	4.2	6.31E-03
NP_055680	NCAPD2	non-SMC condensin I complex, subunit D2	87.9	8.12E-05
NP_005372	NCL	nucleolin	2.8	1.81E-13
NP_001018146	NME1-NME2	NME1-NME2 protein	3.3	3.76E-11
NP_002559	PABPC1	polyadenylate-binding protein 1	1.7	4.22E-03
NP_066953	PPIA	peptidyl-prolyl cis-trans isomerase A	1.8	1.40E-02
NP_006436	PRPF8	pre-mR-processing-splicing factor 8	9.7	2.20E-02
NP_116559	RECQL	ATP-dependent D helicase Q1	1.9	1.43E-02
NP_006704	SUB1	activated RNAPII transcriptional coactivator p15	4.3	6.43E-09
NP_001153147	SYNCRIP	heterogeneous nuclear ribonucleoprotein Q	1.9	4.44E-04
NP_001460	XRCC6	X-ray repair cross-complementing protein 6	1.5	3.58E-03

Compared to nuclear proteins, the number of changed mitochondrial proteins is small (Table 3.1). Nonetheless, it is interesting to note that two proteins relating to heme synthesis and function [14], UQCRB (Table 3.5) and UQCRQ are upregulated, although only 5 mitochondrial proteins were detected to be upregulated (with p values <0.05) in cancer cells. This is consistent with our results from another recent study showing that enhanced heme function promotes lung cancer progression [15].

Table 3.4. A List of Nuclear Proteins Downregulated in NSCLC Cells

Protein ID	Gene Symbol	Description	Fold	p-value
NP_001611	AHNAK	neuroblast differentiation-associated protein AHK	0.3	1.79E-39
NP_612429	AHNAK2	protein AHNAK2	0.2	4.41E-02
NP_653080	AKAP12	A-kinase anchor protein 12	0.4	7.45E-11
NP_060293	DUSP23	dual specificity protein phosphatase 23	0.1	3.09E-03
NP_001387	DYRK1A	dual specificity tyrosine-phosphorylation-regulated kinase 1A	0.2	4.33E-02
NP_055416	EHD2	EH domain-containing protein 2	0.2	2.08E-10
NP_001104026	FLNA	filamin-A	0.2	4.46E-29
NP_057371	HP1BP3	heterochromatin protein 1-binding protein 3	0.3	3.14E-03
NP_001531	HSPB1	heat shock protein beta-1	0.1	4.17E-09
NP_003861	IQGAP1	ras GTPase-activating-like protein	0.5	1.54E-03
NP_015556	Kif22	kinesin family member 22	0.1	1.39E-02
NP_002259	KPNA4	importin subunit alpha-4	0.3	3.04E-02
NP_059447	MVP	major vault protein	0.5	1.77E-04
NP_001074419	MYO1C	myosin-Ic isoform b	0.2	1.84E-05
NP_006087	NDRG1	protein NDRG1	0.1	4.40E-04
NP_002700	PPP1CB	S/T-protein phosphatase PP1-beta catalytic subunit	0.6	4.19E-02
NP_036364	PTRF	polymerase I and transcript release factor	0.3	1.06E-06

Table 3.5. A List of Mitochondrial Proteins Upregulated in NSCLC Cells

Protein ID	Gene Symbol	Description	Fold	p-value
NP_001203	C1QBP	complement 1 Q subcomponent-binding protein	1.5	3.27E-02
NP_001907	CYC1	cytochrome c1, heme protein	4.3	3.61E-02
NP_002147	HSPD1	60 kDa heat shock protein	3.3	5.19E-16
NP_573566	LRPPRC	leucine-rich PPR motif-containing protein	3.9	4.71E-14
NP_006285	UQCRB	cytochrome b-c1 complex subunit 7	6.1	1.68E-02

Immunofluorescence microscopy confirms that the actin cytoskeletal structure is permanently altered in lung cancer cells

The iTRAQ results showing the systematic downregulation of many proteins involved in actin cytoskeleton lead us to postulate that actin cytoskeletal structure is dramatically altered in NSCLC cells. Cytoskeleton and focal adhesions are permanently altered during the transformation of normal lung cells to NSCLC cells. To test this idea, we have performed immunofluorescence microscopy to compare the formation of actin cytoskeletal structures in the normal HBEC30KT cells and two NSCLC cell lines HCC4017 and A549 (Figure 3.3A & 3.3B). We used phalloidin staining to examine and compare stress fiber formation in normal and cancer lung cells. We also stained vinculin in order to examine focal adhesions in the cells [16, 17]. Figure 3.3 shows the result of microscopic analysis. Clearly, stress fiber formation was very strong and prominent in the normal lung cells, as expected (see the prominent thick red fibers in the HBEC panels of 3.3A & 3.3B). In the lung cancer cells, however, stress fiber formation was substantially weakened (see the weak and narrow red fibers in the panels HCC and A549). Likewise, stronger and more prominent adhesions were formed in the normal cells, compared to the cancer cells (see the prominent and thick green bands in the panel HBEC in s 3.3A & 3.3B; in panels HCC and A549, only green spots were detected, showing decreased formation of focal adhesions). These results confirmed the results from the iTRAQ studies and showed that the formation of actin cytoskeleton and focal adhesions is permanently altered during the transformation of normal lung cells to NSCLC cells.

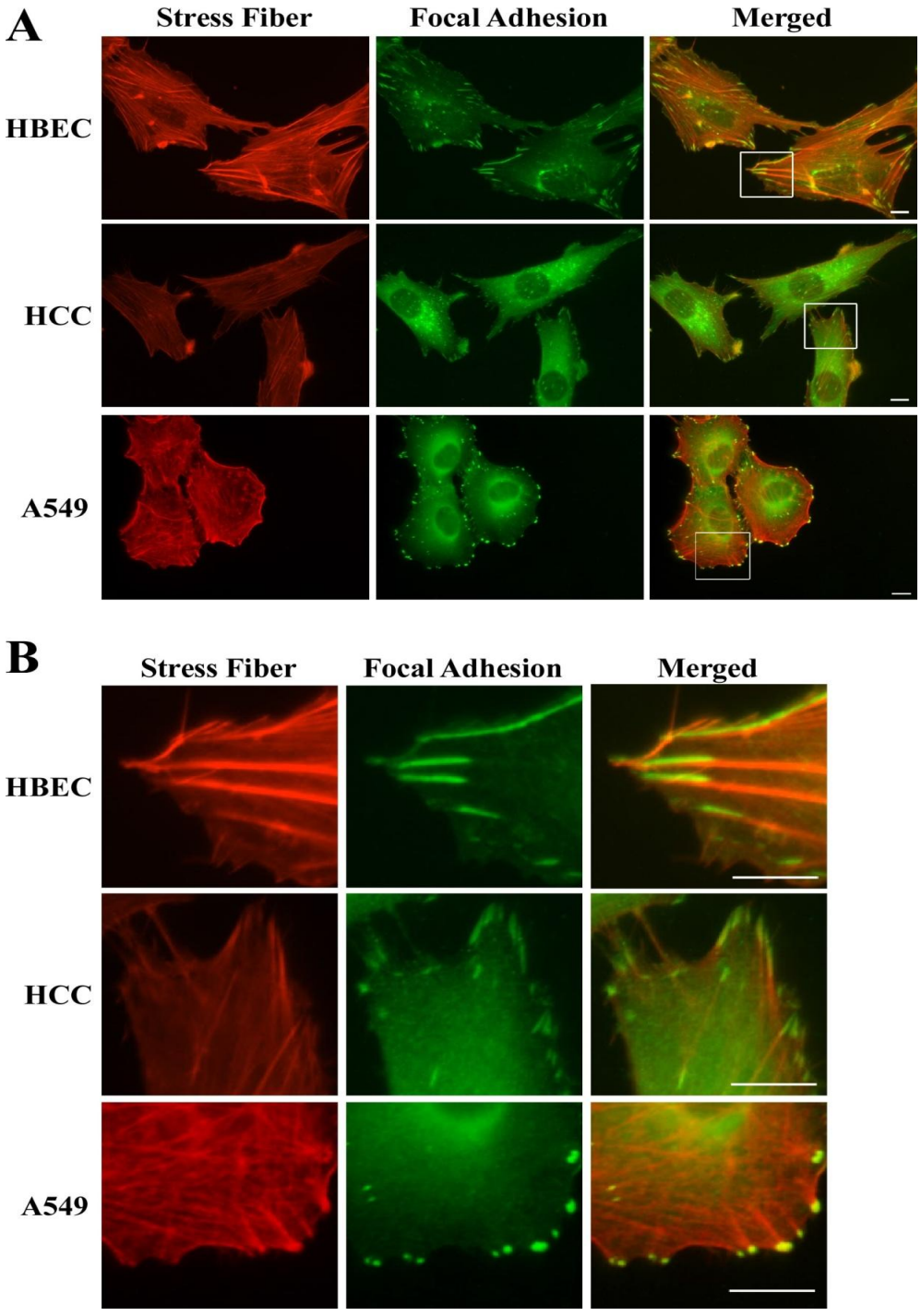

Figure 3.3. Fluorescent microscopic images of stress fibers and focal adhesions formed in normal and cancer lung cells. HBEC30KT, HCC4017 and A549 cells were grown, and F-actin was visualized with Alexa Fluor 568-phalloidin. Focal adhesions were visualized by using a

monoclonal anti-vinculin antibody, followed by detection with a FITC-conjugated goat anti-mouse IgG antibody. Figure 3.3B shows enlarged version of the boxed areas in Figure 3.3A. The bar indicates10 μm.

DISCUSSION

iTRAQ mass spectrometry analysis provides a systematic way to identify the changes in proteins in lung cancer vs normal cells, in the absence of any preconceived limitation and selection. This approach should identify the most prominent protein changes in cancer cells in an unbiased manner. Using iTRAQ, we detected 1584 proteins in the normal HBEC30KT and cancer HCC4017 lung cells. Among them, the levels of 183 (53 with p value cutoff) proteins were significantly upregulated, while the levels of 275 (86 with p value cutoff) proteins were downregulated (Table 3.1). The most striking difference occurred in actin cytoskeleton, where 81 proteins (~3/4 of the detected proteins; 36 with p value cutoff) were downregulated, while only 1 was upregulated, among the 118 detected actin cytoskeletal proteins. The main conclusions from using the information from proteins selected by using only fold changes and from using both fold changes and p value cutoff are largely the same. Thus, the information gained from the analysis of the larger number of changed proteins may also be biologically relevant. Thus, we included all changed proteins in Table 3.2-3.4.

The downregulated actin cytoskeletal proteins include mainly those involved in the formation of stress fibers (both dorsal and ventral), focal adhesions, and cortical actin cytoskeleton (Figure 3.1) [10-13]. These proteins include ACTR2 and ACTR3, which are components of the Arp2/3 complex (see Figure 3.1 and Table 3.2). The Arp2/3 complex stimulates the formation of new actin filaments at the leading edge of motile cells, produces

branches on the sides of existing filaments, and is important for cell motility [18, 19]. Filamin A and B, which are important for regulating the formation of actin cytoskeleton network [20, 21], were downregulated. The downregulated proteins also include myosin and tropomyosin chains, inlcuding MYH9, MYH10, MYL6, MYL9, MYO1C, TPM1, TPM3, TPM4 (see Figure 3.1 and Table 3.2), which have important functions in cell motility and its regulation [22, 23]. Sept2 and other septins, which are key components of cytoskeleton [24], were downregulated. Many of these proteins are critical for stress fiber formation (Figure 3.1) [10, 25]. Furthermore, proteins involved in the formation of focal adhesions [11, 13, 17, 26, 27], such as PFN1 and TLN1, were downregulated. The downregulation of such a high number of proteins involved in the function and regulation of actin cytoskeleton indicates significant changes in actin cytoskeleton and cell motility in lung cancer cells. Notably, this result is also supported by previous comparative proteomic studies of tumor and normal lung tissues. For example, in the study by Li et al, among only 11 identified proteins that are decreased in tumor tissues, 3 are actin cytoskeletal proteins [28]. In another study, it was shown that 3 of the 16 downregulated proteins in tumor tissues are actin cytoskeletal proteins [29].

Indeed, the changes in actin cytoskeleton in NSCLC cells were readily confirmed by fluorescent microscopy. Figure 3.3 shows that the formation of stress fibers and focal adhesions were substantially diminished in NSCLC HCC4017 and A549 cells, compared to the normal cells. Changes in actin cytoskeleton were found to be critical for malignant tumor formation and for promoting the function of oncogenes in tumor progression more than two decades ago [30]. More recent studies have demonstrated the importance of regulation of actin cytoskeleton in cancer cell migration and invasion. Stabilizing actin cytoskeleton is critical for stopping

invading cancer cells and arresting cancer progression [31-34]. Here, our data showed that a systematic and preferential downregulation of actin cytoskeletal proteins diminshes the formation of both stress fibers and focal adhesions, leading to the transformation of normal lung cells to NSCLC cells. While many potential mechanisms can cause changes in actin cytoskeleton [11, 12], our data show that the systematic downregulation of many actin cytoskeletal proteins is a key factor in the progression of NSCLC cells. Perhaps this mechanism to change actin cytoskeleton also operates in other kinds of cancer cells.

Additionally, it is worth noting that NAMPT, TAGLN and EphA2, whose changes were confirmed by Western blotting here, have been investigated peviously regarding their roles in lung cancer. NAMPT, nicotinamide phosphoribosyltransferase precursor, is known to be a therapeutic target for lung cancer and inflammation-related disorders [35, 36]. Hence, its upregulation in NSCLC cells detected here is consistent with its known role in cancer. A previous study identified NAMPT as one of the genes whose transcript levels are downregulated in lung cancer tissues [37]. There are two reasons that can account for the discrepancy with our results. First, we detected proteins, not mRNA. Second, our data are obtained using homogenous cells, while the previous analyzed data used cancer tissues, which contains a combination of different cell types [37]. Our data showed that the levels of both TAGLN (transgelin) and TAGLN2 proteins were downregulated in NSCLC cells. A previous study has shown that the upregulation of TAGLN expression exerts anti-tumour growth and anti-metastasis effects, whereas its levels are inversely correlated with colorectal cancer metastasis [38]. Another study found that TAGLN is upregulated in the tumor-induced reactive myofibroblastic stromal tissue

compartment, while TAGLN2 is upregulated in the neoplastic glandular compartment [39]. These and our results suggest that TAGLN plays an important role in cancer progression.

Further, our Western blotting analysis showed that the levels of both total and ligand-activated (detected by using antibodies to phosphorylated protein) EphA2 proteins were strongly increased in NSCLC cells [9]. Eph receptors are shown to play a wide array of roles in cell adhesion and cell movement, as well as in cancer progression [40-44]. Particularly, the EphA2 receptor has been found to be widely overexpressed in many cancer types [45-47]. The overexpression of EphA2 in NSCLC cells likely contributes to the changes in actin cytoskeleton and adhesions [44].

It is worth noting that a good number of nuclear proteins were up- or downregulated in NSCLC cells (Tables 3.3 and 3.4). These proteins are involved in diverse functions in the nucleus, and many interact directly with each other (Figure 3.2). Interestingly, many of these nuclear proteins also directly interact with the downregulated proteins in actin cytoskeleton (Figure 3.2). The changes in the nucleus and actin cytoskeleton may synergize with each other and further promote the transformation of normal cells to cancer cells. This comparative proteomic study of cancer vs. normal cells employing iTRAQ technology and network analysis shows that permanent systematic changes in a large number of cellular proteins accompany the progression of lung cancer cells, and that iTRAQ is a powerful technique to identify such changes.

CONCLUSIONS

Lung cancer cells exhibit characteristic changes in proteins, when compared to the normal lung epithelial cells. The most dramatic change is the systemic downregulation of many proteins with functions in actin cytoskeleton and adhesion. This downregulation leads to substantial changes in actin cytoskeletal structure, thereby altering cell motility and migration and leading to the progression of lung cancer cells.

METHODS

Lung cell line maintenance and preparation of protein extracts

HBEC30KT and HCC4017 cell lines representing normal and NSCLC cells [3, 4] were provided by Dr. John Minna's lab (UTSW) as a gift. They were developed from the same patient and were maintained in ACL4 supplemented with 2% FBS under 5% CO_2 at 37^{o}C. `HBEC30KT and HCC4017 cells were collected and lysed by using the RIPA buffer (Cell Signaling Technology) containing the protease inhibitor cocktail (Invitrogen) and phosphatase inhibitors. Protein concentrations were determined by using the BCA assay kit (Thermo Scientific).

Protein isobaric labeling with iTRAQ reagents

Proteins from HBEC30KT and HCC4017 cell lines were extracted, and protein concentration was detected, as described above for Western blotting analysis. Isobaric labeling was carried out as described [48] and according to the procedure recommended by the PennState Hershey College of Medicine Mass Spectrometry Core facility (http://med.psu.edu/web/core/proteinsmassspectometry/protocols/itraq). Briefly, 100 μg of

proteins from each sample was reduced with 5mM TCEP (tris-(2-carboxyethyl) phosphine) at 60 °C for 1 h. Cysteine residues were blocked with 18 mM iodoacetamide at room temperature for 30 min. Then, the proteins were precipitated with ice cold acetone (90% v/v) overnight at -20 °C and centrifuged. The protein pellets were washed with ice cold 90% acetone and 20 mM TEAB (triethylammoniumbicarbonate) and air-dried. Protein pellets were then suspended in buffer containing 0.5 M TEAB-0.1% SDS, at a concentration of 5mg/ml, and then digested with trypsin at 40°C overnight. Isobaric labeling reagents were purchased from Applied Biosystems. 8plex isobaric labeling kit containing tags with a reporter mass ranging from 113-121 was used. Isobaric tagging iTRAQ reagent in isopropanol was added directly to the protein digest to reach a final concentration of 61% isopropanol. The mixture was incubated at room temperature for 2h. The reaction was then quenched by addition of 100 µl of water. The eight labeled peptide pools were mixed together and lyophilized.

Mass spectrometry

The iTRAQ protein samples were analyzed by the PennState Hershey College of Medicine Mass Spectrometry Core facility. Prior to MS analysis, protein samples were fractionated and separated into 15 fractions by using 2D-LC. SCX Separations were performed on a passivated Waters 600E HPLC system, using a 4.6 X 250 mm PolySULFOETHYL Aspartamide column (PolyLC, Columbia, MD), at a flow rate of 1 ml/min. Buffer A contained 10 mM ammonium formate, pH 2.7, in 20% acetonitrile/80% water. Buffer B contained 666 mM ammonium formate, pH 2.7, in 20% acetonitrile/80% water. The gradient was Buffer A at 100% (0-22 minutes following sample injection), 0%→40% Buffer B (16-48 min), 40%→100% Buffer B

(48-49 min), then isocratic 100% Buffer B (49-56 min), then at 56 min switched back to 100% Buffer A to re-equilibrate for the next injection. The first 26 ml of eluant (containing all flow-through fractions) was combined into one fraction, then 14 additional 2-ml fractions were collected. All 15 of these SCX fractions were dried down completely to reduce volume and to remove the volatile ammonium formate salts, then resuspended in 9 µl of 2% (v/v) acetonitrile, 0.1% (v/v) trifluoroacetic acid and filtered prior to reverse phase C18 nanoflow-LC separation. The fractionation was performed to purify the peptides and increase the sensitivity of MS. Information from all fractions were combined and analyzed as a whole in the end.

For 2nd dimension separation by reverse phase nanoflow LC, each SCX fraction was autoinjected onto a Chromolith CapRod column (150 X 0.1 mm, Merck) using a 5 µl injector loop on a Tempo LC MALDI Spotting system (ABI-MDS/Sciex). Buffer C was 2% acetonitrile, 0.1% trifluoroacetic acid, and Buffer D was 98% acetonitrile, 0.1% trifluoroacetic acid. The elution gradient was 95% C/ 5% D (2ul per minute flow rate from 0-3 min, then 2.5ul per minute from 3-8.1 min), 5% D→38% D (8.1-40 min), 38% D→80% D (41-44 min), 80% D→5% D (44-49 min) (initial conditions). Flow rate was 2.5 µl/min during the gradient, and an equal flow of MALDI matrix solution was added post-column (7 mg/ml recrystallized CHCA (a-cyano-hydroxycinnamic acid), 2 mg/ml ammonium phosphate, 0.1% trifluoroacetic acid, 80% acetonitrile).

After sample spot drying above, thirteen calibrant spots (ABI 4700 Mix) were added to each plate manually. MALDI target plates (15 per experiment) were analyzed in a data-dependent manner on an ABI 5800 MALDI TOF-TOFs. MS/MS spectra were taken by using up to 2500 laser shots per spectrum at Laser Power 3000, with CID gas Air at 1.2 to 1.3 x 10^{-6} Torr.

As each plate was entered into the instrument, a plate calibration/MS Default calibration update was performed, and then the MS/MS default calibration was updated. MS Spectra were then acquired from each sample spot using the newly updated default calibration, using 500 laser shots per spot, laser intensity 3200. A plate-wide interpretation was then automatically performed, choosing the highest peak of each observed m/z value for subsequent MS/MS analysis.

Up to 2500 laser shots at laser power 4200 were accumulated for each MS/MS spectrum. When the MS and MS/MS spectra from all 15 plates in a sample set had been acquired, protein identification and quantitation were performed using the Paragon algorithm as implemented in Protein Pilot 4.0 software, searching the spectra against either species-specific subsets (plus common contaminants) of the NCBInr database concatenated with a reversed "decoy" version of itself, or the entire NCBInr database. For ProteinPilot analyses, the preset Thorough Search settings were used, and identifications must have a ProteinPilot Unused Score > 1.3 (>95% Confidence interval) in order to be accepted. In addition, the only protein IDs accepted must have a "Local False Discovery Rate" estimation of no higher than 5%, as calculated from the slope of the accumulated Decoy database hits by the PSPEP (Proteomics System Performance Evaluation Pipeline) program by Sean Seymour and colleagues [49]. Note that this Local or "Instantaneous" FDR estimate is much more stringent than $p<0.05$ or 95% confidence scores in Mascot, Sequest, ProteinPilot, or the aggregate False Discovery Rate estimations (2 X number of Decoy database IDs/Total IDs at any chosen threshold score) commonly used in the literature, and combined with the ProGroup algorithm included in ProteinPilot gives a very conservative and fully MIAPE-compliant list of proteins identified. The total human sequences searched

contain 30345 Protein Sequences, plus 360 common lab contaminants. The Local False Discovery Rate (FDR) for the lowest ranking accepted protein ID was less than 5% with the p-value between <0.01 and <0.001.

Mass spectrometry data analysis

8plex iTRAQ MS/MS analysis was performed twice, with each set having 4 normal and 4 cancer cell samples. Therefore, we gained 4 sets of iTRAQ data for each experiment. From two experiments, we gained 8 sets of protein ratios comparing cancer cell line (HCC4017) with the normal cell line (HBEC30KT). Only those proteins that were identified in at least four experiments were considered as detected. Data from each experiment were normalized, and estimated changes in the relative amounts of each identified protein (i.e., cancer vs. normal cells) calculated. Each of the peptides identified from a specific protein is presented as a ratio, with a ratio of 1.0 representing no significant change. The mean and median ratios for each identified proteins were calculated in MS Excel. Proteins that showed ratios higher than 1 in all detected samples and had mean and median ratios of at least 1.3 were considered to be upregulated, while proteins that showed ratios less than 1 in all detected samples and had mean and median ratios of less than 0.76 were considered to be downregulated. The statistical significance of altered proteins were further confirmed by using p values. The p values were calculated based on Fisher's method [50]. For all p-values p_i from n replicates, x=-2*$\sum$[ln(p_i)] was calculated, which follows *chi-squar*e distribution with degree of freedom *2n*, to obtain the combinational p-value for one protein. Those with p values <0.05 are listed in Tables 2-5.

Gene Ontology (GO) analysis of identified proteins and up-or down-regulated proteins in cancer cells was performed by the NIH DAVID application. Protein interaction networks were constructed by using Pathway Studio version 7 and by using the GENEMANIA program.

Immunofluorescence microscopy

For immunofluorescence microscopy, cells were grown on polylysine-coated slides and were fixed with 4% formaldehyde. Cells were washed two times with PBS containing 0.2% BSA and then permeabilized with 0.1% Triton X-100 containing 0.2% BSA. Immunofluorescence staining was performed as described [16]. Fluorescent images were acquired by using a multi-channel Zeiss Axio Observer.Z1 fluorescent microscope with a Zeiss 40X Oil immersion lens and with a high speed AxioCam MRm Rev3 monochrome camera. The software used was Carl Zeiss AxioVision Rel 4.8.1, set to the multi-dimensional mode that allows automatic filter changes and image capturing. Vinculin was stained with monoclonal anti-vinculin antibody (Sigma V9131). The secondary antibody used was FITC-conjugated goat anti-mouse antibody (Invitrogen A11017). F-actin was visualized with Alexa Fluor 568-phalloidin (Invitrogen A12380).

ABBREVIATIONS

ACTR2: ARP2 actin-related protein 2

EphA2: Ephrin type-A receptor 2

GO: Gene ontology

iTRAQ: Isobaric tags for relative and absolute quantitation

MYH9: Myosin heavy chain 9

MYL9: Myosin light chain 9

NAMPT: Nicotinamide phosphoribosyltransferase

NCL: Nucleolin

TAGLN2: Transgelin-2

TLN1: Talin-1

TPM3: Tropomyosin 3

UQCRB: Cytochrome b-c1 complex subunit 7

PFN1: Profilin-1

PPP1CB: S/T-protein phosphatase PP1-beta catalytic subunit

REFERENCES

[1] Jemal A, Siegel R, Xu J, Ward E. Cancer statistics, 2010. CA Cancer J Clin. 2010;60:277-300.

[2] Organization WH. Cancer. Fact sheet no. 297. World Health Organization; 2011.

[3] Ramirez RD, Sheridan S, Girard L, Sato M, Kim Y, Pollack J, et al. Immortalization of human bronchial epithelial cells in the absence of viral oncoproteins. Cancer Res. 2004;64:9027-34.

[4] Whitehurst AW, Bodemann BO, Cardenas J, Ferguson D, Girard L, Peyton M, et al. Synthetic lethal screen identification of chemosensitizer loci in cancer cells. Nature. 2007;446:815-9.

[5] Ross PL, Huang YN, Marchese JN, Williamson B, Parker K, Hattan S, et al. Multiplexed protein quantitation in Saccharomyces cerevisiae using amine-reactive isobaric tagging reagents. Mol Cell Proteomics. 2004;3:1154-69.

[6] Aggarwal K, Choe LH, Lee KH. Shotgun proteomics using the iTRAQ isobaric tags. Brief Funct Genomic Proteomic. 2006;5:112-20.

[7] Shah AN, Cadinu D, Henke RM, Xin X, Dastidar RG, Zhang L. Deletion of a Subgroup of Ribosome-related Genes Minimizes Hypoxia-induced Changes and Confers Hypoxia Tolerance. Physiol Genomics. 2011;43:855-72.

[8] Rubporn A, Srisomsap C, Subhasitanont P, Chokchaichamnankit D, Chiablaem K, Svasti J, et al. Comparative proteomic analysis of lung cancer cell line and lung fibroblast cell line. Cancer Genomics Proteomics. 2009;6:229-37.

[9] Galdi S, Cadinu M, Tomasetto C. The roots of stereotype threat: when automatic associations disrupt girls' math performance. Child Dev. 2014;85:250-63.

[10] Naumanen P, Lappalainen P, Hotulainen P. Mechanisms of actin stress fibre assembly. J Microsc. 2008;231:446-54.

[11] Parsons JT, Horwitz AR, Schwartz MA. Cell adhesion: integrating cytoskeletal dynamics and cellular tension. Nat Rev Mol Cell Biol. 2010;11:633-43.

[12] Olson EN, Nordheim A. Linking actin dynamics and gene transcription to drive cellular motile functions. Nat Rev Mol Cell Biol. 2010;11:353-65.

[13] Zaidel-Bar R, Itzkovitz S, Ma'ayan A, Iyengar R, Geiger B. Functional atlas of the integrin adhesome. Nat Cell Biol. 2007;9:858-67.

[14] Anderson KE, Sassa S, Bishop DF, Desnick RJ. Disorders of heme biosynthesis: X-linked sideroblastic anemia and the porphyrias. In: Scriver CR, Beaudt AL, Sly WS, Valle D, Barton C, Kinzler KW, et al., editors. The metabolic and molecular bases of inherited disease. New York: The McGraw-Hill Companies, Inc.; 2009. p. Chapter 124: 1-53.

[15] Hooda J, Cadinu D, Alam MM, Shah A, Cao TM, Sullivan LA, et al. Enhanced heme function and mitochondrial respiration promote the progression of lung cancer cells. PLoS One. 2013;8:e63402.

[16] Tojkander S, Gateva G, Schevzov G, Hotulainen P, Naumanen P, Martin C, et al. A molecular pathway for myosin II recruitment to stress fibers. Curr Biol. 2011;21:539-50.

[17] Ziegler WH, Gingras AR, Critchley DR, Emsley J. Integrin connections to the cytoskeleton through talin and vinculin. Biochem Soc Trans. 2008;36:235-9.

[18] Pollard TD. Regulation of actin filament assembly by Arp2/3 complex and formins. Annu Rev Biophys Biomol Struct. 2007;36:451-77.

[19] Rotty JD, Wu C, Bear JE. New insights into the regulation and cellular functions of the ARP2/3 complex. Nat Rev Mol Cell Biol. 2013;14:7-12.

[20] Yue J, Huhn S, Shen Z. Complex roles of filamin-A mediated cytoskeleton network in cancer progression. Cell Biosci. 2013;3:7.

[21] Djinovic-Carugo K, Carugo O. Structural portrait of filamin interaction mechanisms. Curr Protein Pept Sci. 2010;11:639-50.

[22] Gunning PW, Schevzov G, Kee AJ, Hardeman EC. Tropomyosin isoforms: divining rods for actin cytoskeleton function. Trends Cell Biol. 2005;15:333-41.

[23] Hartman MA, Finan D, Sivaramakrishnan S, Spudich JA. Principles of unconventional myosin function and targeting. Annu Rev Cell Dev Biol. 2012;27:133-55.

[24] Mostowy S, Cossart P. Septins: the fourth component of the cytoskeleton. Nat Rev Mol Cell Biol. 2012;13:183-94.

[25] Pellegrin S, Mellor H. Actin stress fibres. J Cell Sci. 2007;120:3491-9.

[26] Campbell ID. Studies of focal adhesion assembly. Biochem Soc Trans. 2008;36:263-6.

[27] Zaidel-Bar R, Geiger B. The switchable integrin adhesome. J Cell Sci. 2010;123:1385-8.

[28] Li LS, Kim H, Rhee H, Kim SH, Shin DH, Chung KY, et al. Proteomic analysis distinguishes basaloid carcinoma as a distinct subtype of nonsmall cell lung carcinoma. Proteomics. 2004;4:3394-400.

[29] Park HJ, Kim BG, Lee SJ, Heo SH, Kim JY, Kwon TH, et al. Proteomic profiling of endothelial cells in human lung cancer. J Proteome Res. 2008;7:1138-50.

[30] Holme TC. Cancer cell structure: actin changes in tumour cells--possible mechanisms for malignant tumour formation. Eur J Surg Oncol. 1990;16:161-9.

[31] O'Neill GM. Scared stiff: Stabilizing the actin cytoskeleton to stop invading cancer cells in their tracks. Bioarchitecture. 2011;1:29-31.

[32] Stevenson RP, Veltman D, Machesky LM. actin-bundling proteins in cancer progression at a glance. Journal of Cell Science. 2012;125:1073–9.

[33] Hall A. The cytoskeleton and cancer. Cancer Metastasis Rev. 2009;28:5-14.

[34] Yamaguchi H, Condeelis J. Regulation of the actin cytoskeleton in cancer cell migration and invasion. Biochim Biophys Acta. 2007;1773:642-52.

[35] Okumura S, Sasaki T, Minami Y, Ohsaki Y. Nicotinamide phosphoribosyltransferase: a potent therapeutic target in non-small cell lung cancer with epidermal growth factor receptor-gene mutation. J Thorac Oncol. 2012;7:49-56.

[36] Montecucco F, Cea M, Cagnetta A, Damonte P, Nahimana A, Ballestrero A, et al. Nicotinamide phosphoribosyltransferase as a target in inflammation- related disorders. Curr Top Med Chem. 2013;13:2930-8.

[37] Srivastava M, Khurana P, Sugadev R. Lung cancer signature biomarkers: tissue specific semantic similarity based clustering of digital differential display (DDD) data. BMC Res Notes. 2012;5:617.

[38] Chunhua L, Donglan L, Xiuqiong F, Lihua Z, Qin F, Yawei L, et al. Apigenin up-regulates transgelin and inhibits invasion and migration of colorectal cancer through decreased phosphorylation of AKT. J Nutr Biochem. 2013;24:1766-75.

[39] Rho JH, Roehrl MH, Wang JY. Tissue proteomics reveals differential and compartment-specific expression of the homologs transgelin and transgelin-2 in lung adenocarcinoma and its stroma. J Proteome Res. 2009;8:5610-8.

[40] Kaenel P, Mosimann M, Andres AC. The multifaceted roles of Eph/ephrin signaling in breast cancer. Cell Adh Migr. 2012;6:138-47.

[41] Kandouz M. The Eph/Ephrin family in cancer metastasis: communication at the service of invasion. Cancer Metastasis Rev. 2012;31:353-73.

[42] Nievergall E, Lackmann M, Janes PW. Eph-dependent cell-cell adhesion and segregation in development and cancer. Cell Mol Life Sci. 2012;69:1813-42.

[43] Pasquale EB. Eph receptors and ephrins in cancer: bidirectional signalling and beyond. Nat Rev Cancer. 2010;10:165-80.

[44] Singh A, Winterbottom E, Daar IO. Eph/ephrin signaling in cell-cell and cell-substrate adhesion. Front Biosci. 2012;17:473-97.

[45] Ireton RC, Chen J. EphA2 receptor tyrosine kinase as a promising target for cancer therapeutics. Curr Cancer Drug Targets. 2005;5:149-57.

[46] Landen CN, Kinch MS, Sood AK. EphA2 as a target for ovarian cancer therapy. Expert Opin Ther Targets. 2005;9:1179-87.

[47] Wykosky J, Debinski W. The EphA2 receptor and ephrinA1 ligand in solid tumors: function and therapeutic targeting. Mol Cancer Res. 2008;6:1795-806.

[48] Keshamouni VG, Michailidis G, Grasso CS, Anthwal S, Strahler JR, Walker A, et al. Differential protein expression profiling by iTRAQ-2DLC-MS/MS of lung cancer cells undergoing epithelial-mesenchymal transition reveals a migratory/invasive phenotype. J Proteome Res. 2006;5:1143-54.

[49] Tang WH, Shilov IV, Seymour SL. Nonlinear fitting method for determining local false discovery rates from decoy database searches. J Proteome Res. 2008;7:3661-7.

[50] Fisher RA. Statistical Methods for Research Workers. 12 ed. Edinburgh: Oliver and Boyd; 1954.

CHAPTER 4

DISCUSSION AND CONCLUSIONS

DISCUSSION

Cancer metabolism has drawn considerable attention from researchers worldwide as a crucial factor of cancer progression and survival. Recently, in the past several years many important aspects of metabolic reprogramming of cancer cells has been discovered which is far beyond the accelerated glycolysis under aerobic condition described by Otto Warburg in 1952 [1]. Metabolic reprogramming is now considered as one of the important hallmarks of cancer [1] which is contributed by both genetic and epigenetic changes [2]. Metabolic reprogramming is an important factor to promote various stages in cancer development, such as, growth survival and metastasis [3-10].

Lung cancer is the most diagnosed cancer and the leading cause of cancer death worldwide [11]. NSCLC account for about 85% of the lung cancer cases with 5 years overall survival rate of less than 15% [12]. Previous work in our lab identifies a key alteration in NSCLC's metabolism. We found that the level of oxygen utilizing hemoproteins and the rate of respiration are increased in NSCLC cells compare to normal cell [13]. In the first chapter I discussed about metabolic reprogramming of cancer cell metabolism. In the second chapter of I have studied the effect of CycT on NSCLC cell's respiration and how it affects mitochondrial function to induce mitochondrial fragmentation that leads to cell death via apoptosis. CycT is derived from natural product Cyclopamine to improve its water solubility, is a teratogen that inhibits hedgehog signaling [14]. I also studied the effect of Glucose and Glutamine on NSCLC's oxygen consumption as glucose and glutamine are the two major fuels for cancer [15,

16]. I found that Glutamine is the major respiratory fuel for NSCLC cells as in the absence of glutamine respiration is greatly reduced where as in the absence of Glucose it is either increased or remains unaffected. Interestingly , CycT also reduces the respiration in these NSCLC cells. I also found that CycT increases the ROS production in the NSCLC cells in a time dependent manner, the increase in ROS production is preceded by membrane hyperpolarization. Mitochondrial staining showed that the Mitochondria is fragmented in CycT treated NSCLC cells, that is due to the increase level and recruitment of fission protein, DRP1 to the fission site. The mitochondrial fragmentation may release the apoptotic factors that cause apoptosis and cell death.

I also examined the effect of CycT on Heme synthesis and metabolism as our previous work showed that heme plays a critical role in NSCLC's respiration and survival [13]. CycT does not affect the rate of heme synthesis as well as it does not affect the level of proteins involved in heme metabolism. However, CycT greatly reduces the level of Hh signaling target protein Gli1 as expected . Therefore, the impact of CycT on NSCLC's respiration is not through affecting heme metabolism. I have also shown that CycT reduces the level of phosphorylated p44/42 MAPK which is critical for the activation of Hh signaling [17].

In the third chapter of my dissertation I have shown data of a comparative proteomic study using two isogenic cell line representing NSCLC cell (HCC4017) and normal lung cell (HBEC30KT). iTRAQ technology was used in this study, which employs tags with the same total mass but a different reporter group mass to label the peptides [18] is a power technology to identify differentially expressed proteins [19]. In total, 1584 proteins were detected in the two cell line, majority of the protein detected was Cytoplasmic including 241 mitochondrial proteins

and 118 cytoskeletal proteins. The number of nuclear proteins detected was 532. Among all the detected proteins, 183 proteins were upregulated and 275 proteins were downregulated , with the similar number of proteins in different organelles is either up or downregulated in NSCLC cell line. However , the proteins involved in actin cytoskeleton were preferentially downregulated in with 81 proteins showing downregulation and only 1 protein showing upregulation. The down regulated actin cytoskelatal proteins are involved in the formation of stress fiber, focal adhesion and cortical actin filaments [20-25]. this finding was supported by imuunofluorescence microscopy showing that the such actin cytoskelatal structures are much weaker and thinner in NSCLC cell lines (HCC4017 and A549) compare to the normal cell line (HBEC30KT). It has been reported previously that stabilized acitn cytoskelatal structures (stress fiber and focal adhesion) arrests tumorigenic transformation and cancer progression [26-30]. Therefore, the preferential downregulation of actin cytoskelatal proteins causing weaker stress fiber and focal adhesion, might play an important role in the transformation of normal lung cell to NSCLC cell. Our data also shows that the levels of TAGLN (transgelin) TAGLN2 are downregulated in NSCLC cells , these proteins was shown to have anti tumor growth and anti metastasis activity [31]. Furhthermore, our data shows that the level of both total and phosphorylated EphA2 is upregulated in NSCLC cell [32]. EphA2 has been shown to play critical role in cell adhesion and cell movement aiding cancer progression [33-37]. The over expression of EphA2 might contribute to the changes in actin cytoskelatal structure leading to the malignancy of lung cell [37]. A good number of nuclear proteins were also up or downregulated in NSCLC cells, these proteins form inter connected network with themselves as well as with the downregulated actin

cytoskelatal proteins. Therefore the changes in nuclear protein may cause/coordinate the changes in cytoskelatal proteins leading to tumorigenesis and progression of NSCLC cells

CONCLUSIONS

The increased rate of Glycolysis in cancer cell is often accompanied by higher rate of mitochondrial respiration. Tumors with defective OXPHOS sometimes regain the capacity of mitochondrial respiration through the transfer mitochondria, which is critical for initiation and progression of such tumors. The heme influx as well as the rate of OXPHOS is intensified in NSCLC cells. As heme is the part of many OXPHOS complexes and diminishing heme availability reduces the rate of OXPHOS as well as selectively kills NSCLC cells. Therefore, increased heme availability might causes the intensified mitochondrial respiration in NSCLC cells that promote tumor development and progression.

The depletion of glutamine reduces the rate of respiration in NSCLC cell lines. Hh signaling inhibitor, CycT and SANT1 reduces the mitochondrial respiration in NSCLC cell lines without affecting the heme metabolism. These Hh inhibitors cause mitochondrial hyperpolarization, increased ROS generation, increased mitochondrial fission thereby promoting mitochondrial fragmentation and apoptosis of NSCLC cells. This novel mechanism of Hh inhibitors can provide insights of how to optimize anti Hh signaling strategy to treat cancer with aberrant Hh signaling.

Comparative proteomic study using an isogenic pair of normal and NSCLC cell line reveals changes in proteins of different organelle carrying different function. The most remarkable change is the preferential downregulation of protein involved in actin cytoskeleton.

Downregulation of such proteins leads to the thinner stress fiber and weaker focal adhesion complex, which might play important role in the malignant transformation of lung epithelial cells.

REFERENCES

[1] Fan TW, Warmoes MO, Sun Q, Song H, Turchan-Cholewo J, Martin JT, et al. Distinctly perturbed metabolic networks underlie differential tumor tissue damages induced by immune modulator beta-glucan in a two-case ex vivo non-small-cell lung cancer study. Cold Spring Harb Mol Case Stud. 2016;2:a000893.

[2] Tan AS, Baty JW, Berridge MV. The role of mitochondrial electron transport in tumorigenesis and metastasis. Biochim Biophys Acta. 2014;1840:1454-63.

[3] Dang L, White DW, Gross S, Bennett BD, Bittinger MA, Driggers EM, et al. Cancer-associated IDH1 mutations produce 2-hydroxyglutarate. Nature. 2009;462:739-44.

[4] Nomura DK, Long JZ, Niessen S, Hoover HS, Ng SW, Cravatt BF. Monoacylglycerol lipase regulates a fatty acid network that promotes cancer pathogenesis. Cell. 2010;140:49-61.

[5] Le A, Lane AN, Hamaker M, Bose S, Gouw A, Barbi J, et al. Glucose-independent glutamine metabolism via TCA cycling for proliferation and survival in B cells. Cell Metab. 2012;15:110-21.

[6] Mullen AR, Wheaton WW, Jin ES, Chen PH, Sullivan LB, Cheng T, et al. Reductive carboxylation supports growth in tumour cells with defective mitochondria. Nature. 2012;481:385-8.

[7] Son J, Lyssiotis CA, Ying H, Wang X, Hua S, Ligorio M, et al. Glutamine supports pancreatic cancer growth through a KRAS-regulated metabolic pathway. Nature. 2013;496:101-5.

[8] Xie H, Hanai J, Ren JG, Kats L, Burgess K, Bhargava P, et al. Targeting lactate dehydrogenase--a inhibits tumorigenesis and tumor progression in mouse models of lung cancer and impacts tumor-initiating cells. Cell Metab. 2014;19:795-809.

[9] Kim D, Fiske BP, Birsoy K, Freinkman E, Kami K, Possemato RL, et al. SHMT2 drives glioma cell survival in ischaemia but imposes a dependence on glycine clearance. Nature. 2015;520:363-7.

[10] Sellers K, Fox MP, Bousamra M, 2nd, Slone SP, Higashi RM, Miller DM, et al. Pyruvate carboxylase is critical for non-small-cell lung cancer proliferation. J Clin Invest. 2015;125:687-98.

[11] Zeng Y, Ruan W, He J, Zhang J, Liang W, Chen Y, et al. Adoptive Immunotherapy in Postoperative Non-Small-Cell Lung Cancer: A Systematic Review and Meta-Analysis. PLoS One. 2016;11:e0162630.

[12] Goldstraw P, Ball D, Jett JR, Le Chevalier T, Lim E, Nicholson AG, et al. Non-small-cell lung cancer. Lancet. 2011;378:1727-40.

[13] Hooda J, Cadinu D, Alam MM, Shah A, Cao TM, Sullivan LA, et al. Enhanced heme function and mitochondrial respiration promote the progression of lung cancer cells. PLoS One. 2013;8:e63402.

[14] Fan Q, Gu D, He M, Liu H, Sheng T, Xie G, et al. Tumor shrinkage by cyclopamine tartrate through inhibiting hedgehog signaling. Chin J Cancer. 2011;30:472-81.

[15] Anastasiou D, Cantley LC. Breathless cancer cells get fat on glutamine. Cell Res. 2012;22:443-6.

[16] Ward PS, Thompson CB. Metabolic reprogramming: a cancer hallmark even warburg did not anticipate. Cancer Cell. 2012;21:297-308.

[17] Liu H, Jian Q, Xue K, Ma C, Xie F, Wang R, et al. The MEK/ERK signalling cascade is required for sonic hedgehog signalling pathway-mediated enhancement of proliferation and inhibition of apoptosis in normal keratinocytes. Exp Dermatol. 2014;23:896-901.

[18] Shah AN, Cadinu D, Henke RM, Xin X, Dastidar RG, Zhang L. Deletion of a subgroup of ribosome-related genes minimizes hypoxia-induced changes and confers hypoxia tolerance. Physiol Genomics. 2011;43:855-72.

[19] Ross PL, Huang YN, Marchese JN, Williamson B, Parker K, Hattan S, et al. Multiplexed protein quantitation in Saccharomyces cerevisiae using amine-reactive isobaric tagging reagents. Mol Cell Proteomics. 2004;3:1154-69.

[20] Naumanen P, Lappalainen P, Hotulainen P. Mechanisms of actin stress fibre assembly. Journal of microscopy. 2008;231:446-54.

[21] Parsons JT, Horwitz AR, Schwartz MA. Cell adhesion: integrating cytoskeletal dynamics and cellular tension. Nature reviews Molecular cell biology. 2010;11:633-43.

[22] Olson EN, Nordheim A. Linking actin dynamics and gene transcription to drive cellular motile functions. Nature reviews Molecular cell biology. 2010;11:353-65.

[23] Zaidel-Bar R, Itzkovitz S, Ma'ayan A, Iyengar R, Geiger B. Functional atlas of the integrin adhesome. Nature cell biology. 2007;9:858-67.

[24] Yue J, Huhn S, Shen Z. Complex roles of filamin-A mediated cytoskeleton network in cancer progression. Cell & bioscience. 2013;3:7.

[25] Djinovic-Carugo K, Carugo O. Structural portrait of filamin interaction mechanisms. Current protein & peptide science. 2010;11:639-50.

[26] O'Neill GM. Scared stiff: Stabilizing the actin cytoskeleton to stop invading cancer cells in their tracks. Bioarchitecture. 2011;1:29-31.

[27] Stevenson RP, Veltman D, Machesky LM. Actin-bundling proteins in cancer progression at a glance. Journal of cell science. 2012;125:1073-9.

[28] Hall A. The cytoskeleton and cancer. Cancer metastasis reviews. 2009;28:5-14.

[29] Yamaguchi H, Condeelis J. Regulation of the actin cytoskeleton in cancer cell migration and invasion. Biochim Biophys Acta. 2007;1773:642-52.

[30] Holme TC. Cancer cell structure: actin changes in tumour cells--possible mechanisms for malignant tumour formation. European journal of surgical oncology : the journal of the European Society of Surgical Oncology and the British Association of Surgical Oncology. 1990;16:161-9.

[31] Chunhua L, Donglan L, Xiuqiong F, Lihua Z, Qin F, Yawei L, et al. Apigenin up-regulates transgelin and inhibits invasion and migration of colorectal cancer through decreased phosphorylation of AKT. The Journal of nutritional biochemistry. 2013;24:1766-75.

[32] Cadinu D, Hooda J, Alam M, Balamurugan P, Henke RM, Zhang L. Comparative proteomic analysis reveals characteristicmolecular changes accompanying the transformation ofnonmalignant to cancer lung cells. EuPA OPEN PROTEOMICS. 2014;3:1-12.

[33] Kandouz M. The Eph/Ephrin family in cancer metastasis: communication at the service of invasion. Cancer metastasis reviews. 2012;31:353-73.

[34] Nievergall E, Lackmann M, Janes PW. Eph-dependent cell-cell adhesion and segregation in development and cancer. Cellular and molecular life sciences : CMLS. 2012;69:1813-42.

[35] Kaenel P, Mosimann M, Andres AC. The multifaceted roles of Eph/ephrin signaling in breast cancer. Cell adhesion & migration. 2012;6:138-47.

[36] Genander M, Frisen J. Ephrins and Eph receptors in stem cells and cancer. Current opinion in cell biology. 2010;22:611-6.

[37] Singh A, Winterbottom E, Daar IO. Eph/ephrin signaling in cell-cell and cell-substrate adhesion. Frontiers in bioscience. 2012;17:473-97.

VITA

Md Maksudul Alam was born in a distant village of Dhaka, Bangladesh on December 31, 1981. He started his schooling at the Rasulpur Primary Govt. school, then he started middle school at Madhabdi S. P. Institution. Md Maksudul Alam attended the Govt. Science College to get higher secondary education from 1997 to 1999. In 2000, Md Maksudul Alam enrolled at the University of Dhaka to pursue a B.Sc. in Biochemistry and Molecular Biology which he received in 2006. Md Maksudul Alam then joined Dr. Haseena Khan's lab at the University of Dhaka as a research associate and continued working until 2010. In 2010, Md Maksudul Alam enrolled at The University of Texas at Dallas to pursue a PhD degree in the department of Molecular and Cell Biology.